UNIVERSIDAD NACIONAL AUTÓNOMA DE MÉXICO
POSGRADO EN CIENCIAS FÍSICAS
INSTITUTO DE FÍSICA
FÍSICA CUÁNTICA, ATÓMICA Y MOLECULAR

PAULI CHANNELS OF MULTIPARTICLE SYSTEMS

T E S I S
QUE PARA OPTAR POR EL GRADO DE
MAESTRO EN CIENCIAS (FÍSICA)

PRESENTA
JOSÉ ALFREDO DE LEÓN GARRIDO

TUTOR PRINCIPAL:
DR. CARLOS FRANCISCO PINEDA ZORRILLA
INSTITUTO DE FÍSICA, UNAM

MIEMBROS DEL COMITÉ TUTOR:
DR. FRANCOIS ALAIN LEYVRAZ WALTZ
INSTITUTO DE CIENCIAS FÍSICAS, UNAM

DR. ALEJANDRO PEREZ RIASCOS
DEPARTAMENTO DE FÍSICA, UNIVERSIDAD NACIONAL DE COLOMBIA

CIUDAD UNIVERSITARIA, CD. MX., ENERO 2024

**PROTESTA UNIVERSITARIA DE INTEGRIDAD Y
HONESTIDAD ACADÉMICA Y PROFESIONAL
(Graduación con trabajo escrito)**

De conformidad con lo dispuesto en los artículos 87, fracción V, del Estatuto General, 68, primer párrafo, del Reglamento General de Estudios Universitarios y 26, fracción I, y 35 del Reglamento General de Exámenes, me comprometo en todo tiempo a honrar a la Institución y a cumplir con los principios establecidos en el Código de Ética de la Universidad Nacional Autónoma de México, especialmente con los de integridad y honestidad académica.

De acuerdo con lo anterior, manifiesto que el trabajo escrito titulado:

"Pauli channels of multiparticle systems"

que presenté para obtener el grado de -----Maestria--- es original, de mi autoría y lo realicé con el rigor metodológico exigido por mi programa de posgrado, citando las fuentes de ideas, textos, imágenes, gráficos u otro tipo de obras empleadas para su desarrollo.

En consecuencia, acepto que la falta de cumplimiento de las disposiciones reglamentarias y normativas de la Universidad, en particular las ya referidas en el Código de Ética, llevará a la nulidad de los actos de carácter académico administrativo del proceso de graduación.

Atentamente

José Alfredo de León Garrido, No. de cuenta 522463105

(Nombre, firma y Número de cuenta de la persona alumna)

Pauli channels of multiparticle systems

José Alfredo de León Garrido

Resumen

Los canales cuánticos son un formalismo para describir la evolución unitaria y no unitaria de sistemas cuánticos. Más específicamente, los canales de Pauli han sido estudiados en el contexto del ruido cuántico y la dinámica de sistemas de qubits. Un canal de Pauli es un mapeo lineal que actúa sobre el espacio en el que viven las matrices de densidad de un sistema de qubits y es diagonal en la base de las matrices de Pauli.

En este trabajo, investigamos dos clases de canales cuánticos de muchas partículas. La primera de estas clases es un subconjunto de los canales de Pauli de muchos qubits, que nombramos canales "Pauli Component Erasing" (PCE). Estos canales eliminan o preservan las componentes de Pauli de la matriz de densidad. La segunda clase que estudiamos es una generalización de los canales de Pauli para sistemas multipartitos de dimensión arbitraria, para lo cual utilizamos la base de las matrices de Weyl. Estas matrices representan una generalización unitaria de las matrices de Pauli para dimensiones arbitrarias.

Realizamos una caracterización exhaustiva de los canales PCE y los canales de Weyl. En primer lugar, establecimos una correspondencia uno a uno de los canales PCE con subespacios vectoriales finitos. A partir de esto, dedujimos sus propiedades e identificamos el subconjunto de canales PCE que puede generarse mediante la composición de canales que preservan la mitad de las componentes de Pauli. Además, demostramos dos implementaciones de los canales PCE: en primer lugar, como el límite asintótico de procesos de decoherencia de qubits markovianos, y en segundo lugar, utilizando modelos de colisiones.

Después de esto, presentamos los canales de Weyl de muchas partículas, que engloban tanto a los canales de Pauli como a los canales PCE. Determinamos los puntos extremos de este conjunto y comprendimos que la estructura algebraica generalizada de los canales PCE está embebida dentro de todos los canales de Weyl. En otras palabras, no se limita solo a los canales de "component erasing". Finalmente, a través de esta investigación, contribuimos a una mejor comprensión de los canales cuánticos en el contexto de sistemas de muchas partículas.

Supervisor: Dr. Carlos Francisco Pineda Zorrilla

Pauli channels of multiparticle systems
José Alfredo de León Garrido

Abstract

Quantum channels are a formalism to describe the unitary and non-unitary evolution of quantum systems. More specifically, the so-called Pauli channels have been studied in the context of quantum noise and the dynamics of qubit systems. A Pauli channel is a linear map acting on the space in which density matrices of a qubit system live, and is diagonal in the basis of tensor products of Pauli matrices.

In this work, we explore two classes of multi-particle quantum channels. The first one is an intriguing class of Pauli channels, which we refer to as "Pauli Component Erasing" (PCE) channels. These channels either erase or preserve the Pauli components of the density matrix. The second class of channels is one that generalizes Pauli channels for multipartite and arbitrary-dimensional systems, for which we employ the basis of Weyl matrices. These matrices represent a unitary generalization of Pauli matrices for arbitrary dimensions.

We conducted a comprehensive characterization of PCE channels and Weyl channels. Firstly, we established a one-to-one correspondence between finite vector spaces and PCE channels. From this, we deduced their properties and identified the subset of PCE channels that can be generated through channel composition of those preserving half the Pauli components. Furthermore, we demonstrated two implementations of PCE channels: firstly, as the asymptotic limit of Markovian qubit decoherence processes, and secondly, using collision models.

Following this, we introduced many-particle Weyl channels, which encompass both Pauli and PCE channels. We determined the extreme points of this set and understood that the generalized vector structure of PCE channels is embedded within all Weyl channels. In other words, it doesn't only pertain to "component erasing" channels. Finally, through this research, we contribute to a better understanding of quantum channels in the context of many-particle systems.

Supervisor: Dr. Carlos Francisco Pineda Zorrilla

Agradecimientos

Le agradezco a mi asesor, Carlos Pineda, por su tiempo, paciencia y orientación durante la maestría.

Les agradezco al equipo de trabajo en este proyecto que comenzó con "los PCEs", pero que resultó en muchas más cosas interesantes: Alejandro Fonseca, Tomás Basile, David Dávalos, François Leyvraz y, de nuevo, Carlos Pineda. Ha sido una experiencia muy enrriquecedora trabajar junto a ustedes.

Le agradezco a Cindy por estar incondicionalmente para mí y por contar siempre con su apoyo para mi superación profesional.

Le agradezco a mi mamá, la Ednita Moda, por su apoyo para continuar con mis estudios de posgrado.

Les agradezco a las amistades que he hecho o forjado durante estos dos años en México: Adrián, Cristian, Elser, Emi y Juan Camilo (orden alfabético).

Finalmente, les agradezco a los reales: Benja, Gómez y Papaya (orden alfabético), por seguir contando con su sincera amistad y apoyo moral a pesar de la distancia física.

Contents

Declaration

Some of the work presented in this thesis has been published in a journal and prepared as a preprint. Both are listed below.

Publications

de Leon, J. A., Fonseca, A., Leyvraz, F., Davalos, D., & Pineda, C. (2022). "Pauli component erasing quantum channels". *Physical Review A, 106*(4), 042604.

Preprints

Basile, T., de Leon, J. A., Fonseca, A., Leyvraz, F., & Pineda, C. (2023). "Weyl channels for multipartite systems". *arXiv preprint arXiv:2310.10947.*

List of Figures

List of Tables

Introduction

Quantum channels play a fundamental role in quantum information theory and quantum computation [1–4]. They represent the mathematical formalism for describing quantum noise and the evolution of open quantum systems, capturing the non-unitarity from interaction between the system and its environment. Understanding and characterizing quantum channels is relevant for designing quantum protocols [5–7], analyzing quantum algorithms [1, 8, 9], studying quantum error correction [10–12], quantum communication [13, 14], quantum entanglement manipulation [15, 16] and investigating phenomena such as decoherence [17–19]. By studying the properties and characteristics of quantum channels, we gain insights into the behavior of quantum systems and develop powerful tools for harnessing quantum resources [20]. In general, exploring the framework of quantum channels and their mathematical properties is of paramount importance.

The phenomenon of unintended dissipation of quantum correlations, known as "decoherence" [21], plays a pivotal role in quantum physics. To investigate the effects of decoherence, quantum channels serve as an useful tool. However, characterizing quantum channels presents a formidable challenge, particularly due to the rapidly escalating number of parameters required as the Hilbert-space dimension expands. Additionally, these parameters are constrained in complicated way by physical constraints, such as the requirement of complete positivity [22].

A detailed exploration of classes of channels possessing specific properties sheds light on the complex realm of quantum channels. Notably, in the case of qubits, numerous studies have been dedicated to the "unital" case, that is, the class of quantum channels leaving the maximally mixed state invariant. This class of channels, characterized by three parameters, forms the well-known tetrahedron of Pauli channels [23, 24].

Moreover, most of the applications in the field of quantum information have been built upon qubits. Nevertheless, many real-world realizations of quantum systems have more than two levels that can be used to provide an important technical advantage. Such advantage is indeed employed to develop several important tasks like quantum cryptography [25, 26], quantum computation [27–29], violation of Bell inequalities [30], randomness generation [31], among others. For this reason, the study of high-dimensional and multiparticle systems is of relevance.

One relevant theoretical study of quantum channels beyond the qubit case has been provided by Nathason and Ruskai [32]. They examine families of convex combinations of quantum-classical channels, defined through mutually umbiased bases, related to unital qubit channels with positive eigenvalues, thereby providing a generalization of the Bloch sphere. The geometry of these channels have further been investigated [33]. Furtheremore, several related works have used or studied quantum channels of systems of qudits [34–37].

In this thesis, we undertake a comprehensive study of two classes of quantum channels. The first class focuses on qubits and their potential to describe decoherence processes, while the second class encompasses arbitrary-dimensional systems. This manuscript begins with a review of the formalism of quantum channels in Chapter 1. Subsequently, in Chapter 2, we introduce the Pauli maps of qubits. Here, we investigate the conditions for them to be quantum channels, i.e. complete positivity. In Chapter 3, we shift our attention to the maps that we introduced as Pauli component erasing (PCE) maps, examining their complete positivity conditions and establishing a correspondence between PCE channels and finite vector spaces. This correspondence enables us to identify the smallest subset of PCE channels that, when composed, generates the complete set. In Chapter 4, we delve into a demonstration of how the generators of PCE channels represent the fixed point of a pure dissipative Markovian process. Finally, in Chapter 5, we broaden our scope to a generalization of Pauli maps, considering systems of arbitrary dimension, and introduce the Weyl maps. Here, we investigate complete positivity and reveal the presence of a generalized algebraic structure within all Weyl channels, dispelling the notion that this structure is not exclusive to the "component erasing" type of channels.

Quantum channels

In this chapter, we introduce the theoretical framework of quantum channels. While the unitary evolution of an ideal isolated quantum system can be described by the Schrödinger equation [38], the dynamics of an open quantum system require a different approximation. In the literature, two main approaches are proposed: one for continuous systems and another for discrete ones. Continuous systems are typically addressed with the Lindblad equation [39]. Conversely, discrete systems, which we focus on, are approached with the theory of quantum channels [3, 4]. Both descriptions capture the non-unitary effects attributed to the interaction with an environment, which is not necessarily known.

The chapter is organized as follows. We begin introducing the density matrix as the mathematical tool to describe quantum states in Section 1.1. Next, we define a quantum channel in Section 1.2. We will discuss the duality between quantum states and quantum channels given by a correspondence between them in Section 1.3. In Section 1.4 we present the Kraus representation of a quantum channel. Finally, we illustrate the concepts and mathematical tools introduced in this chapter by deriving the characterization of a general quantum channel of a single-qubit in Section 1.5.

1.1. Density matrix formalism: quantum states

The density matrix formalism uses operators to represent quantum states. It is especially useful when describing the state of an open quantum system [40, 41], which refers to a system that interacts with its environment. Examples of open quantum systems include subsystems of a spin chain [42] and a two-level atom embedded in an electromagnetic field [43]. In these cases, the quantum states are typically represented as statistical mixtures of pure states, and the density matrix allows us to capture this statistical nature and study the system's properties and evolution.

We will now introduce the mathematical definition of density matrices and justify it with a physical situation. A density matrix $\rho \in \mathcal{B}(\mathcal{H}_S)$ is a positive semi-definite operator of trace one that acts on the Hilbert space $\mathcal{H}_S$ of the system [3, 4]. From a physical perspective, let us consider a situation where the quantum state of a system is prepared in the laboratory. However the exact state after preparation is not fully known. Instead, what we have is a statistical ensemble of possible preparations, where the state after each preparation is $|\psi_k\rangle$ with probability p_k. In this case, the density matrix for the state of system after the preparation is given by the expression:

$$\rho = \sum_k p_k \, |\psi_k\rangle\langle\psi_k| \,. \tag{1.1}$$

This formulation of quantum states allows us to account for the statistical mixture of different pure states.

All postulates of quantum mechanics can be reformulated straightforwardly, with the exception being the measurement postulate. Within the density matrix formalism, quantum measurements are characterized by a set of measurement operators denoted as $\{M_m\}$ [3]. Operators M_m act on the Hilbert space of the system being measured and satisfy the completeness equation $\sum_m M_m^\dagger M_m = \mathbb{1}$, with $\mathbb{1}$ the identity operator. Given the system is in the state ρ, the probability $p(m)$ of measuring

M and obtain m as a result is

$$p(m) = \text{Tr}\left(M_m^\dagger M \rho\right). \tag{1.2}$$

After the measurement of M_m the state of the system is

$$\rho' = \frac{M_m \rho M_m^\dagger}{\text{Tr}\left(M_m^\dagger M \rho\right)}. \tag{1.3}$$

As in the state vector formalism, not all density matrices of composite systems are separable. This is easy to assimilate for the states of a bipartite system with Hilbert space $\mathcal{H}_A \otimes \mathcal{H}_B$. Not all states of the total system can be expressed as a convex superposition of tensor products $\sum_k p_k \rho_A^k \otimes \rho_B^k$. In such instances, the density matrix ρ represents an entangled state [4].

Within the vector space of Hermitian matrices, which contains the set of all density matrices, it is possible to select a basis to expand ρ with. The vector space of Hermitian matrices is a real subspace of $\mathcal{B}(\mathcal{H})$ with dimension N^2, where $\mathcal{B}(\mathcal{H})$ is equipped with the inner product $\langle A, B \rangle = \text{Tr}\, A^\dagger B$. Consequently, any general Hermitian matrix can be expressed as [4]

$$A = \alpha_0 \mathbb{1} + \sum_{i=1}^{N^2-1} \alpha_i \sigma_i. \tag{1.4}$$

Here, $\{\sigma_i\}$ are any basis for the $N^2 - 1$ dimensional subspace of Hermitian matrices with zero trace, denoted as M_N. These matrices serve as generators for the group $SU(N)$ and satisfy the following relations:

$$\sigma_i \sigma_j = \frac{2}{N}\delta_{ij} + d_{ijk}\sigma_k + i f_{ijk}\sigma_k, \tag{1.5}$$

where d_{ijk} (f_{ijk}) is totally symmetric (anti-symmetric).

An orthogonal basis of unitary matrices can be employed to expand a density matrix ρ. This basis comprises a set $\{V_s\}$ of d^2 matrices, with $V_0 = \mathbb{1}$, that satisfy

the condition $\mathrm{Tr}\, V_i V_k = d\delta_{k,d}$ for all j and k. As a result, any density matrix ρ can be expressed as [32]

$$\rho = \frac{1}{d}\left[\mathbb{1} + \sum_{s=1}^{d^2} \alpha_s V_s\right], \tag{1.6}$$

where $\alpha_s = \mathrm{Tr}\, V_s^\dagger \rho$. This specific basis is important because, for $d > 2$, this representation of ρ extends the Bloch representation.

The density matrix formalism also describes reduced states. Consider a composite system S plus its environment E, with Hilbert space $\mathcal{H}_S \otimes \mathcal{H}_E$. When measuring an observable A_S, which acts only on $\mathcal{H}_S$, the expectation value can be computed using the *reduced density matrix* ρ_S as [3]

$$\mathrm{Tr}\left[\rho(A_S \otimes \mathbb{1})\right] = \mathrm{Tr}\left(\rho_S A_S\right), \tag{1.7}$$

where $\rho_S = \mathrm{Tr}_E\,\rho$, with Tr_E indicating the partial trace over the environmental degrees of freedom. Similarly, considering the environment as the system, we can derive the reduced density matrix of the environment, denoted as ρ_E, by performing the partial trace over the system degrees of freedom: $\rho_E = \mathrm{Tr}_S\,\rho$.

1.2. Completely positive and trace-preserving maps: quantum dynamics

The evolution of an open quantum system is typically non unitary. However, by expanding the system to include an appropriate environment, the reduced evolution of the system can be described as originating from a unitary evolution of the larger system. Consider the Hilbert space of the system to be denoted as $\mathcal{H}_S$ and that of the environment $\mathcal{H}_E$, so the total Hilbert space of the composed system is $\mathcal{H}_S \otimes \mathcal{H}_E$. We assume the initial state of the total system is a product state $\rho \otimes |\nu\rangle\langle\nu|$, and that it evolves with an unitary operator U. Therefore, the final state ρ' of the system alone is obtained by tracing out the environment from the evolved joint state. This

is expressed as [3, 4]

$$\rho' = \text{Tr}_E\left(U(\rho \otimes |\nu\rangle\langle\nu|)U^\dagger\right) = \sum_i \langle\mu_i|U|\nu\rangle \, \rho \, \langle\nu|U^\dagger|\mu_i\rangle, \qquad (1.8)$$

with $\{|\mu_i\rangle\}$ an orthonormal basis of $\mathcal{H}_E$, and we shall remark that U acts on $\mathcal{H}_S \otimes \mathcal{H}_E$ while $|\mu_i\rangle, |\nu\rangle \in \mathcal{H}_E$, so $\langle\mu_i|U|\nu\rangle$ is an operator acting on $\mathcal{H}_S$. It is also important to note that $\langle\mu_i|U|\nu\rangle$ is, in general, not unitary. Equation (1.8) is in essence what is known as the operator-sum or Kraus representation of a completely positive map, which we will discuss in more detail in section 1.4.

The requirement for a quantum map $\mathcal{E}$ to be completely positive, and thus represent a physical quantum evolution, stems from the fact that it is not enough for $\mathcal{E}$ to solely preserve the positivity of the density matrix ρ. When describing the evolution of a quantum state ρ, we must consider ρ to be a reduced density matrix derived from an unknown state of a larger system. Then, complete positivity guarantees that any extension of the map $\mathcal{E} \otimes \mathbb{1}_K$, where $\mathbb{1}_K$ is the identity acting on a system of arbitrary dimension K, preserves the positivity of all states, including those that are entangled.

The precise mathematical formulation of complete positivity is the following. A map $\mathcal{E}$ is completely positive if and only if, upon extending the Hilbert space $\mathcal{H}_S$ to $\mathcal{H}_S \otimes \mathcal{H}_E$, where $\mathcal{H}_E$ is of any finite dimension K, the map $\mathcal{E} \otimes \mathbb{1}_K$ is positive semidefinite. Observe that the states giving meaning to this condition are those that are entangled, as otherwise, all quantum maps would be trivially completely positive.

From an operational point of view, evaluating the complete positivity of a map $\mathcal{E}$ is impractical, as it would require verifying the positivity of $\mathcal{E} \otimes \mathbb{1}_K$ for the infinite possibilities of the dimension K. In the next section, we will discuss a connection between quantum maps and states that will enable a simple verification of complete positivity.

1.3.   Duality between density matrices and quantum channels

While quantum states and dynamics may initially appear distinct, there actually exists a duality between quantum channels and quantum states. This duality proves to be very important, as it simplifies evaluating the complete positivity of a map $\mathcal{E}$. It allows to only asses the positivity of the resulting state computed from the application of the extended map $\mathcal{E} \otimes \mathbb{1}$ to the maximally entangled state between the system that $\mathcal{E}$ acts upon and another system of the same dimension.

The duality between channels $\Phi : \mathcal{B}(H_S) \mapsto \mathcal{B}(H_S)$ and states $\rho : H_S \otimes H_S \mapsto H_S \otimes H_S$ is known as the Choi-Jamiołkowski isomorphism [44, 45]. Although it is known that this duality does not strictly meet the conditions of an isomorphism, e.g. [46], it is still referred to as the Choi-Jamiołkowski isomorphism in the literature. Considering a quantum channel $\mathcal{E}$ that acts on states $\rho : \mathcal{H}_S \mapsto \mathcal{H}_S$, the so-called isomorphism is expressed as

$$\mathcal{E} \leftrightarrow \mathcal{D}_{\mathcal{E}} = [\mathcal{E} \otimes \mathbb{1}]\left(\varrho^+\right) \qquad \varrho^+ = \frac{1}{d} \sum_{k,l=0}^{d-1} |k,k\rangle\langle l,l| \,, \tag{1.9}$$

where $d = \dim \mathcal{H}_S$ and $\varrho^+ \in \mathcal{B}(\mathcal{H}_S \otimes \mathcal{H}_S)$ is the density matrix of the maximally entangled state between the system $\mathcal{E}$ acts upon and another system of the same dimension. To avoid cluttering the notation we have dropped the Kronecker product symbol in $|k\rangle \otimes |k\rangle$. The matrix $\mathcal{D}_{\mathcal{E}}$ is known as the Choi-Jamiołkowski matrix of the quantum channel $\mathcal{E}$. As all quantum states, it is a trace one and positive operator. The correspondence between a quantum channel and a Choi-Jamiołkowski matrix is one-to-one.

The Choi-Jamiołkowski isomorphism serves a tool for evaluating complete positivity. It has been proved that a map $\Phi : \mathcal{B}(H_S) \mapsto \mathcal{B}(H_S)$ is trace-preserving and completely positive if and only if the corresponding Choi-Jamiołkowski matrix $\mathcal{D}_{\Phi}$ is positive semidefinite [4].

1.4.   Kraus representation

In Section 1.2, we introduced completely positive maps from an environmental perspective and arrived at its representation in eq. (1.8). In general, any completely positive map Φ can be expressed in *Kraus form*:

$$\Phi(\rho) = \sum_i K_i \rho K_i^\dagger, \tag{1.10}$$

where K_i are the eigenvectors of the Choi-Jamiołkowski matrix $(\mathcal{E} \otimes \mathbb{1})(\varrho^+)$. Furthermore, if the Kraus operators K_i satisfy the completeness condition $\sum_i K_i^\dagger K_i = \mathbb{1}$, then Φ is trace-preserving and called a quantum channel. Kraus [47] and Surdashan [48] showed independently that (1.10) follows from the dilation Stinespring theorem [49].

There is no unique set of Kraus operators for a completely positive map Φ. This fact follows from the theorem of *unitary freedom in Kraus representation* introduced by Nielsen and Chuang [3]. According to this theorem, if we have two distinct sets of Kraus operators $\{E_1, \ldots, E_m\}$ and $\{F_1, \ldots, F_m\}$, they represent the same map Φ if and only if there is a unitary matrix u such that $E_i = \sum_j u_{ij} F_j$.

To illustrate the consequences of unitary freedom in Kraus representation, let us consider an example. We have a single-qubit quantum channel $\mathcal{E}$ with Kraus operators $\{\mathbb{1}/\sqrt{2}, \sigma_z/\sqrt{2}\}$, and "another" quantum channel $\mathcal{F}$ with Kraus operators $\{|0\rangle\langle 0|, |1\rangle\langle 1|\}$. From a physical point of view, $\mathcal{E}$ represents a quantum evolution where, with equal probability, either no operation is performed or the unitary operation σ_z is applied to the state ρ. On the other hand, $\mathcal{F}$ corresponds to a projective measurement of ρ in the basis $\{|0\rangle, |1\rangle\}$. Both sets of Kraus operators are related via the Hadamard matrix.

A canonical set of Kraus operators for a quantum channel can be defined from the eigenvectors of its Choi-Jamiołkowski matrix. This set is called canonical in the sense that K_i are linearly independent [44]. By employing the spectral decomposi-

tion of the Choi-Jamiołkowski matrix $\mathcal{D}_\Phi$ of a quantum chanenl Φ, it is expressed as

$$\mathcal{D}_\Phi = \sum_i \lambda_i \ket{k(i)}\bra{k(i)}, \quad \ket{k(i)} = \sum_\alpha c_\alpha(i)\ket{\alpha}. \tag{1.11}$$

By reshaping the vectors $\sqrt{\lambda_i}\ket{k(i)}$, we obtain a canonical set of Kraus operators, denoted by $K(i)$, for the quantum channel Φ, where

$$K_{\beta\gamma}(i) = c_\alpha(i), \quad \alpha = \beta N + \gamma - 1 \quad \beta, \gamma = 1\dots, N. \tag{1.12}$$

1.5. Single-qubit quantum channels

In this last section we characterize the unital and some non-unital single-qubit quantum channels. While a comprehensive treatment has been previously presented by Ruskai et al. [50], we will provide our own distinct approach. By developing our unique treatment, we aim to offer a perhaps easier characterization, as well as an illustration of how to use the tools introduced in preceding sections.

We begin by expressing the density matrix of a single-qubit system in the basis composed by the identity plus Pauli matrices, which allows us to expand ρ as in eq. (1.6):

$$\rho = \frac{1}{2}\sum_{m,n=0}^{1} r_{m,n}\sigma_{m,n} \quad r_{0,0} = 1, \tag{1.13}$$

where the two-indices notation is used to compactly represent all Pauli matrices as

$$\sigma_{m,n} = \sum_{k=0}^{1}(-1)^{mk}\ket{k}\bra{k+n}, \tag{1.14}$$

including the identity operator $\sigma_{0,0} = \mathbb{1}$. In this notation the Pauli basis is ordered as $\{\mathbb{1}, \sigma_x, \sigma_z, i\sigma_y\}$. Note that $r_{0,0} = 1$ for ρ to have unit trace. The projections $r_{m,n} = \text{Tr}\,\sigma_{m,n}\rho$, with $(m,n) \neq (0,0)$, are the components of the so-called Bloch vector, which represents uniquely the state of a qubit. The Bloch vector is a vector lying in the unit ball, where $|(r_{0,1}, r_{1,0}, r_{1,1})| = 1$ corresponds to a pure state, and
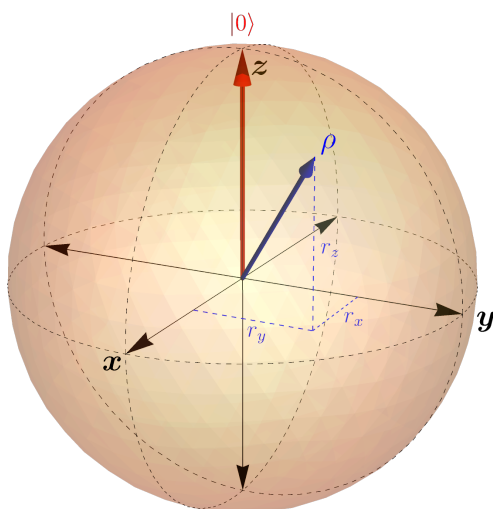
Figure 1.1: All quantum states ρ of a single-qubit are represented in the unit ball. Pure states lie in the surface ($|\vec{r}| = 1$), and mixed states are those within the surface ($|\vec{r}| < 1$).

$|(r_{0,1}, r_{1,0}, r_{1,1})| < 1$ corresponds to a mixed state, as illustrated in Fig. 1.1.

Every trace-preserving linear map $\mathcal{E}$ of a single-qubit system transforms the components $r_{m,n}$ of the density matrix ρ, as expressed in eq. (1.13), according to [51]:

$$r_{m,n} \mapsto \tau_{m,n} r_{m,n} + \kappa_{m,n} \quad \tau_{0,0} + \kappa_{0,0} = 1. \tag{1.15}$$

Furthermore, since $\mathcal{E}$ preserves the Hermiticity of ρ, both $\tau_{m,n}$ and $\kappa_{m,n}$ must be real parameters.

An important subset of trace-preserving maps for single-qubit systems is the class of unital maps [3, 51]. These unital maps, denoted $\mathcal{E}_{\vec{\tau}}$, are those defined in eq. (1.15) with the specific choice of parameters $(\kappa_{0,1}, \kappa_{1,0}, \kappa_{1,1}) = (0, 0, 0)$. To establish the conditions for $\mathcal{E}_{\vec{\tau}}$ to be completely positive, we examine the positivity of the Choi-Jamiołkowski matrix, which can be computed using eq. (1.9) as follows:

$$\mathcal{D}_{\mathcal{E}_{\vec{\tau}}} = \sum_{m,n} \tau_{m,n} \sigma_{m,n} \otimes \sigma_{m,n} \quad \tau_{0,0} = 1, \tag{1.16}$$

Recall that a map $\mathcal{E}$ is completely positive if and only if its Choi-Jamiołkowski
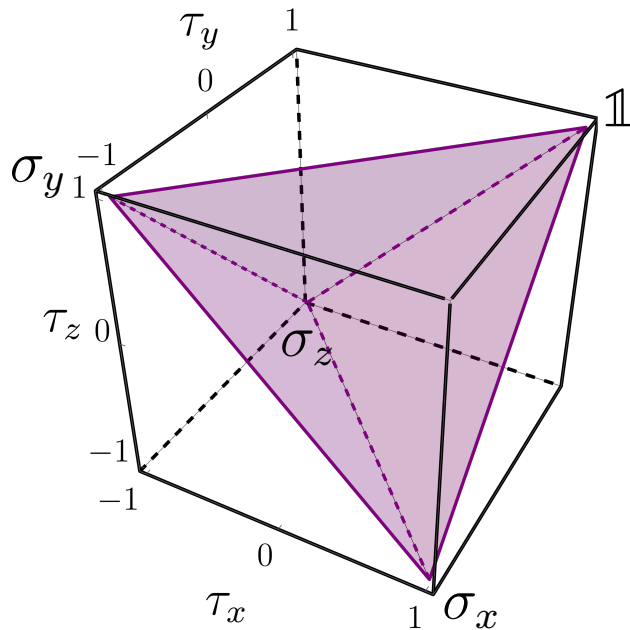
Figure 1.2: Tetrahedron of all unital single-qubit quantum channels.

matrix $\mathcal{D}$ is positive semidefinite. We proceed to diagonalize $\mathcal{D}_{\Phi_{\vec{\tau}}}$ using the steps detailed in Sec. 2.3 and obtain its eigenvalues $\lambda_{r,s}$. The conditions for $\mathcal{E}_{\vec{\tau}}$ to be completely positive can then be expressed as:

$$\lambda_{r,s} = \sum_{m,n}(-1)^{-ms+nr}\tau_{m,n} \geq 0. \tag{1.17}$$

These four inequalities define the well-known tetrahedron where all unital single-qubit quantum channels lie within. We illustrate it in Fig. 1.2. These conditions have been known since the work of Fujiwara and Algoet in 1999 [52]. All unital single-qubit quantum channel are then a convex combination of the four extreme points.

For the broader class of non-unital single-qubit maps, we will focus on two significant cases. The first case consider maps, denoted as $\mathcal{E}$ and defined in eq. (1.15) with the specific parameters $(\kappa_{0,0}, \kappa_{1,0}, \kappa_{1,1}) = (0, 0, \kappa_z)$. This case was studied by Fujiwara and Algoet [53]. They established the necessary and sufficient condition

for $\mathcal{E}$ to be completely positive:

$$\tau_{0,1}^2 + \kappa_z^2 \leq (1 - |\tau_{1,1}|)^2. \tag{1.18}$$

The second case of interest pertains to maps $\mathcal{E}_{\vec{\kappa}}$, with all $\tau_{m,n} = 1$ and arbitrary $\kappa_{m,n}$ values. Using eq. (1.9) we compute the Choi-Jamiołkowski matrix to be

$$\mathcal{D}_{\mathcal{E}_{\vec{\kappa}}} = \sum_{m,n} \kappa_{m,n} \sigma_{m,n} \otimes \mathbb{1} \quad \kappa_{0,0} = 1. \tag{1.19}$$

Diagonalizing $\mathcal{E}_{\vec{\kappa}}$ and identifying that the eigenvalues $\mu_{\pm}$ are doubly degenerated, we obtain the conditions for complete positivity:

$$\mu_{\pm} = 1 \pm |(\kappa_{0,0}, \kappa_{1,0}, \kappa_{1,1})| \geq 0. \tag{1.20}$$

Not all single-qubit quantum channels are the composition $\mathcal{E}_{\vec{\kappa}} \circ \mathcal{E}_{\vec{\tau}}$ of a quantum channel that contracts the Bloch sphere and another that displaces the origin of coordinates. Even though eq. (1.15) may suggest the contrary, a single-qubit quantum channel can be composed by a not completely positive map deforming the Bloch sphere and a quantum channel displacing the origin of coordinates. An specific example of this is the amplitude damping channel, see Tab 1.1.

Sec. 2.3 In Table 1.1 we show a summary of the different types of single-qubit quantum channels. The first channel is the trivial one, which does nothing to the state ρ of a single-qubit. The second represents a unitary evolution. Similar channels describing rotations around any other axis exist. The third channel takes a pure state to a mixed state. The phase-flip describes a decoherence process, in which suppresses the off-diagonal elements of ρ in eigenbasis of σ_z. Finally, the amplitude-damping describes a relevant physical process because it can take a mixed state to a pure state.

In this chapter, we have introduced the framework of quantum channels. We began by presenting the density matrix as the primary tool for describing the
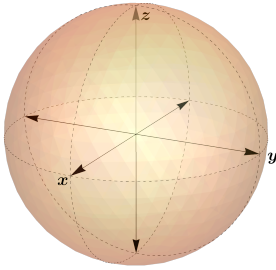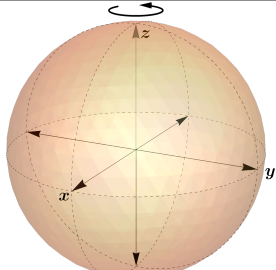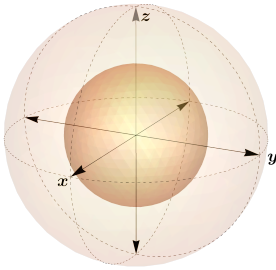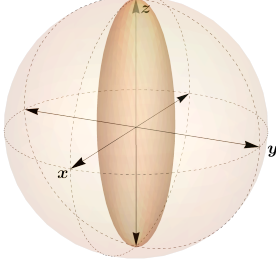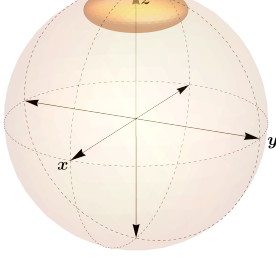
	Channel	$\vec{\tau}$	$\vec{\kappa}$	Bloch representation
1	Identity	$(1, 1, 1)$	$(0, 0, 0)$	
2	Rotation around z-axis	$(\tau_x, \tau_y, 1)$	$(0, 0, 0)$	
3	Depolarizing	(τ_x, τ_x, τ_x)	$(0, 0, 0)$	
4	Phase-flip	$(\tau_x, \tau_x, 1)$	$(0, 0, 0)$	
5	Amplitude-damping	$(\tau_x, \tau_x, \tau_x^2)$	$(0, 0, 1 - \tau_x^2)$	

Table 1.1: Summary of single-qubit quantum channels.

quantum state of an open quantum system. We then moved to quantum channels, which capture the evolution of the density matrix. These mathematical objects are completely positive and trace-preserving maps. Subsequently, we discussed the Choi-Jamiołkowski isomorphism, which provides a practical method for assessing the complete positivity of a linear map. To illustrate these framework in practical terms, we provided a derivation of the quantum channels for a single qubit. In the next chapter, we turn to study a specific but relevant class of N-qubit system maps.

Pauli quantum channels

Our approach to present Pauli quantum channels begins with introducing Pauli diagonal maps. We recall that, in our terminology, maps are not necessarily completely positive. Subsequently, we perform the diagonalization of the Choi-Jamiołkowski matrix of a Pauli diagonal map. We obtain the linear relationship between the parameters characterizing a Pauli diagonal quantum channel, which describes how the channel operates on the *Pauli components* of the density matrix, and the eigenvalues of its Choi-Jamiołkowski matrix.

2.1. Pauli diagonal maps

To introduce the definition of a Pauli diagonal map we shall begin by expressing the density matrix of a multi-qubit system in the basis of tensor products of Pauli matrices. We will denote a N-qubit Pauli operator, also referred to as Pauli string [54], as

$$\sigma_{\vec{m},\vec{n}} = \sigma_{m_1,n_1} \otimes \sigma_{m_2,n_2} \otimes \ldots \otimes \sigma_{m_N,n_N}, \qquad m_j, n_j = 0, 1. \tag{2.1}$$

This notation allows us to associate each N-qubit Pauli operator with a pair of "vectors" $(\vec{m}, \vec{n})$, where every pair of numbers (m_j, n_j) corresponds to a local Pauli operator. From the properties of Pauli matrices it is verified that the N-qubit

Pauli operators satisfy both the orthogonality condition $\operatorname{Tr} \sigma_{\vec{m},\vec{n}} \sigma_{\vec{r},\vec{s}} = 2^N \delta_{\vec{m},\vec{r}} \delta_{\vec{n},\vec{s}}$ and the completeness condition $1/2^N \sum \sigma_{\vec{m},\vec{n}} \sigma_{\vec{m},\vec{n}}^{\dagger} = \mathbb{1}_{2^N}$. Hence, this set, including the identity, forms a basis of the space $\mathcal{B}\left(\mathbb{C}^{2^{\otimes N}}\right)$. Finally, the density matrix of a N-qubit system is expressed as

$$\rho = \frac{1}{2^N} \sum_{\vec{m},\vec{n}} r_{\vec{m},\vec{n}} \sigma_{\vec{m},\vec{n}}, \tag{2.2}$$

where the projections $r_{\vec{m},\vec{n}} = \operatorname{Tr} \sigma_{\vec{m},\vec{n}} \rho$ will be referred to as Pauli components.

We define a Pauli diagonal map, or simply a Pauli map, as a linear map that transforms the Pauli components of the density matrix of a N-qubit system, as given in eq. (2.2), according to:

$$r_{\vec{m},\vec{n}} \mapsto \tau_{\vec{m},\vec{n}} r_{\vec{m},\vec{n}} \quad \tau_{\vec{0},\vec{0}} = 1, \, \tau_{\vec{m},\vec{n}} \in \mathbb{R}. \tag{2.3}$$

By imposing these conditions on the parameters $\tau_{\vec{m},\vec{n}}$ of a Pauli map we ensure the map is trace-preserving and positive. That is, by definition a Pauli map preserves the normalization condition and transforms positive matrices to positive matrices. Consequently, we need only investigate the conditions that $\tau_{\vec{m},\vec{n}}$ must satisfy for a Pauli map to be complete positivity, thus becoming a quantum channel. This is what we do in the next section.

2.2. Choi-Jamiołkowski matrix

In this section, we present two results. Firstly, we derive the generic form of the Choi-Jamiołkowski matrix for a broader class of diagonal maps than just Pauli diagonal maps. Secondly, we perform the diagonalization of the Choi-Jamiołkowski matrix specifically for Pauli diagonal maps to determine the necessary conditions that $\tau_{\vec{m},\vec{n}}$ must satisfy for the map to be completely positive.

2.2.1. Generic form of the Choi-Jamiołkowski matrix of any diagonal map

We demonstrate that the Choi-Jamiołkowski matrix of any map that is diagonal in an orthogonal basis $U_{\vec{m},\vec{n}}$ of $\mathcal{B}(\mathcal{H}_1 \otimes \ldots \otimes \mathcal{H}_N)$, with $\dim(\mathcal{H}_j)$ arbitrary, has the following generic form:

$$\mathcal{D} = \sum \tau_{\vec{m},\vec{n}} \, U_{\vec{m},\vec{n}} \otimes U^*_{\vec{m},\vec{n}}. \tag{2.4}$$

Recall that the Choi-Jamiołkowski matrix of a map $\mathcal{E}$ is computed by applying the extended map $\mathcal{E} \otimes \mathbb{1}$ to the maximally entangled state between the system that $\mathcal{E}$ acts upon and another system of the same dimension. To prove eq. (2.4) we express the maximally entangled state in the orthogonal basis $U_{\vec{m},\vec{n}}$ and use the definition of a diagonal map:

$$\mathcal{E}(U_{\vec{m},\vec{n}}) = \tau_{\vec{m},\vec{n}} U_{\vec{m},\vec{n}}. \tag{2.5}$$

We express $\left| \vec{k} \right\rangle\!\left\langle \vec{l} \right|$, which is the standard matrix that have only one entry 1 in position $(\vec{k}, \vec{l})$ and 0 elsewhere, in an orthogonal basis $U_{\vec{m},\vec{n}}$:

$$\left| \vec{k} \right\rangle\!\left\langle \vec{l} \right| = \sum_{\vec{m},\vec{n}} \mathrm{Tr}\left(U^\dagger_{\vec{m},\vec{n}} \left| \vec{k} \right\rangle\!\left\langle \vec{l} \right| \right) U_{\vec{m},\vec{n}}. \tag{2.6}$$

Following this, we perform a change of basis for the maximally entangled state $\varrho^{\mathrm{max\,ent}}$, leading to:

$$\varrho^{\mathrm{max\,ent}} = \frac{1}{d} \sum_{\vec{k},\vec{l},\vec{m},\vec{n},\vec{m}',\vec{n}'} \mathrm{Tr}\left(U^\dagger_{\vec{m},\vec{n}} \left| \vec{k} \right\rangle\!\left\langle \vec{l} \right| \right) \mathrm{Tr}\left(U_{\vec{m}',\vec{n}'} \left| \vec{l} \right\rangle\!\left\langle \vec{k} \right| \right) U_{\vec{m},\vec{n}} \otimes U^*_{\vec{m}',\vec{n}'}. \tag{2.7}$$

Here, we have used (2.6) and its complex conjugate for the first and second factors of the tensor product in eq. (1.9), respectively. By applying the definition of the

trace and the orthogonality condition, we arrive at:

$$\varrho^{\text{max ent}} = \frac{1}{d} \sum_{\vec{m},\vec{n}} U_{\vec{m},\vec{n}} \otimes U_{\vec{m},\vec{n}}^*. \tag{2.8}$$

This immediately leads us to the result that $[\mathcal{E} \otimes \mathbb{1}](\varrho^{\text{max ent}})$ corresponds to (2.4). We emphasize that this generic form of the Choi-Jamiołkowski matrix holds for any number of particles, even regardless of their dimension. The sole requirement is that $\{U_{\vec{m},\vec{n}}\}$ is an orthogonal basis.

Equation (2.4) provides a representation of any map diagonal in an orthogonal basis of operators, allowing for a direct evaluation of complete positivity, as a map is completely positive if and only if its Choi-Jamiołkowski is positive.

2.3.   Pauli quantum channels

We now focus on deriving the conditions under which a Pauli map is a quantum channel. To do so, we investigate the conditions of trace preservation and complete positivity of a Pauli map in terms of its Choi-Jamiołkowski matrix.

We begin by writing the Choi-Jamiołkowski matrix of a Pauli diagonal map of N qubits. Straightforwardly, by using eq. (2.4), we obtain:

$$\mathcal{D} = \frac{1}{2^N} \sum_{\vec{m},\vec{n}} \tau_{\vec{m},\vec{n}} \, \sigma_{\vec{m},\vec{n}} \otimes \sigma_{m,\vec{n}}. \tag{2.9}$$

A Pauli map is trace-preserving by definition, as $\tau_{\vec{0},\vec{0}} = 1$. This fixes the trace of the Choi-Jamiołkowski matrix as:

$$\text{Tr}\,\mathcal{D} = \frac{1}{2^N} \sum_{\vec{m},\vec{n}} \tau_{\vec{m},\vec{n}} 2^{2N} \delta_{\vec{m},\vec{0}} \delta_{\vec{n},\vec{0}}$$

$$= 2^N \tau_{\vec{0},\vec{0}} = 2^N. \tag{2.10}$$

Recall that a Pauli map is completely positive, if and only if its corresponding Choi-

Jamiołkowski matrix $\mathcal{D}$ is positive. Thus, we diagonalize the matrix $\mathcal{D}$, carrying a series of steps in the following. We begin by observing that all operators in the sum of right-hand side of eq. (2.9) commute:

$$\left[\sigma_{\vec{m},\vec{n}} \otimes \sigma^*_{\vec{m},\vec{n}}, \sigma_{\vec{m}',\vec{n}'} \otimes \sigma^*_{m',\vec{n}'}\right] = 0 \quad \forall\, \vec{m}, \vec{n}, \vec{m}', \vec{n}', \tag{2.11}$$

which follows from the following relation:

$$\left(\sigma_{\vec{m},\vec{n}} \otimes \sigma^*_{\vec{m},\vec{n}}\right)\left(\sigma_{\vec{m}',\vec{n}'} \otimes \sigma^*_{\vec{m}',\vec{n}'}\right) = \sigma_{\vec{m},\vec{n}}\sigma_{\vec{m}',\vec{n}'} \otimes \sigma_{-\vec{m},\vec{n}}\sigma_{-\vec{m}',\vec{n}'} \tag{2.12}$$

$$= \sigma_{\vec{m}+\vec{m},\vec{n}+\vec{n}} \otimes \sigma_{-\vec{m}-\vec{m}',\vec{n}+\vec{n}'}. \tag{2.13}$$

We have used $\sigma_{\vec{m},\vec{n}}\sigma_{\vec{m}',\vec{n}'} = (-1)^{\vec{m}'\cdot\vec{n}}\sigma_{\vec{m}+\vec{m},\vec{n}+\vec{n}}$, which can be proved using the compact expression for all Pauli matrices.

The commutation relations in eq. (2.11) yield two important implications we now discuss. On one hand, they allow us to diagonalize $\mathcal{D}$ as

$$P^{-1}\mathcal{D}P = 1/2^N \sum_{\vec{m},\vec{n}} \tau_{\vec{m},\vec{n}} \; P^{-1}\sigma_{\vec{m},\vec{n}} \; \otimes \; \sigma^*_{m,\vec{n}} \, P, \tag{2.14}$$

where the columns of P are the common eigenvectors shared by all $\sigma_{\vec{m},\vec{n}} \otimes \sigma^*_{m,\vec{n}}$. On the other hand, the second implication follows directly from eq. (2.14). There is a linear relationship between the parameters $\tau_{\vec{m},\vec{n}}$ of a Pauli diagonal map and the eigenvalues $\lambda_{\vec{r},\vec{s}}$ of its Choi-Jamiołkowski matrix. This allows us to easily study Pauli diagonal maps either in their superoperator or Choi-Jamiołkowski matrix representation.

The next step in our diagonalization of $\mathcal{D}$ takes advantage of the fact that operators $\sigma_{\vec{m},\vec{n}} \otimes \sigma^*_{\vec{m},\vec{n}}$ and $|\sigma_{\vec{r},\vec{s}}\rangle\!\rangle\langle\!\langle\sigma_{\vec{r},\vec{s}}|$ commute for all $\vec{m}, \vec{n}, \vec{r}, \vec{s}$, which follows from:

$$\sigma_{\vec{m},\vec{n}} \otimes \sigma^*_{\vec{m},\vec{n}} |\sigma_{\vec{r},\vec{s}}\rangle\!\rangle = (-1)^{\vec{m}\cdot\vec{s}+\vec{n}\cdot\vec{r}} |\sigma_{\vec{r},\vec{s}}\rangle\!\rangle, \tag{2.15}$$

where $|\sigma_{\vec{r},\vec{s}}\rangle\!\rangle$ are the vectorized N-qubit Pauli operators in eq. (2.1) and can be
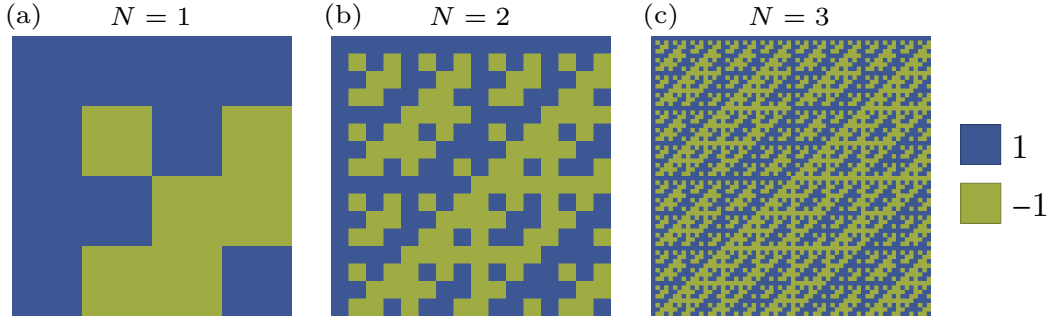
Figure 2.1: Plots of matrix $(F_2 \otimes F_2)^{\otimes N}$ for $N =1$, 2 and 3 qubits. This matrix represents the linear relationship between the $\tau_{\vec{m},\vec{n}}$ of a Pauli map and the eigenvalues $\lambda_{\vec{r},\vec{s}}$ of its Choi-Jamiołkowski matrix, see eq. (2.18).

expressed as:

$$|\sigma_{\vec{m},\vec{n}}\rangle\rangle = \sum_{\vec{k}} (-1)^{\vec{k}\cdot\vec{m}} \left|\vec{k}, \vec{k}+\vec{n}\right\rangle, \tag{2.16}$$

where the sum $\vec{k}+\vec{n}$ is performed component-wise.

Finally, from eq. (2.15) the eigenvalues of $\mathcal{D}$ are computed straightforwardly to be:

$$\lambda_{\vec{r},\vec{s}} = \frac{1}{2^N} \sum_{\vec{m},\vec{n}} (-1)^{\vec{m}\cdot\vec{s}+\vec{n}\cdot\vec{r}} \tau_{\vec{m},\vec{n}}. \tag{2.17}$$

The eigenvalues of the Choi-Jamiołkowski may be expressed in terms of the Fourier transform matrix. If we recognize $(-1)^{\vec{m}\cdot\vec{s}+\vec{n}\cdot\vec{r}} = \left(\bigotimes_\alpha F_2 \otimes F_2\right)_{2\vec{m}+\vec{n},2\vec{s}+\vec{r}}$, where F_2 is the 2×2 discrete Fourier transform matrix, we then can re-write eq. (2.17) in an elegant and compact equation as:

$$\vec{\lambda} = (F_2 \otimes F_2)^{\otimes N} \vec{\tau}. \tag{2.18}$$

We illustrate in Fig. 2.1 some plots of this linear transformation between $\lambda_{\vec{r},\vec{s}}$ and $\tau_{\vec{m},\vec{n}}$ for Pauli maps of systems with $N = 1$, 2 and 3 qubits. Note that all rows and columns are either symmetric or anti-symmetric when reflected. This will become important when we introduce Pauli component erasing channels in the next chapter.

We have diagonalized the Choi-Jamiołkowski matrix of a Pauli diagonal map. Therefore, from the Choi-Jamiołkowski isomorphism we can state that a Pauli diagonal map is a quantum channel if and only if

$$\lambda_{\vec{r},\vec{s}} = \frac{1}{2^N} \sum_{\vec{m},\vec{n}} (-1)^{\vec{m}\cdot\vec{s}+\vec{n}\cdot\vec{r}} \tau_{\vec{m},\vec{n}} \geq 0 \qquad \forall\, \vec{r}, \vec{s}; \tag{2.19}$$

$$\sum_{\lambda_{\vec{r},\vec{s}}} \lambda_{\vec{r},\vec{s}} = d^N. \tag{2.20}$$

From the diagonalization of the Choi-Jamiołkowski we can derive the canonical Kraus representation of a Pauli diagonal quantum channel. From eq. (2.15) follows the vectorized N-qubit Pauli operators serve as the eigenvectors of $\mathcal{D}$. Thus, the canonical Kraus representation of a Pauli diagonal quantum channel is given by:

$$\mathcal{E}(\rho) = \sum_{\vec{r},\vec{s}} p_{\vec{r},\vec{s}}\, \sigma_{\vec{r},\vec{s}} \rho \sigma_{\vec{r},\vec{s}}, \tag{2.21}$$

where $p_{\vec{r},\vec{s}} = \sqrt{\lambda_{\vec{r},\vec{s}}}$. Vector $\vec{p}$ contains the probabilities that matrices $\sigma_{\vec{r},\vec{s}}$ act on the density matrix [55]. Thus, provided $\vec{p}$, eq. (2.18) tells us how a Pauli diagonal channel acts over the Pauli components of the density matrix.

Pauli component erasing quantum channels

We wish now to study a specific class of Pauli channels of N qubits, which we call *Pauli component erasing.* For a single qubit these channels are those projecting the Bloch sphere to any of the Cartesian axes, see Figure 3.1. These channels describe the limiting points of the decoherence processes that erase the non-diagonal terms of the density matrix, also called coherences, in the eigenbases of each of the Pauli matrices. Nevertheless, this matter will be left for the next chapter, as here we only investigate the mathematical structure of PCE channels and some of its properties.
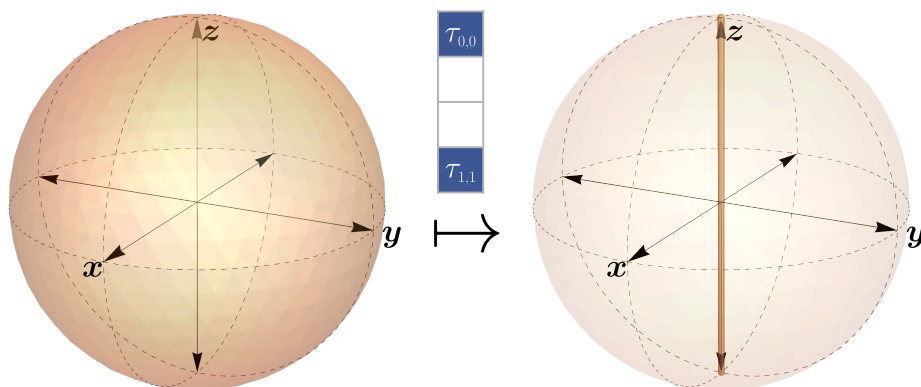
Figure 3.1: Single-qubit PCE channel $\vec{\tau} = (1, 0, 0, 1)$ projecting the Bloch sphere onto the z axis. This channel may be seen as the completely phase-flipping channel.

3.1. PCE maps

We define a Pauli component erasing (PCE) map as a Pauli map of N qubits, see eq. (2.3), which acts over the Pauli components as follows:

$$r_{\vec{m},\vec{n}} \mapsto \tau_{\vec{m},\vec{n}} r_{\vec{m},\vec{n}} \quad \tau_{\vec{0},\vec{0}} = 1, \quad \tau_{\vec{m},\vec{n}} = 0, 1. \tag{3.1}$$

That is, a PCE map either preserves or erases the Pauli components of the density matrix. Analogously, a PCE map projects the density matrix onto a subspace spanned by a subset of all possible N-qubit Pauli operators.

We shall be interested in investigating how to constrain the components of $\vec{\tau}$ for a PCE map to be completely positive. Without these conditions, a PCE map $\vec{\tau}$ could be a mathematical object without physical meaning. We delve into the conditions of complete positivity in the subsequent section, but we provide an illustrative example before to understand which kind of PCE maps are not associated with a quantum evolution of a single qubit.

All PCE maps of a single qubit projecting the Bloch sphere to a disk are not completely positive. Let us consider the PCE map that transforms the Bloch sphere into a disk in the x-y plane. That PCE map is represented by:

$$\vec{\tau} = (1, 1, 1, 0). \tag{3.2}$$

By computing the eigenvalues of the corresponding Choi-Jamiołkowski matrix, using eq. (2.18), we obtain:

$$\vec{\lambda} = \left(\frac{3}{2}, \frac{1}{2}, \frac{1}{2}, -\frac{1}{2} \right). \tag{3.3}$$

Therefore, the negative eigenvalue indicates that the PCE map (3.2) is not completely positive, as the extended PCE map acting on two qubits, when they are maximally entangled, transforms the two-qubit density matrix to a matrix that is not positive semi-definite. Rotations of the Bloch sphere do not alter the eigenval-

ues $\vec{\tau}$ of a PCE map. Consequently, the Choi-Jamiołkowski matrices of the other two PCE maps projecting the Bloch sphere onto a disk in either the *x-z* or *y-z* planes, possess identical eigenvalues as those in eq. (3.3). These eigenvalues, however, correspond to different eigenvectors. In consequence, despite the fact that PCE maps similar to that defined in (3.2) are indeed positive, as they transform single-qubit density matrices to single-qubit density matrices, they do not represent a physical quantum evolution because they are not completely positive.

When studying PCE maps of more than a single qubit, we have no such geometrical representation as the Bloch sphere to keep visualizing the maps. It is important to be able to have such a illustrative representation, as it provides intuition about the mathematical structure. Thus, to visualize PCE maps we have developed a pictorial tool. This tool represents the components of the PCE map $\vec{\tau}$ in a *N*-dimensional grid. Each square at position $(\vec{m}, \vec{n})$ is colored either black $(\tau_{\vec{m},\vec{n}} = 1)$ or white $(\tau_{\vec{m},\vec{n}} = 0)$ depending on the corresponding $\tau_{\vec{m},\vec{n}}$. We show in Fig. 3.2 some examples of PCE maps of a single qubit: the identity map, the map projecting the Bloch sphere to a disk in the *y-z* plane, the map projecting the Bloch sphere to the *z* axis, and the completely depolarizing map. Similarly, we depict in Fig. 3.3 three two-qubit PCE maps: the identity, a map projecting the density matrix to the subspace where the maximally entangled state lives, and another map preserving the local components $\langle \sigma_x \otimes \mathbb{1} \rangle$ and $\langle \mathbb{1} \otimes \sigma_y \rangle$ of both qubits, and the two correlations $\langle \sigma_x \otimes \sigma_y \rangle$ and $\langle \sigma_y \otimes \sigma_x \rangle$.

Though our tool to visualize PCE maps is helpful, it does have its limitations. Visualizing 3D grids becomes cumbersome, especially those representing PCE maps with colored cubes in the center. Moreover, when dealing with systems of more than three qubits the complexity of visualization escalates further. Despite these limitations, the representation of two-qubit PCE maps will be enough to understand the structure of PCE maps in the coming section.

We would like to highlight two points regarding our representation of PCE maps. On one hand, this tool can be employed to represent the density matrix of *N* qubits
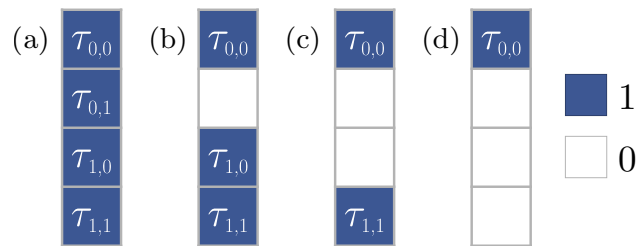
Figure 3.2: Some PCE maps of a single-qubit system. (a) Identity map: $\vec{\tau} = (1, 1, 1, 1)$, (b) PCE map that projects the Bloch sphere to a disk in the y-z plane: $\vec{\tau} = (1, 0, 1, 1)$, (c) totally phase-flip channel: see Table 1.1, $\vec{\tau} = (1, 0, 0, 1)$, and (d) completely depolarizing channel: $\vec{\tau} = (1, 0, 0, 0)$. Figure taken and modified from [56].

as well, by using a gradient to depict the values $-1 \leq r_{\vec{m}, \vec{n}} \leq 1$ instead of the binary coloring scheme. On the other hand, for $N \geq 3$, the complexity of visualizing the grids can be mitigated by representing PCE maps in a two-dimensional grid format, where the indices $(\vec{m}, \vec{n})$ are viewed as coming from a tensor product of N 2×2 matrices, as we show in Appendix 5.4.

In the following section, it will become more clear how useful the representation of PCE maps is to distinguish intuitively between quantum channels and non completely positive maps.

3.2. PCE quantum channels as vector spaces

We now study the subset of PCE maps that describe the physical quantum evolution of systems of qubits. We begin by deriving the complete positivity conditions
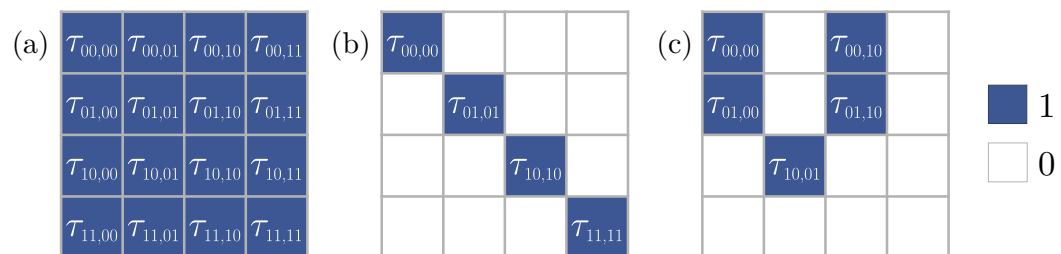
Figure 3.3: Some PCE maps of a two-qubit system. (a) identity map, (b) PCE map projecting the density matrix to the subspace where the maximally entangled state lives, and (c) a map preserving the local components x and y of qubits one and two, respectively, and two correlations between them.
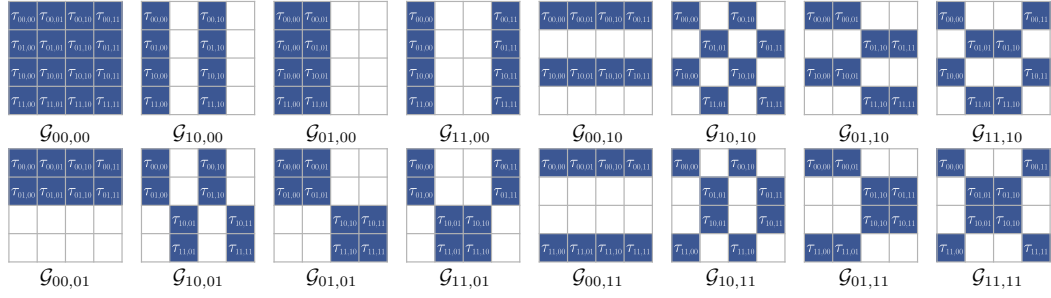
Figure 3.4: All two-qubit PCE channels that preserve 8/16 of the Pauli components of the density matrix. The indices (m_1, n_1) and (m_2, n_2) of the labels $\mathcal{G}_{\vec{m},\vec{n}}$ indicate how the corresponding PCE channel acts locally on each individual qubit. Figure taken and modified from [56].

for a PCE map to be a quantum channel. Then, we derive from them an elegant algebraic structure of finite vector spaces for PCE channels.

The complete set of two-qubit PCE maps that preserve eight Pauli components is presented in Fig. 3.4. Notably, out of the huge number of PCE maps within this category—totaling 6,435, to be exact—only sixteen are found to be completely positive. To calculate the number of PCE maps preserving eight Pauli components, one can determine the number of different subsets $\{(m,n)\}|_{(\vec{m},\vec{n})\neq(\vec{0},\vec{0})}$ with seven elements. For each of the PCE channels depicted in Fig. 3.4, there are more than four hundred additional PCE maps that do not meet the criteria for complete positivity. Indeed, this highlights how the complete positivity plays a key role to determine whether a PCE map represent a physical evolution.

Furthermore, upon closer examination of the grids in Fig. 3.4 we are led to the conclusion that a mathematical structure must underlay these distinctive patterns. By looking carefully at all the grids a heuristic rule is clear. If a PCE channel either preserves or erases the local components $\langle \sigma_i \otimes \mathbb{1} \rangle$ and $\langle \mathbb{1} \otimes \sigma_j \rangle$ of the density matrix of both individual qubits, then the correlation $\langle \sigma_i \otimes \sigma_j \rangle$ is preserved as well.

The heuristic rule and, more importantly, the patterns that underlie all PCE channels are elucidated through an algebraic structure. Each PCE channel is uniquely characterized by a subspace within $\bigoplus_N (\mathbb{Z}_2 \oplus \mathbb{Z}_2)$ over the field $\{0, 1\}$.

Proof. We show that a PCE map is completely positive if and only if $W = \{(\vec{m}, \vec{n}) : \tau_{\vec{m},\vec{n}} = 1\}$ forms a subspace within the aforementioned finite vector space. We begin proving that completely positive and trace-preserving conditions of a PCE channel imply the subspace structure. Consider two components $\tau_{\vec{m},\vec{n}}$ and $\tau_{\vec{m}',\vec{n}'}$ of the channel such that $\tau_{\vec{m},\vec{n}} = \tau_{\vec{m}',\vec{n}'} = 1$. Inverting eq. (2.17) we obtain:

$$\tau_{\vec{m},\vec{n}} = \frac{1}{2^N} \sum_{\vec{r},\vec{s}} (-1)^{\vec{m}\cdot\vec{s}+\vec{n}\cdot\vec{r}} \lambda_{\vec{r},\vec{s}} \tag{3.4}$$

$$1 = \frac{1}{2^N} \sum_{\vec{r},\vec{s}} (-1)^{\vec{m}\cdot\vec{s}+\vec{n}\cdot\vec{r}} \lambda_{\vec{r},\vec{s}}. \tag{3.5}$$

A similar equation holds for $\tau_{\vec{m}',\vec{n}'}$. We note that $-1 \leq (-1)^{\vec{m}\cdot\vec{s}+\vec{n}\cdot\vec{r}} \leq 1$. Furthermore, we take into account that the complete positivity constraints the eigenvalues of the Choi-Jamiołkowski matrix as $\lambda_{\vec{r},\vec{s}} \geq 0$, and trace preservation condition dictates that $\sum_{\vec{r},\vec{s}} \lambda_{\vec{r},\vec{s}} = 2^N$. Hence, for eq. (3.5) to hold, we conclude that $(-1)^{\vec{m}\cdot\vec{s}+\vec{n}\cdot\vec{r}} = 1$ for all $(\vec{r}, \vec{s})$, which means:

$$\vec{m} \cdot \vec{s} + \vec{n} \cdot \vec{r} = 0 \quad \forall\, (\vec{r}, \vec{s}), (\vec{m}, \vec{n}) : \tau_{\vec{m},\vec{n}} = 1. \tag{3.6}$$

An analogous condition is derived for the primed versions $(\vec{m}', \vec{n}')$. Now, calculating $\tau_{\vec{m}+\vec{m}',\vec{n}+\vec{n}'}$ using eq. (3.4), and inserting in that expression equations (3.6) and its primed version, we obtain:

$$\tau_{\vec{m}+\vec{m}',\vec{n}+\vec{n}'} = \frac{1}{2^N} \sum_{\vec{r},\vec{s}} (-1)^{(\vec{m}+\vec{m}')\cdot\vec{s}+(\vec{n}+\vec{n}')\cdot\vec{r}} \lambda_{\vec{r},\vec{s}} \tag{3.7a}$$

$$= \frac{1}{2^N} \sum_{\vec{r},\vec{s}} \lambda_{\vec{r},\vec{s}} = 1. \tag{3.7b}$$

We have used trace-preserving condition once again in the last line. We have showed that, if a PCE map is completely positive, then

$$\tau_{\vec{m},\vec{n}} \tau_{\vec{m}',\vec{n}'} = \tau_{\vec{m}+\vec{m}',\vec{n}+\vec{n}'} \tag{3.8}$$
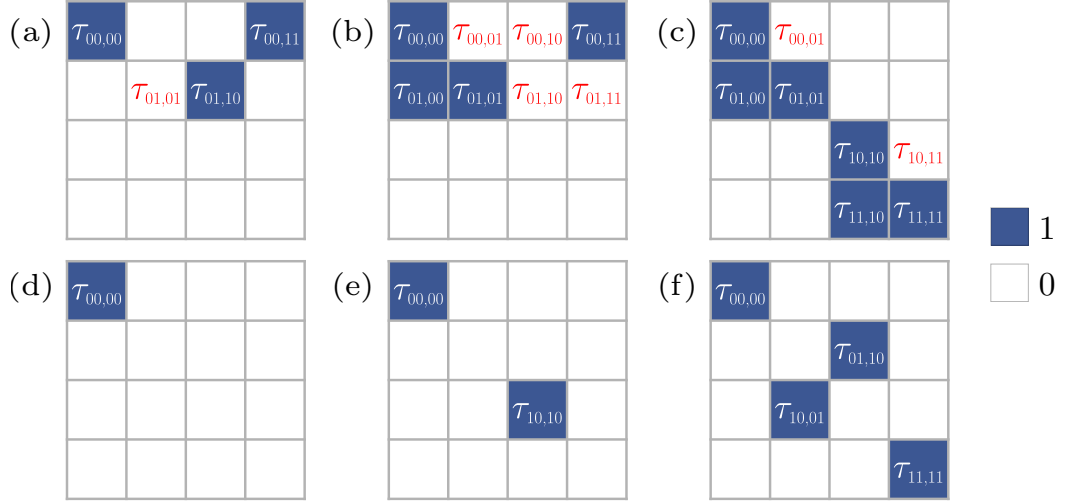
Figure 3.5: Examples of two-qubit PCE maps exhibiting non-completely positive and completely positive behaviors. In (a) to (c) we illustrate three non-completely positive maps, each accompanied by the corresponding $\tau_{\vec{m},\vec{n}}$ that are missing to complete the vector subspace in red font. In (d) to (f) we present three PCE channels.

holds for all $\tau_{\vec{m},\vec{n}} = 1$. To prove the converse, we only need to prove that the vector structure implies the complete positivity condition, as a PCE map is already defined as trace-preserving. Let us assume that the set of indices $W = \left\{ (\vec{m}, \vec{n}) : \tau_{\vec{m},\vec{n}} = 1 \right\}$ forms a vector subspace of $\bigoplus_N \left(\mathbb{Z}_2 \oplus \mathbb{Z}_2 \right)$, given that eq. (3.6) holds. The eigenvalue $\lambda_{\vec{r},\vec{s}}$ in eq. (2.17) can then be computed by summing exclusively over those indices in vector space W, allowing us to obtain:

$$\lambda_{\vec{r},\vec{s}} = \frac{1}{2^N} \sum_{(\vec{m},\vec{n}) \in W} \tau_{\vec{m},\vec{n}} = \frac{|W|}{2^N}, \qquad (3.9)$$

where $|W|$ denotes the cardinality of vector subspace W. From this, it follows the inequality:

$$\frac{1}{2^N} \leq \lambda_{\vec{r},\vec{s}} \leq 2^N, \qquad (3.10)$$

as the lowest and highest cardinality of W are those of the trivial and complete vector spaces, respectively. This inequalities imply that $\lambda_{\vec{r},\vec{s}} \geq 0$, which are the complete positivity conditions. $\qquad \square$

Now, the vector structure provides a tool either to check if a PCE map is a quan-

tum channel or to construct a PCE channel. For instance, take the PCE map represented in Fig. 3.3(c). The set indices W are not closed under sum modulo 2, as $(01, 00) + (10, 01) = (11, 01)$ but $\tau_{11,01} = 0$. Another six examples are shown in Fig. 3.5. On the other hand, to construct the PCE channel in Fig. 3.3 or, more generally, a PCE channel preserving $4 = 2^2$ Pauli components we need only to determine two linearly independent vectors $(\vec{m}, \vec{n})$ and $(\vec{m}', \vec{n}')$; for instance, $(01, 01)$ and $(10, 10)$.

3.3. Some properties of PCE channels

From the correspondence between PCE channels and vector subspaces, some properties are derived. These follow from well-known properties of finite vector spaces, for which we refer to Ref. [57].

Property 1 (Power of two)**.** *The number of Pauli components preserved by a PCE channel is a power of two.*

Proof. Given a vector space of dimension K over the finite field of p elements, with p a prime number, the number of elements of the vector space is p^K. PCE channels correspond to a vector subspace of dimension K over the field $\{0, 1\}$. Thus, a the corresponding subspace to a PCE channel $\vec{\tau}$ has 2^K elements. $\qquad\square$

Property 2. *The number $\mathcal{S}_{N,K}$ of PCE channels of N qubits preserving 2^K Pauli components is:*

$$\mathcal{S}_{N,K} = \prod_{j=0}^{K-1} \frac{2^{2N-j} - 1}{2^{K-j} - 1}. \tag{3.11}$$

Proof. The number $\mathcal{S}_{N,K}$ is equal to the number of different subspaces W with dimension K, and can be calculated as the ratio $\mathcal{N}_{N,K}/\mathcal{M}_K$, which is the number of subsets with K linearly independent vectors out of a set containing $2^{2N} - 1$ vectors,

divided by the number of different bases that a given subspace of dimension K can have.

To evaluate $\mathcal{N}_{N,K}$ we proceed in K steps:

1. We choose one of the $2^{2N} - 1$ non-zero vectors.

2. We choose a second vector out of the complement of the initial $2^{2N} - 1$ non-zero vectors and the subset spanned by the first selected vector, which has $2^{2N} - 2$ elements.

   $\vdots$

$j + 1$. We choose a $j + 1$-th vector from the complement of the initial $2^{2N} - 1$ non-zero vectors and the subset spanned by the first j vectors, which has $2^{2N} - 2^j$ elements.

   $\vdots$

K. We choose a K-th vector from the complement of the initial $2^{2N} - 1$ non-zero vectors and the subset spanned by the first $K - 1$ vectors, which has $2^{2N} - 2^{K-1}$ elements.

From this, it is clear that $\mathcal{N}_{N,K}$ evaluates to:

$$\mathcal{N}_{N,K} = \prod_{j=0}^{K-1} \left(2^{2N} - 2^j \right) \tag{3.12}$$

On the other hand, we use that the number of different bases for a subspace W of dimension K is equal to the number of different linear transformations from W to itself [57]. Therefore, we consider that all of these linear transformations are all $K \times K$ non-singular matrices over the field $\{0, 1\}$. These can be constructed as:

1. We choose one of the $2^K - 1$ non-zero vectors of subspace W with dimension K.

2. We choose a second vector out of the complement of the initial $2^K - 1$ non-zero vectors of subspace W with dimension K and the subset spanned by the first selected vector, which has $2^K - 2$ elements.

⋮

$j + 1$. We choose a $j+1$-th vector from the complement of the initial $2^K - 1$ non-zero vectors of subspace W with dimension K and the subset spanned by the first j vectors, which has $2^K - 2^j$ elements.

⋮

K. We choose a K-th vector from the complement of the initial $2^K - 1$ non-zero vectors of subspace W with dimension K and the subset spanned by the first $K - 1$ vectors, which has $2^K - 2^{K-1}$ elements.

It is then clear that:

$$\mathcal{M}_K = \prod_{j=0}^{K-1} \left(2^K - 2^j \right). \tag{3.13}$$

From this, we see that the ratio $\mathcal{N}_{N,K}/\mathcal{M}_K$ is equal to eq. (3.11). □

Property 3. *There are the same number of PCE channels of N qubits preserving 2^K and 2^{2N-K} Pauli components.*

Proof. This can be proved using eq. (3.11) and showing that $\mathcal{S}_{N,2N-K} = \mathcal{S}_{N,K}$, as in the following:

$$\mathcal{S}_{N,2N-K} = \prod_{j=0}^{2N-K-1} \frac{2^{2N-j} - 1}{2^{2N-K-j} - 1} \tag{3.14}$$

$$= \frac{(2^{2N} - 1)(2^{2N-1} - 1) \cdots (2^{2N-K} - 1) \cdots (2^{K+1} - 1)}{(2^{2N-K} - 1)(2^{2N-K-1} - 1) \cdots (2^{K+1} - 1) \cdots (2 - 1)} \tag{3.15}$$

$$= \frac{\prod_{x=2N-K+1}^{2N} 2^x - 1}{\prod_{y=1}^{K} 2^y - 1}. \tag{3.16}$$

Then, using the change of indices $x \to 2N - j$ and $y \to K - j$, and taking into account that swapping the limits of the product leaves the product invariant :

$$= \prod_{j=0}^{K-1} \frac{2^{2N-j} - 1}{2^{K-j} - 1} \tag{3.17}$$

$$= \mathcal{S}_{N,K}. \tag{3.18}$$

$\square$

This symmetry indicates a type of duality between individual PCE channels preserving 2^K and 2^{2N-K} Pauli components. However, for the time being we have been unable to find it, as well as we have failed to recognize if it is of physical importance.

Property 4. *The computational complexity of specifying all PCE channels for a system of N qubits, denoted as $\mathcal{O}(N)$, scales linear in the number of qubits.*

Proof. The specification of a PCE channel $\vec{\tau}$ is equivalent to specifying the basis elements of the corresponding W, which grows linearly in the number of qubits. $\square$

A straightforward, albeit naive, approach to specifying PCE channels is to enumerate all possible PCE maps $\vec{\tau}$ and then verify complete positivity with eq. (2.19). In fact, this was the initial method we employed at the beginning of this study. However, the total number of maps, which is 2^{2N-1}, becomes exponential in the number of qubits, making it computationally inefficient.

3.4. Kraus representation of a PCE

We can further investigate the eigenvalues of the Choi-Jamiołkowski matrix of a PCE quantum channel to derive its canonical Kraus representation.

We can re-express the eigenvalues of the Choi-Jamiołkowski matrix of a PCE channel in eq. (2.17) as:

$$\lambda_{\vec{r},\vec{s}} = \frac{1}{2^N} \sum_{(\vec{m},\vec{n}) \in W} (-1)^{\phi_{\vec{r},\vec{s}}(\vec{m},\vec{n})},$$

(3.19)

where we are summing only over the non-zero components $\tau_{\vec{m},\vec{n}}$. Adittionally, we have denoted

$$\phi_{\vec{r},\vec{s}}(\vec{m},\vec{n}) = \vec{m} \cdot \vec{s} + \vec{n} \cdot \vec{r}$$

(3.20)

as we have recognized $\phi_{\vec{r},\vec{s}}$ as a linear map from the vector space of all indices $\{(\vec{m},\vec{n})\}$ to the vector space $\mathbb{Z}_2 = \{0,1\}$. This is useful, given that a linear map preserves the vector structure. In other words, the subspace W of indices is mapped either to the trivial space or $\mathbb{Z}_2$. Thus, it follows that the sum reduces either to a sum of ones or a sum of the same number of 1s and -1s:

$$\lambda_{\vec{r},\vec{s}} = \begin{cases} |W|/2^N, & \phi_{\vec{r},\vec{s}}(\vec{m},\vec{n}) = 0 \quad \forall\, (\vec{m},\vec{n}) \in W, \\ 0, & \text{otherwise}, \end{cases}$$

(3.21)

where $|W|$ denotes the cardinality of the subspace W, which is the number of components $\tau_{\vec{m},\vec{n}}$ equal to one. Let us define the vector subspace $W^\perp = \{(\vec{r},\vec{s}) : \phi_{\vec{r},\vec{s}}(\vec{m},\vec{n}) = 0,\, \forall\, (\vec{m},\vec{n}) \in W\}$. The non-zero $\lambda_{\vec{r},\vec{s}}$ are then those eigenvalues with indices $(\vec{r},\vec{s}) \in W^\perp$. Once we have obtained the non-zero eigenvalues, the Kraus representation follows from the diagonalization of the Choi-Jamiołkowski matrix:

$$\mathcal{E}(\rho) = \sum_{(\vec{r},\vec{s}) \in W^\perp} \lambda_{\vec{r},\vec{s}}\, \sigma_{\vec{r},\vec{s}} \rho \sigma_{\vec{r},\vec{s}}.$$

(3.22)

3.5. PCE Generators

The set of PCE channels is itself a semigroup under the composition operation. That is, the composition of two PCE channels $\vec{\tau}$ and $\vec{\tau}'$ is another PCE channel $\vec{\tau} \circ \vec{\tau}'$, where $\circ$ denotes component-wise or Haddmard product. From this, the question about PCE channels impossible to be obtained from the composition of

any other two PCE channels is natural. Once again, the vector structure provides a way to answer this.

By standard theorems of linear algebra, any proper subspace W can be extended to a maximal non-trivial subspace of dimension $2N - 1$. Then, the intersections of these maximal subspaces reduce to any other subspace W. In other words, those maximal subspaces corresponding to PCE channels generate, under composition, the rest of PCEs. We shall now focus on how to determine this set of PCE generators, which we call from now on PCEGs and denote $\mathcal{G}_{\vec{m},\vec{n}}$.

One way to specify the set of PCE generators is to determine all different bases of subspaces with dimension $2N - 1$. However, there is a connection between PCEGs and linear transformation between the components of the Wey channel $\vec{\tau}$ and the eigenvalues $\vec{\lambda}$ of its Choi-Jamiołkowski matrix.

The indices $(\vec{m}, \vec{n})$ of all matrix elements equal to one in rows or columns of $(F_2 \otimes F_2^*)^{\otimes N}$ can be identified as maximal vector subspaces of W as well as PCE generators. We see that $(-1)^{\vec{m} \cdot \vec{s} + \vec{n} \cdot \vec{r}}$ is the matrix element of $(F_2 \otimes F_2^*)^{\otimes N}$ in row $(\vec{m}, \vec{n})$ and column $(\vec{s}, \vec{r})$. Therefore, we require a similar condition to the one expressed in eq. (3.6) to identify those matrix elements given row $(\vec{m}, \vec{n})$ or column $(\vec{r}, \vec{s})$ that are equal to one:

$$\vec{m} \cdot \vec{s} + \vec{n} \cdot \vec{r} = 0. \tag{3.23}$$

From this, considering another matrix element equal to one satisfies a similar condition for a primed version $(\vec{m}', \vec{n}')$. Then multiplying both matrix elements, similar to the proof of the vector space of PCE channels, we arrive at the same closure relation. Similar to an observation we made before in section 3.4, eq. (3.23) can be seen as linear map of either the indices $(\vec{m}, \vec{n})$ or $(\vec{r}, \vec{s})$ from the whole vector space to $\mathbb{Z}_2$. The indices are maped either to zero, in which case all matrix elements are one, or to zero and one, in which case half the matrix elements are one and the others minus one. That is the subspaces correspond to those with cardinality 2^{2N} or 2^{2N-1}.
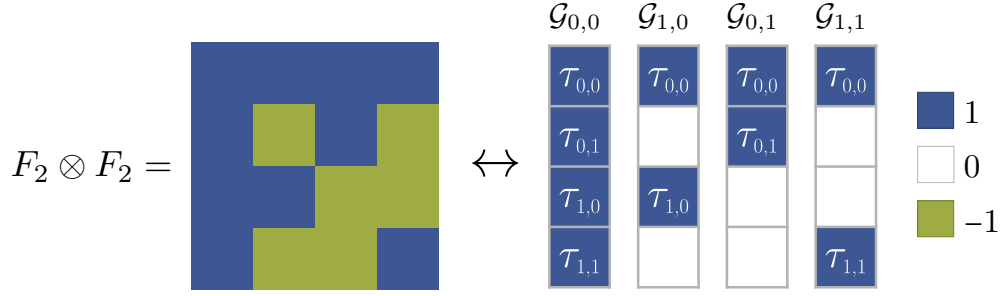
Figure 3.6: Connection between the linear transformation between $\vec{\tau}$ and $\vec{\lambda}$, and the PCEGs $\mathcal{G}_{\vec{m},\vec{n}}$ for a single-qubit system. By taking every row or column and changing the color green for white, that is, reassigning $-1 \mapsto 0$, we obtain the $\vec{\tau}$ of all PCEGs of a single qubit.

In fact, the only indices mapped all to zero are those in the first row or column. Now, it only remains showing that every subspace is different. This may be proved from the fact that the Fourier matrix F_2 has full rank and the rank of a tensor product is the product of the ranks. Thus, the linear transformation between $\vec{\tau}$ and $\vec{\lambda}$ has always full rank. In consequence, if two rows or columns with half the elements 1 and the other half -1 would be characterized by the same maximal subspace W, the matrix would no have full rank. Therefore, all subspaces characterizing the -1 in every row or column are indeed different.

The elegant algebraic structure we have used not only to characterize the PCE channels, but for the 1s in the matrix $(F_2 \otimes F_2^*)^{\otimes N}$ as well, establishes a connection between PCEGs and matrix $(F_2 \otimes F_2^*)^{\otimes N}$. In turn, this provides a way to specify all PCEGs in a very efficient way. By replacing all -1s with zeroes in matrix $(F_2 \otimes F_2^*)^{\otimes N}$, every row or column is the vector $\vec{\tau}$ of a PCE generator $\mathcal{G}_{\vec{m},\vec{n}}$. We show the example of a single-qubit in Fig. 3.6.

What is more, we see that PCE generators are either symmetric or anti-symmetric under reflection of the j-th axis. That is, if we consider the map Σ^k defined as follows:

$$\vec{m} = (m_1, \ldots, m_j, \ldots, m_N) \rightarrow \Sigma^j(\vec{m}) = (m_1, \ldots, 1 - m_j, \ldots, m_N) \tag{3.24}$$

$$\vec{n} = (n_1, \ldots, n_j, \ldots, n_N) \rightarrow \Sigma^j(\vec{n}) = (n_1, \ldots, 1 - n_j, \ldots, n_N), \tag{3.25}$$
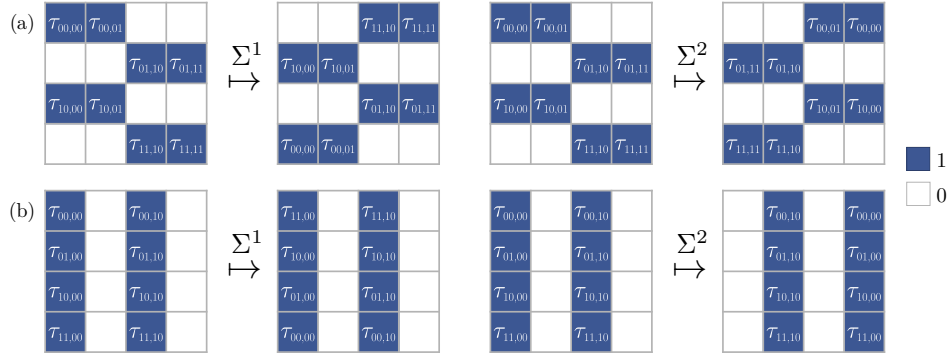
Figure 3.7: Two example of reflections over the first and second particle of two-qubit PCEGs: (a) $\mathcal{G}_{10,01}$, and (b) $\mathcal{G}_{01,00}$. Here, we reordered the indices of $\tau_{\vec{m},\vec{n}}$ as $(m_1 n_1, m_2 n_2)$ for the purpose of being able to see the symmetry or anti-symmetry under vertical and horizontal reflection of the grids, correspondingly. We see that $\mathcal{G}_{10,01}$ is anti-symmetric under reflections over both particles, and $\mathcal{G}_{01,00}$ is symmetric under reflection over the first particle and anti-symmetric over the second one.

we can conclude from the properties of Σ^k and the dimension of the maximal subspaces $2N-1$, that $\vec{\tau}$ of a PCE generator is either symmetric or anti-symmetric under the action of Σ^k over the indices. We illustrate an example in Fig. 3.7. In Ref. [56] we use this symmetry to connect the PCEGs $\mathcal{G}_{\vec{m},\vec{n}}$ with matrix $(F_2 \otimes F_2^*)^{\otimes N}$. We have presented another way to do that in this work, but for the time being, we have been unable to find another connection of this symmetry with physical properties of PCEGs. However, symmetries in physics have been always important to characterize.

PCE channels and decoherence

In this chapter, we study two implementations of PCE channels. To do so, we begin by deriving the Kraus representation for PCE generators, as any other PCE can be obtained through the composition of these.

4.1. Kraus operators of PCE generators

We can further examine the Kraus representation we derived in eq. (3.22) in Sec. 3.4, specifically focusing on PCE generators. Here, we investigate the vector subspaces $W^{\perp}$ associated with each maximal non-trivial subspace W.

It is important to recall that vector subspaces $W^{\perp}$ are associated with homomorphisms $\phi_{\vec{r},\vec{s}}$ that map a subspace W to the trivial vector space. We proceed by identifying that homomorphisms $\phi_{\vec{r},\vec{s}}$ determine whether the matrix element of $(F_2 \otimes F_2^*)^{\otimes N}$ in column $(\vec{s}, \vec{r})$ and row $(\vec{m}, \vec{n})$ is -1 or 1. As discussed in Sec. 3.5, the positions of ones in the matrix correspond to the maximal non-trivial subspaces W^*. Now, we consider two homomorphisms, $\phi_{\vec{r},\vec{s}}(\vec{m}, \vec{n})$ and $\phi_{\vec{r}',\vec{s}'}(\vec{m}, \vec{n})$, such that $(\vec{r}, \vec{s}) \neq (\vec{r}', \vec{s}') \neq (\vec{0}, \vec{0})$. Both homomorphisms map the same maximal subspace W^* to the trivial vector space if and only if the columns $(\vec{s}, \vec{r})$ and $(\vec{s}', \vec{r}')$ of matrix $(F_2 \otimes F_2^*)^{\otimes N}$ are the same, which is not true. Therefore, by contradiction, only the homomorphisms $\phi_{\vec{0},\vec{0}}$ and $\phi_{\vec{r},\vec{s}}$ map all elements of one maximal non-trivial subspace

to the trivial vector space $\{(\vec{0},\vec{0})\}$. With eqs. (3.21) and (3.22) we can express the Kraus representation of a PCEG $\mathcal{G}_{\vec{m},\vec{n}}$ as:

$$\mathcal{G}_{\vec{m},\vec{n}}(\rho) = \frac{1}{2}\left(\rho + \sigma_{\vec{m},\vec{n}}\rho\sigma_{\vec{m},\vec{n}}\right). \tag{4.1}$$

4.2. Pure dissipative implementation

We can demonstrate that a PCEG can be seen as a fixed point of pure dissipative processes. Consequently, every PCE channel can be regarded as the fixed point of another pure dissipative process.

Examining eq. (4.1), we can identify that a PCEG is the asymptotic limit of the following dynamical process:

$$\mathcal{G}_{\vec{m},\vec{n},t}(\rho) = \left(\frac{1+e^{-\gamma t}}{2}\right)\rho + \left(\frac{1-e^{-\gamma t}}{2}\right)\sigma_{\vec{m},\vec{n}}\rho\sigma_{\vec{m},\vec{n}} \quad \gamma > 0. \tag{4.2}$$

Now, we shall prove that this family of quantum channels with the parameter t is indeed constitutes a dynamical process, satisfying the semi-group property $\mathcal{G}_{\vec{m},\vec{n},t_2} \circ \mathcal{G}_{\vec{m},\vec{n},t_2} = \mathcal{G}_{\vec{m},\vec{n},t_1+t_2}$:

$$\mathcal{G}_{\vec{m},\vec{n},t_2}\Big(\mathcal{G}_{\vec{m},\vec{n},t_1}(\rho)\Big) = \mathcal{G}_{\vec{m},\vec{n},t_2}\left(\left(\frac{1+e^{-\gamma t_1}}{2}\right)\rho + \left(\frac{1-e^{-\gamma t_1}}{2}\right)\sigma_{\vec{m},\vec{n}}\rho\sigma_{\vec{m},\vec{n}}\right) \tag{4.3}$$

$$= \left(\frac{1+e^{-\gamma t_1}}{2}\right)\left[\left(\frac{1+e^{-\gamma t_2}}{2}\right)\rho + \left(\frac{1-e^{-\gamma t_2}}{2}\right)\sigma_{\vec{m},\vec{n}}\rho\sigma_{\vec{m},\vec{n}}\right)\right]$$

$$+ \left(\frac{1-e^{-\gamma t_1}}{2}\right)\left[\left(\frac{1+e^{-\gamma t_2}}{2}\right)\sigma_{\vec{m},\vec{n}}\rho\sigma_{\vec{m},\vec{n}} + \left(\frac{1-e^{-\gamma t_2}}{2}\right)\rho\right]$$

$$\tag{4.4}$$

$$= \left(\frac{1+e^{-\gamma(t_1+t_2)}}{2}\right)\rho + \left(\frac{1-e^{-\gamma(t_1+t_2)}}{2}\right)\sigma_{\vec{m},\vec{n}}\rho\sigma_{\vec{m},\vec{n}} \tag{4.5}$$

$$= \mathcal{G}_{\vec{m},\vec{n},t_1+t_2}(\rho). \tag{4.6}$$
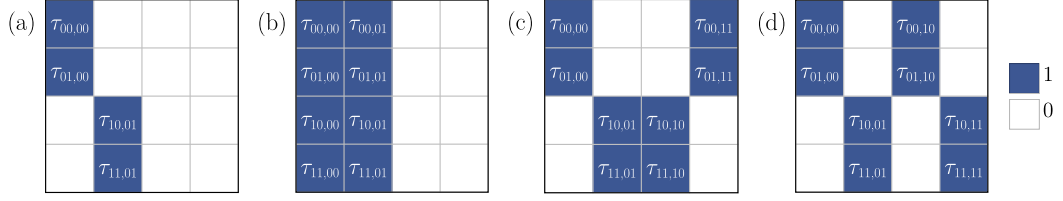
Figure 4.1: One PCE channel is the fixed point of more than one Markovian dissipative process. The two-qubit PCE channel in (a) is the fixed point of a Markovian process with the Lindblad generators of any two PCEGs in (b)-(d).

The Lindblad generator can be obtained by the standard procedure:

$$\mathcal{L}_{\vec{m},\vec{n}}[\rho] = \left.\frac{d\mathcal{G}_{\vec{m},\vec{n},t}(\rho)}{dt}\right|_{t=0} = \frac{\gamma}{2}\left(\sigma_{\vec{m},\vec{n}}\rho\sigma_{\vec{m},\vec{n}} - \rho\right), \qquad (4.7)$$

where the unique Lindblad operator corresponding to the relaxation ratio $\gamma/2$ is $\sigma_{\vec{m},\vec{n}}$. Thus, the process is purely dissipative [58].

Since PCEGs commute, every PCE channel can also be regarded as the asymptotic limite of a decoherence process. Let us consider the example of the PCE channel depicted in Fig. 4.1(a). First, we see that this channel can be obtained as the composition of $\mathcal{G}_{01,10}$ and $\mathcal{G}_{01,11}$. Thus, it is the fixed point of the dissipation process described by:

$$\mathcal{L}(\rho) = \frac{\gamma_{01,10}}{2}(\sigma_{01,10}\rho\sigma_{01,10} - \rho) + \frac{\gamma_{01,11}}{2}(\sigma_{01,11}\rho\sigma_{01,11} - \rho). \qquad (4.8)$$

This process has the Lindbladian operators $\sigma_{01,10} = \sigma_x \otimes \sigma_z$ and $\sigma_{01,11} = i\sigma_x \otimes \sigma_y$, each with relaxation ratios $\gamma_{01,10}$ and $\gamma_{01,11}$, respectively. Nonetheless, such election of Lindblad operators is not unique, as the PCE channel is also equal to the composition of $\mathcal{G}_{00,01}$ with any of the aforementioned PCEGs. Thus, the corresponding dissipative process can be such with one of the aforementioned Lindbladian operators and $\sigma_{00,01} = \mathbb{1} \otimes \sigma_x$.

Figure 4.2: Illustration of a collision model in (a) vs a conventional system-bath model in (b). Taken from [59].

4.3. Collision model implementation

Another way to implement PCE channels is through collision models. A collision model is a tool used to describe the interaction between the system and its environment. In this model, the environment is composed of a large, discrete collection of smaller units, and the open system interacts with these units one at a time. In contrast, in a conventional system-bath model, the bath typically consists of a continuum of normal modes, and the system interacts with all of them simultaneously. We illustrate this in Fig. 4.2.

The collision model for implementing a PCEG $\mathcal{G}_{\vec{m},\vec{n}}$ is constructed as follows. Since $\mathcal{G}_{\vec{m},\vec{n}}$ have two Kraus operators, we can choose a single qubit in the environment. The system interacts with the ancilla qubit through a unitary transformation defined as:

$$U_{\vec{m},\vec{n}} \ket{\psi} \ket{0} = \frac{1}{\sqrt{2}} \big(\ket{\psi} \ket{0} + \sigma_{\vec{m},\vec{n}} \ket{\psi} \ket{0} \big), \tag{4.9}$$

$$U_{\vec{m},\vec{n}} \ket{\psi} \ket{1} = \frac{1}{\sqrt{2}} \big(\ket{\psi} \ket{0} - \sigma_{\vec{m},\vec{n}} \ket{\psi} \ket{0} \big). \tag{4.10}$$

It is straightforward to show that if the system of qubits interacts with an ancilla qubit in the state $\ket{0}$ the reduced dynamics is that of a PCEG, that is:

$$\mathcal{G}_{\vec{m},\vec{n}}(\rho) = \mathrm{Tr}_E \left[U_{\vec{m},\vec{n}} (\rho \otimes \ket{0}\!\bra{0}), U_{\vec{m},\vec{n}}^\dagger \right], \tag{4.11}$$

where Tr_E denotes the partial trace over the environment.

Every PCE channel can be then implemented with a collision model as well. Given that a PCE channel is the composition of M PCEGs as $\mathcal{E} = \mathcal{G}_{\vec{m}_M, \vec{n}_M} \circ \cdots \circ \mathcal{G}_{\vec{m}_1, \vec{n}_1}$, there are two approaches for implementation:

1. The channel $\mathcal{E}$ can be implemented as a single collision with M ancilla qubits in the product state $|0\rangle^{\otimes M}$.

2. Alternatively, it can be realized through M collisions with a single qubit reset to state $|0\rangle$ after each collision.

Weyl channels for multipartite systems

In the preceding chapters, we established the significance of PCE channels in describing qubit decoherence processes, emphasizing their elegant vector structure. This chapter aims to explore the potential for extending this algebraic framework to quantum channels of more general systems. Specifically, we seek to investigate the generalization of these concepts for quantum channels in systems involving multiple particles with arbitrary dimensions, a class of channels that has received limited attention thus far.

In this chapter, we introduce a generalization of Pauli maps for arbitrary-dimensional multi-particle systems, employing Weyl matrices. These matrices are a unitary generalization of Pauli matrices that have a number of useful properties. Notably, these properties enable us to diagonalize the Choi-Jamiołkowski matrix of a Weyl quantum map, thereby enabling the study of the subset of physically meaningful quantum maps: Weyl channels.

The chapter is organized as follows. We begin by discussing in Sec. 5.1 the reasons of why we choose Weyl matrices to study quantum maps of many particles. Subsequently, in Sec. 5.2, we define a Weyl map and diagonalize its Choi-Jamiołkowski matrix to establish the conditions of complete positivity for the map to represent

a quantum channel. From these conditions, we investigate in Sec. 5.3 the extreme points within the convex set of quantum channels and, in Sec. 5.4, uncover the embedded group structure within all channels.

The group structure offers an answer to the initial question that initiated the study of Weyl maps, a motivation drawn from our results of PCE channels. However, our most significant discovery lies in the universality of these structure. They are not exclusive to the "component erasing" type of channels but are a property of all Weyl channels.

5.1. Why the basis of Weyl matrices?

We shall begin by discussing, from a mathematical point of view, what characteristics we desire the basis of $\mathcal{B}(\mathcal{H}_d \otimes \mathcal{H}_d)$ to have. It is worth noting that all the properties of PCE channels are derived from the underlying vector structure. This vector structure, in turn, originates from the complete positivity conditions. These conditions are a direct outcome of the diagonalization of the Choi-Jamiołkowski matrix of a Pauli map. Fundamentally, the derivation of all results about PCE channels rely on performing the diagonalization the Choi-Jamiołkowski matrix.

We desire a basis of $\mathcal{B}(\mathcal{H}_d \otimes \mathcal{H}_d)$ having analogous properties to those of the N-qubit operators $\sigma_{\vec{m},\vec{n}}$ that allowed us to diagonalize the Choi-Jamiołkowski matrix in Sec. 2.3. Those properties are:

1. All operators in $\{\sigma_{\vec{m},\vec{n}} \otimes \sigma^*_{\vec{m},\vec{n}}\}$ mutually commute. From this follows the linear relationship between eigenvalues of the map and those of its corresponding Choi-Jamiołkowski matrix.

2. All operators in $\{\sigma_{\vec{m},\vec{n}} \otimes \sigma^*_{\vec{m},\vec{n}}\}$ commute with all operators in $\{|\sigma_{\vec{r},\vec{s}}\rangle\!\rangle\langle\!\langle\sigma_{\vec{r},\vec{s}}|\}$. In consequence, $|\sigma_{\vec{r},\vec{s}}\rangle\!\rangle$ are the eigenvectors of $\mathcal{D}$ and the derivation of its eigenvalues is straightforward.

The second property might have appeared fortuitous in Sec. 2.3, In fact, that was the case when we first realized it. Nevertheless, we later uncovered a deeper understanding, which we have saved until this moment.

Both sets of operators $\{|\sigma_{\vec{r},\vec{s}}\rangle\!\rangle\langle\!\langle\sigma_{\vec{r},\vec{s}}|\}$ and $\{\sigma_{\vec{m},\vec{n}} \otimes \sigma^*_{\vec{m},\vec{n}}\}$ actually span the same space. From the properties of Pauli matrices, it follows that $\{\sigma_{\vec{m},\vec{n}} \otimes \sigma^*_{\vec{m},\vec{n}}\}$ forms a basis of $\mathcal{B}\big((\mathbb{C}^2)^{\otimes N} \otimes (\mathbb{C}^2)^{\otimes N}\big)$. Then, the linear transformation between both sets, specified by:

$$\mathrm{Tr}\left[\left(\sigma_{\vec{m},\vec{n}} \otimes \sigma^*_{\vec{m}',\vec{n}'}\right)^\dagger |\sigma_{\vec{r},\vec{s}}\rangle\!\rangle\langle\!\langle\sigma_{\vec{r},\vec{s}}|\right] = 2^N(-1)^{\vec{m}\cdot\vec{s}+\vec{n}\cdot\vec{r}}\delta_{\vec{m},\vec{m}'}\delta_{\vec{n},\vec{n}'}, \tag{5.1}$$

implies that operators $|\sigma_{\vec{r},\vec{s}}\rangle\!\rangle\langle\!\langle\sigma_{\vec{r},\vec{s}}|$ are expanded only over elements of the form $\sigma_{\vec{m},\vec{n}} \otimes \sigma^*_{\vec{m},\vec{n}}$.

Proof. To prove this, we begin by computing the following product:

$$\left(\sigma_{\vec{m},\vec{n}} \otimes \sigma_{\vec{m}',\vec{n}'}\right)^\dagger |\sigma_{\vec{r},\vec{s}}\rangle\!\rangle\langle\!\langle\sigma_{\vec{r},\vec{s}}| = \sum_{\vec{k},\vec{l},\vec{\mu},\vec{\nu}} (-1)^{\vec{m}\cdot(\vec{k}+\vec{n})+\vec{m}'\cdot(\vec{l}+\vec{n}')+\vec{r}\cdot(\vec{\mu}+\vec{\nu})} \left|\vec{k},\vec{l}\right\rangle\!\Big\langle \vec{k}+\vec{n},\vec{l}+\vec{n}'\Big| \times$$

$$|\vec{\mu},\vec{\mu}+\vec{s}\rangle\langle\vec{\nu},\vec{\nu}+\vec{s}|$$

$$= \sum_{\vec{k},\vec{\nu}} (-1)^{\vec{m}\cdot(\vec{k}+\vec{n})+\vec{m}'\cdot(\vec{k}+\vec{s}+\vec{n})+\vec{r}\cdot(\vec{k}+\vec{n}+\vec{\nu})} \times$$

$$\left|\vec{k},\vec{k}+\vec{s}+\vec{n}-\vec{n}'\right\rangle\!\Big\langle\vec{\nu},\vec{\nu}+\vec{s}\Big|$$

$$\tag{5.2}$$

Then, computing the trace, we obtain:

$$\mathrm{Tr}\left[\left(\sigma_{\vec{m},\vec{n}} \otimes \sigma_{\vec{m}',\vec{n}'}\right)^\dagger |\sigma_{\vec{r},\vec{s}}\rangle\!\rangle\langle\!\langle\sigma_{\vec{r},\vec{s}}|\right] = \sum_{\vec{k},\vec{\nu}} (-1)^{\vec{m}\cdot(\vec{k}+\vec{n})+\vec{m}'\cdot(\vec{k}+\vec{n}+\vec{s})+\vec{r}\cdot(\vec{k}+\vec{n}+\vec{\nu})} \times$$

$$\delta_{\vec{k},\vec{\nu}}\delta_{\vec{k}+\vec{s}+\vec{n}-\vec{n}',\vec{\nu}+\vec{s}}$$

$$= \sum_{\vec{k}} (-1)^{\vec{m}\cdot(\vec{k}+\vec{n})+\vec{m}'\cdot(\vec{k}+\vec{n}+\vec{s})+\vec{r}\cdot\vec{n}}\delta_{\vec{n},\vec{n}'}$$

$$= (-1)^{\vec{m}'\cdot\vec{s}+\vec{r}\cdot\vec{n}}(-1)^{\vec{m}'\cdot\vec{n}+\vec{m}\cdot\vec{n}} \sum_{\vec{k}} (-1)^{\vec{k}\cdot(\vec{m}+\vec{m}')}\delta_{\vec{n},\vec{n}'}$$

$$= 2^N(-1)^{\vec{m}'\cdot\vec{s}+\vec{r}\cdot\vec{n}}(-1)^{\vec{m}'\cdot\vec{n}+\vec{m}\cdot\vec{n}}\delta_{\vec{m},\vec{m}'}\delta_{\vec{n},\vec{n}'}, \quad (5.3)$$

which reduces to eq. (5.1). □

This serves as a way more clear explanation of why the commutation relations between operators $|\sigma_{\vec{r},\vec{s}}\rangle\!\rangle\langle\!\langle\sigma_{\vec{r},\vec{s}}|$ and $\sigma_{\vec{m},\vec{n}} \otimes \sigma^*_{\vec{m},\vec{n}}$ hold.

A basis of matrices for $\mathcal{B}(\mathcal{H}_d \otimes \mathcal{H}_d)$ satisfying the aforementioned relations are the Weyl matrices. Weyl matrices were first introduced by Weyl [60] and can be all expressed in the following compact expression [61]:

$$U_{m,n} = \sum_k \omega^{mk} |k\rangle\langle k+n| \quad \omega = e^{2\pi i/d}. \quad (5.4)$$

From now on, all arithmetical operations are taken modulo d. Furthermore, we introduce the multi-particle Weyl matrices as:

$$U_{\vec{m},\vec{n}} = \bigotimes_\alpha U_{m_\alpha,n_\alpha}, \quad (5.5)$$

where $1 \leq \alpha \leq N$ labels the particles in the system. Some well-known properties of these matrices are:

$$\mathrm{Tr}\left(U^\dagger_{m,n}U_{m',n'}\right) = d\delta_{m,m'}\delta_{n,n'} \quad (5.6)$$

$$U_{m,n}U_{m',n'} = \omega^{m'n}U_{m+m',n+n'} \quad (5.7)$$

$$U_{m,n}U_{m',n'} = \omega^{m'n-mn'}U_{m',n'}U_{m,n} \quad (5.8)$$

$$U^\dagger_{m,n} = \omega^{mn}U_{-m,-n}, \quad (5.9)$$

as well as their vector equivalents [61].

We now discuss how the previously discussed conditions for N-qubit Pauli operators also apply to operators $U_{\vec{m},\vec{n}} \otimes U^*_{\vec{m},\vec{n}}$ and $|U_{\vec{r},\vec{s}}\rangle\!\rangle\langle\!\langle U_{\vec{r},\vec{s}}|$. They come as a consequence

of the properties of Weyl matrices. The first condition, which concerns the commutation relations between different $\left(U_{m,n} \otimes U_{m,n}^* \right)$, arises from the symmetry in the following expression:

$$\left(U_{m,n} \otimes U_{m,n}^* \right)\left(U_{m',n'} \otimes U_{m',n'}^* \right) = \left(U_{m,n} U_{m',n'} \right) \otimes \left(U_{-m,n} U_{-m',n'}^* \right) \tag{5.10}$$

$$= U_{m+m',n+n'} \otimes U_{-(m+m'),n+n'}. \tag{5.11}$$

In the first line, we have applied the property from eq. (5.4), and in the second line, we used the property from eq. (5.7). On the other hand, the second condition, concerning the commutation relations between $U_{\vec{m},\vec{n}} \otimes U_{\vec{m},\vec{n}}^*$ and $|U_{\vec{r},\vec{s}}\rangle\!\rangle\langle\!\langle U_{\vec{r},\vec{s}}|$ is a result from the linear relationship between them, established in:

$$\text{Tr}\left[\left(U_{\vec{m},\vec{n}} \otimes U_{\vec{m}',\vec{n}'}^* \right)^\dagger |U_{\vec{r},\vec{s}}\rangle\!\rangle\langle\!\langle U_{\vec{r},\vec{s}}| \right] = d^N \omega^{\vec{m}\cdot\vec{s} - \vec{n}\cdot\vec{r}} \delta_{\vec{m},\vec{m}'} \delta_{\vec{n},\vec{n}'}. \tag{5.12}$$

In the next section we use the Weyl matrices to define a Weyl map.

5.2. Weyl chanels

The density matrix of a system of N d-level particles can be expressed in the basis of multi-particle Weyl matrices as:

$$\rho = \frac{1}{d^N} \sum_{\vec{m},\vec{n}} \alpha_{\vec{m},\vec{n}} U_{\vec{m},\vec{n}} \qquad \alpha_{\vec{m},\vec{n}}^* = \omega^{-\vec{m}\cdot\vec{n}} \alpha_{-\vec{m},-\vec{n}}. \tag{5.13}$$

Unlike the basis of Pauli matrices, $\alpha_{\vec{m},\vec{n}}$ is generally a complex coefficient. We define a Weyl map through the transformation of the components of the density matrix (5.13) as:

$$\alpha_{\vec{m},\vec{n}} \mapsto \tau_{\vec{m},\vec{n}} \alpha_{\vec{m},\vec{n}} \qquad \tau_{\vec{0},\vec{0}} = 1 \qquad \tau_{\vec{m},\vec{n}} \in \mathbb{C}. \tag{5.14}$$

See that we have defined a Weyl map as a trace-preserving map already. We will refer to $\vec{\tau}$ as the Weyl map. This vector, comprising the eigenvalues of the superoperator of a Weyl map, uniquely characterizes the map.

We shall find the complete positivity conditions for a Weyl map $\vec{\tau}$ to be a quantum channel. To achieve this, we proceed diagonalizing the Choi-Jamiołkowski matrix and investigate the conditions under which it is positive semidefinite. Let us begin by writing the Choi-Jamiołkowski matrix $\mathcal{D}$ from eq. (2.4) in Sec. 2.2.1:

$$\mathcal{D} = \frac{1}{d^N} \sum_{\vec{m},\vec{n}} \tau_{\vec{m},\vec{n}} U_{\vec{m},\vec{n}} \otimes U_{\vec{m},\vec{n}}^*. \tag{5.15}$$

We follow the same steps for the diagonalization as presented in Sec. 2.3 to obtain the eigenvalues $\lambda_{\vec{r},\vec{s}}$. From this, the complete positivitity conditions on a Weyl map $\vec{\tau}$ read:

$$\tau_{\vec{m},\vec{n}} = \tau_{-\vec{m},-\vec{n}}^*, \tag{5.16a}$$

$$\lambda_{\vec{r},\vec{s}} = \frac{1}{d^N} \sum_{\vec{m},\vec{n}} \omega^{\vec{m}\cdot\vec{r}-\vec{n}\cdot\vec{s}} \tau_{\vec{m},\vec{n}} \geq 0. \tag{5.16b}$$

The first condition ensures that $\lambda_{\vec{r},\vec{s}}$ are real. Furthermore, the linear relationship between $\vec{\lambda}$ and $\vec{\tau}$ can be expressed, once again, in terms of Fourier matrices, similar to Pauli maps, as:

$$\vec{\tau} = \left(\bigotimes_\alpha F_{d_\alpha} \otimes F_{d_\alpha}^* \right) \vec{\lambda}. \tag{5.17}$$

We shall add that the trace-preserving condition in the Choi-Jamiołkowski matrix representation reads:

$$\sum_{\vec{r},\vec{s}} \lambda_{\vec{r},\vec{s}} = d^N. \tag{5.18}$$

This condition follows directly computing the trace of (5.15) and recalling that all Weyl matrices $U_{\vec{m},\vec{n}}$ are traceless except for the identity $U_{\vec{0},\vec{0}}$.

As a consequence of the structure of multi-particle Weyl matrices $U_{\vec{m},\vec{n}}$, interesting and beautiful different patterns arise in matrix $\bigotimes_\alpha F_{d_\alpha} \otimes F_{d_\alpha}^*$, the argument of which
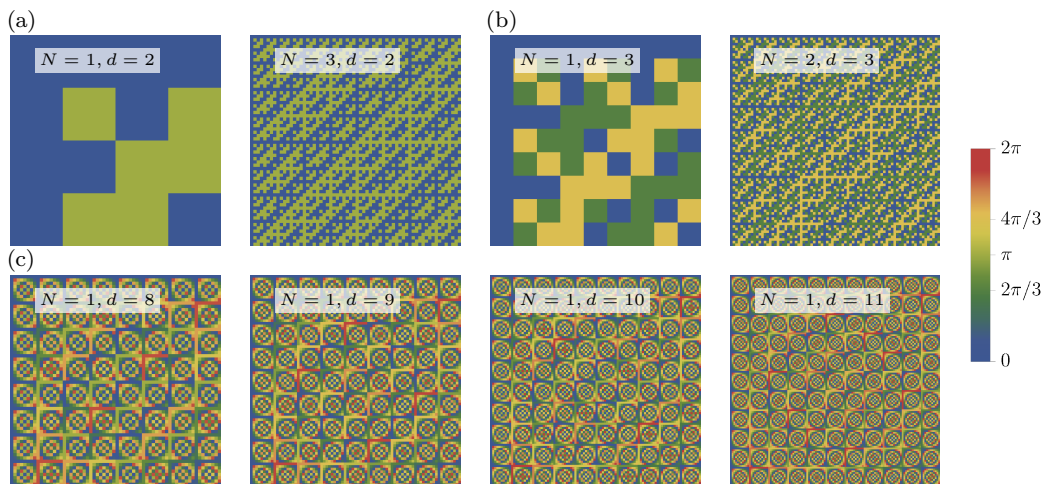
Figure 5.1: Plots of the argument of matrix $\bigotimes_\alpha F_{d_\alpha} \otimes F_{d_\alpha}^*$ for systems of (a) qubits, (b) qutrits and (c) higher single d-level systems. Taken from [62].

we illustrate in Fig. 5.1. We present plots for qubits, qutrits and higher single-d level particles. Even though a system of 3 qubits and a single 8-level system are similar, in the sense that their Hilbert spaces are isomorphic, the corresponding plots in Fig. 5.1(a) and Fig. 5.1(c) remind us that their corresponding bases are different.

5.3. Convex structure of Weyl channels

From the eigenvalues in eq. (5.16b) of the Choi-Jamiołkowski matrix we can unveil the convex structure of Weyl channels and identify its extreme points. Given that all eigenvalues $\lambda_{\vec{r},\vec{s}}$ are non-negative and sum up to d^N, they form the standard d^{2N-1} dimensional simplex. Furthermore, since the transformation between $\lambda_{\vec{r},\vec{s}}$ and $\tau_{\vec{m},\vec{n}}$ is linear and invertible, the set of all $\tau_{\vec{m},\vec{n}}$ forms also a d^{2N-1} dimensional simplex.

From the diagonalization of the Choi-Jamiołkowski of a Weyl map, we see that the Kraus representation of generic Weyl channels is:

$$\mathcal{E}(\rho) = \sum_{\vec{m},\vec{n}} U_{\vec{m},\vec{n}} \rho U_{\vec{m},\vec{n}}^\dagger. \tag{5.19}$$

Therefore, the extreme points of the λ's simplex are clearly

$$\lambda_{\vec{r},\vec{s}} = d^N \delta_{\vec{r},\vec{r}_0} \delta_{\vec{s},\vec{s}_0}, \tag{5.20}$$

where $(\vec{r}_0, \vec{s}_0)$ is fixed and labels the extreme point. Then, the extreme points of the τ's simplex are obtained by inverting eq. (5.16a) and inserting eq. (5.20):

$$\tau_{\vec{m},\vec{n}} = \frac{1}{d^N} \sum_{\vec{r},\vec{s}} \left(d^N \delta_{\vec{r},\vec{r}_0} \delta_{\vec{s},\vec{s}_0} \right) \omega^{-\vec{m}\cdot\vec{r}+\vec{n}\cdot\vec{s}} \tag{5.21}$$

$$= \omega^{-\vec{m}\cdot\vec{r}_0+\vec{n}\cdot\vec{s}_0}. \tag{5.22}$$

Such Weyl channels $\vec{\tau}$ can be called extreme Weyl channels.

An important fact about extreme Weyl channels $\vec{\tau}$ can be concluded from eq. (5.22). A Weyl channel $\vec{\tau}$ is extreme if and only if $|\tau_{\vec{m},\vec{n}}| = 1$. We have already proved that an extreme Weyl channel has roots of unity for the components of its corresponding vector $\vec{\tau}$, see eq. (5.22). The converse holds as the linear transformation between $\tau_{\vec{m},\vec{n}}$ and $\lambda_{\vec{r},\vec{s}}$ is invertible. That is, if we can go from eq. (5.20) to eq. (5.22), we can go back as well.

All Weyl channels can be identified as random unitary channels. For these channels, all Kraus operators are unitary [63]. Random unitary channels are important because their Kraus operators may be experimentally realized through quantum gates. Recall that the vectorized Weyl matrices $|U_{\vec{m},\vec{n}}\rangle\!\rangle$ diagonalize the Choi-Jamiołkowski matrix. Thus, from eq. (5.20) the Kraus representation of a Weyl channels follows:

$$\mathcal{E}(\rho) = \sum_{\vec{r},\vec{s}} \lambda_{\vec{r},\vec{s}} U_{\vec{r},\vec{s}} \rho U_{\vec{r},\vec{s}}^\dagger. \tag{5.23}$$

5.4. A mathematical structure within Weyl channels

In this section, we show how the vector structure of PCE channels generalizes for Weyl channels. Nevertheless, which is more important, we show that the algebraic

structure is embedded within all Weyl channels $\vec{\tau}$. It is not exclusive to the type of "component erasing" channels, like PCEs.

The subset of indices $(\vec{m}, \vec{n})$ for which its corresponding components in $\vec{\tau}$ of a Weyl channel satisfy $\left|\tau_{\vec{m},\vec{n}}\right| = 1$, form a subgroup of a finite abelian group.

Proof. We will proceed trying to recycle the elements from the proof for vector spaces corresponding to PCE channels in Sec. 3.2. Let us invert eq. (5.16b):

$$\tau_{\vec{m},\vec{n}} = \frac{1}{d^N} \sum_{\vec{r},\vec{s}} \lambda_{\vec{r},\vec{s}} \omega^{-\vec{m}\cdot\vec{r}+\vec{n}\cdot\vec{s}}. \tag{5.24}$$

We see here that $\tau_{\vec{m},\vec{n}}$ is a convex combination of roots of unity. Thus, for $\left|\tau_{\vec{m},\vec{n}}\right| = 1$ we can take, without loss of generality, $\tau_{\vec{m},\vec{n}} = \omega^k$, with k a positive integer. Then:

$$\omega^k = \frac{1}{d^N} \sum_{\vec{r},\vec{s}} \lambda_{\vec{r},\vec{s}} \omega^{-\vec{m}\cdot\vec{r}+\vec{n}\cdot\vec{s}} \tag{5.25}$$

$$1 = \frac{1}{d^N} \sum_{\vec{r},\vec{s}} \lambda_{\vec{r},\vec{s}} \omega^{-\vec{m}\cdot\vec{r}+\vec{n}\cdot\vec{s}-k}. \tag{5.26}$$

Once more, the key here is to note that $-1 \leq \mathrm{Re}(\omega^{-\vec{m}\cdot\vec{r}+\vec{n}\cdot\vec{s}-k}) \leq 1$. Therefore, even if $\sum_{\vec{r},\vec{s}} \lambda_{\vec{r},\vec{s}} \mathrm{Im}(\omega^{-\vec{m}\cdot\vec{r}+\vec{n}\cdot\vec{s}-k}) = 0$, it is impossible that $\sum_{\vec{r},\vec{s}} \lambda_{\vec{r},\vec{s}} \mathrm{Re}(\omega^{-\vec{m}\cdot\vec{r}+\vec{n}\cdot\vec{s}})$ equals d^N unless $\omega^{-\vec{m}\cdot\vec{r}+\vec{n}\cdot\vec{s}-k} = 1$, for all $(\vec{r}, \vec{s})$. Hence, the following condition holds:

$$-\vec{m}\cdot\vec{r} + \vec{n}\cdot\vec{s} = jd + k \qquad j, k \in \mathbb{Z} \qquad \forall\, (\vec{r}, \vec{s}). \tag{5.27}$$

Obviously, without loss of generality, we can choose $j = 0$. A similar equation to eq. (5.27) holds for the primed version of indices. Computing $\tau_{\vec{m}+\vec{m}',\vec{n}+\vec{n}'}$ we obtain:

$$\tau_{\vec{m}+\vec{m}',\vec{n}+\vec{n}'} = \frac{1}{d^N} \sum_{\vec{r},\vec{s}} \omega^{-(\vec{m}+\vec{m}')\cdot\vec{r}+(\vec{n}+\vec{n}')\cdot\vec{s}} \lambda_{\vec{r},\vec{s}} = \omega^{k+k'}, \tag{5.28}$$

where we have used equations (5.27) and its primed version, as well as $\sum_{\vec{r},\vec{s}} \lambda_{\vec{r},\vec{s}} =$

d^N. Finally, we have proved that:

$$\tau_{\vec{m},\vec{n}}\tau_{\vec{m}',\vec{n}'} = \tau_{\vec{m}+\vec{m}',\vec{n}+\vec{n}'}. \tag{5.29}$$

This establishes that the set $\mathcal{H} = \{(\vec{m},\vec{n}) : |\tau_{\vec{m},\vec{n}}| = 1\}$ forms a subgroup of the direct product $\mathcal{G} = \bigoplus_N \mathbb{Z}_d \oplus \mathbb{Z}_d$. $\qquad\square$

In general, a vector structure does not exist, as $\mathbb{Z}_d$ is a field only when d is prime. In any other case, one encounters elements in the group without inverses.

The group structure within Weyl channels described in eq. (5.29) does not specify the actual values those $\tau_{\vec{m},\vec{n}}$ can take. In the case of PCE channels, we did not need to concern ourselves with how to assign values to the $\tau_{\vec{m},\vec{n}}$ of those $(\vec{m},\vec{n})$ in the vector subspace, as the only option is to assign the value 1. However, for Weyl channels, we may identify $\tau_{\vec{m},\vec{n}}$ as a map from the group $\mathcal{H}$ to the roots of unity. These elements form also a group, which is isomorphic to $\mathbb{Z}_d$. Therefore, determining how to assign an appropriate root of unity given a subgroup $\mathcal{H}$ is equivalent to asking for the homomorphisms $\tau : \mathcal{H} \mapsto \mathbb{Z}_d$.

As established in eq. (5.29) we have shown that the indices for which $|\tau_{\vec{m},\vec{n}}| = 1$ form a subgroup. We intentionally have not explored the reverse relationship as it leads to an important result: the group structure can coexist with other $\tau_{\vec{m},\vec{n}}$ with indices not in the group and whose modulus is different from one.

Now, let us break down the expression for the eigenvalues $\lambda_{\vec{r},\vec{s}}$ in eq. (5.16b) into two separate sums, one over the elements within the group $\mathcal{H}$ and the other over the rest:

$$\lambda_{\vec{r},\vec{s}} = \frac{1}{d^N} \sum_{(\vec{m},\vec{n})\in\mathcal{H}} \omega^{\vec{m}\cdot\vec{r}-\vec{n}\cdot\vec{s}}\tau_{\vec{m},\vec{n}} + \frac{1}{d^N} \sum_{(\vec{m},\vec{n})\notin\mathcal{H}} \omega^{\vec{m}\cdot\vec{r}-\vec{n}\cdot\vec{s}}\tau_{\vec{m},\vec{n}} \tag{5.30}$$

$$= \frac{1}{d^N} \sum_{(\vec{m},\vec{n})\in\mathcal{H}} \omega^{\vec{m}\cdot(\vec{r}+\vec{r}_0)-\vec{n}\cdot(\vec{s}+\vec{s}_0)} + \frac{1}{d^N} \sum_{(\vec{m},\vec{n})\notin\mathcal{H}} \omega^{\vec{m}\cdot\vec{r}-\vec{n}\cdot\vec{s}}\tau_{\vec{m},\vec{n}} \tag{5.31}$$

The first term can be evaluated identifying that the function $\phi(\vec{m},\vec{n}) = \vec{m} \cdot (\vec{r} +$

$\vec{r}_0) - \vec{n} \cdot (\vec{s} + \vec{s}_0)$ is an homomorphism $\phi : \mathcal{H} \mapsto \mathbb{Z}_d$. This lead to:

$$
\frac{1}{d^N} \sum_{(\vec{m},\vec{n}) \in \mathcal{H}} \omega^{\vec{m} \cdot (\vec{r}+\vec{r}_0) - \vec{n} \cdot (\vec{s}+\vec{s}_0)} =
\begin{cases}
|\mathcal{H}|/d^N, & \phi_{\vec{r},\vec{s}}(\vec{m}, \vec{n}) = 0 \quad \forall\, (\vec{m}, \vec{n}) \in \mathcal{H}, \\[2ex]
0, & \text{otherwise.}
\end{cases}
\tag{5.32}
$$

The homomorphisms $\phi_{\vec{r},\vec{s}}$ mapping $\mathcal{H}$ to zero form a group as well, which we denote $\mathcal{H}^\perp$. Therefore, the conditions of complete positivity of a Weyl map read:

$$
-|H| \leq \frac{1}{d^N} \sum_{(\vec{m},\vec{n}) \notin \mathcal{H}} \omega^{\vec{m} \cdot \vec{r} - \vec{n} \cdot \vec{s}} \tau_{\vec{m},\vec{n}} \quad (\vec{r}, \vec{s}) \in \mathcal{H}^\perp
\tag{5.33a}
$$

$$
0 \leq \frac{1}{d^N} \sum_{(\vec{m},\vec{n}) \notin \mathcal{H}} \omega^{\vec{m} \cdot \vec{r} - \vec{n} \cdot \vec{s}} \tau_{\vec{m},\vec{n}} \quad (\vec{r}, \vec{s}) \notin \mathcal{H}^\perp.
\tag{5.33b}
$$

This inequality is significant since the right-hand sides are real numbers due to the property $\tau_{\vec{m},\vec{n}}^* = \tau_{-\vec{m},-\vec{n}}$, which still holds because all elements in $\mathcal{H}$ have an inverse $-(\vec{m}, \vec{n})$; consequently, those not in $\mathcal{H}$ have inverses as well. This shows that the group structure is inherent in all Weyl channels. In other words, a Weyl channel have a subset of $\tau_{\vec{m},\vec{n}}$ with indices forming a subgroup, while the rest are constrained by inequalities (5.33).

All Weyl channels may be algorithmically constructed in the following steps:

1. Find all subgroups $\mathcal{H} \subseteq \mathcal{G}$.

2. Find all homomorphisms $\tau : \mathcal{G} \mapsto \mathbb{Z}_{d^-}$

3. Assign the values of $\tau_{\vec{m}',\vec{n}'}$, for $(\vec{m}', \vec{n}') \notin \mathcal{H}$, according to completely positivity inequalities.

We devote Appendix 5.4 to present an algorithm to find the subgroups of the most general group we may encounter for Weyl channels. Additionally, in Appendix 5.4 we present how to determine all homomorphisms. We show single-qutrit Weyl channels examples in Fig. 5.2 where we are using the PCE representation of Appendix 5.4.
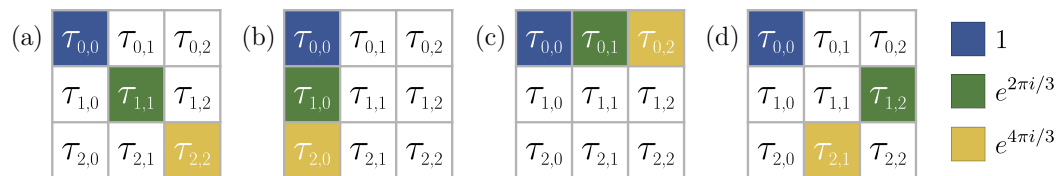
Figure 5.2: Examples of single-qutrit Weyl channels. The colored squared form a subgroup of $\mathbb{Z}_3 \oplus \mathbb{Z}_3$, and the colors are assigned by some homomorphism $\mathbb{Z}_3 \oplus \mathbb{Z}_3 \mapsto \mathbb{Z}_3$. Those $\tau_{\vec{m},\vec{n}}$ in the white squares are indicated, as they need not to be zero, but instead be constrained by inequalities in Eq. (5.33).

Conclusions

In this thesis, we have explored two classes of quantum channels. Firstly, we introduced and conducted a comprehensive study of Pauli component erasing (PCE) maps for systems of qubits. Subsequently, we occupied with the task of studying a generalization of the Pauli maps for multipartite systems with arbitrary-dimensional particles. To achieve this, we used the Weyl matrices, which are unitary generalization of Pauli matrices. Using tools drawn of linear algebra and finite group theory, we have uncovered insightful characterizations for both classes of quantum channels.

We revised the theory of quantum channels in Chapter 1. In Chapter 2, we introduced the Pauli maps for systems of qubits. We defined a Pauli map as a diagonal in the basis of N-qubit Pauli operators. Then, we took a detour to show the generic form of the Choi-Jamiołkowski matrix of any quantum map diagonal in an orthogonal basis. Afterwards, we returned to Pauli maps and diagonalized its Choi-Jamiołkowski matrix to derive the conditions of complete positivity which dictates when the map is a quantum channel.

Moving forward to Chapter 3, we introduced the concept of Pauli component erasing (PCE) maps and systematically explored the subset of quantum channels within this domain. We defined a PCE map as a trace-preserving quantum map that either preserves or erases the Pauli components of the density matrix of a system

of qubits. From the complete positivity conditions we obtained in the preceding chapter, we showed that PCE quantum channels are completely characterized by finite vector subspaces. In turn, these vector structure enabled us to derive several properties of PCE channels. Additionally, we identified the smallest subset that generate, under composition, the entire set of PCE channels. Finally, we studied the Kraus representation of PCE channels.

To ground these mathematical concepts, Chapter 4 was dedicated to present physical implementations of PCE channels We showed that PCE channels can be viewed as fixed points of Markovian processes, and derived their corresponding Lindbladian generators. Furthermore, we demonstrated that simple collision models can implement PCE channels as well.

The intriguing vector structure of PCE channels naturally prompted us to ponder the possibility of a generalization for systems of arbitrary-dimensional particles. Thus, we introduced and studied the Weyl maps for systems of qudits in Chapter 5. Our choice of the Weyl matrices was because these have similar properties to the Pauli matrices, enabling the analytical diagonalization of the Choi-Jamiołkowski matrix. Through the complete positivity conditions, we unveiled two pivotal results. Firstly, we identified the extreme points of the set, elucidating that Weyl channels are random unitary channels. Secondly, we revealed a non-trivial fact–the generalization of the vector structure of PCE channels is a group structure, embedded within all Weyl channels.

Our work contributes significantly to the comprehension of many-body quantum channels, as well as the dynamics of both qubits and d-level systems, an area of escalating importance for theoretical and practical endeavors. Future research directions include extending the notion of "component erasin" channels within the set of Weyl channels, probing other properties of these channels such as divisibility, non-Markovianity, channel capacity, and characterizing the subset of entanglement breaking channels. Additionally, we aim to delve deeper into the interplay between the algebraic structure of Weyl channels and quantum error-correcting codes, while

exploring physical implementations and systems whose interactions are described by such channels.

Beyond PCE figures

In this appendix, we will explore a method for adapting our representation of PCE maps, as discussed in Section 3.1, to visualize an N-qubit PCE map within a 2D grid. The underlying concept involves treating the vector $\vec{\tau}$ as a matrix that is the tensor product of single-qubit matrices τ_j of dimension 2×2.

Consequently, the indices (i, j) of the matrix element $\tau_{i,j}$ correspond with the indices $(\vec{m}, \vec{n})$ according to the following relation:

$$(i,j) = \left(2^{N-1}m_1 + 2^{N-2}m_2 + \ldots + m_N, 2^{N-1}n_1 + 2^{N-2}n_2 + \ldots + n_N \right). \quad (34)$$

This perspective allows us to envision $\vec{\tau}$ as divided into four $2^{N-1} \times 2^{N-1}$ subgrids, each determined by the positions (m_1, n_1). Simultaneously, these subgrids can be further divided into four $2^{N-2} \times 2^{N-2}$ subgrids, with their positions being (m_2, n_2). This grid subdivision process can be iterated until $j = N$. Examples of systems with $N = 1, 2, 3$ qubits are illustrated in Figures 1-3 for clarity.
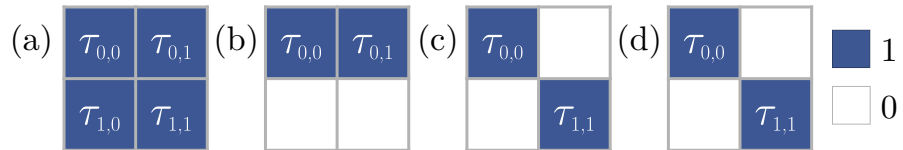
Figure 1: All single-qubit PCE channels in the new representation.
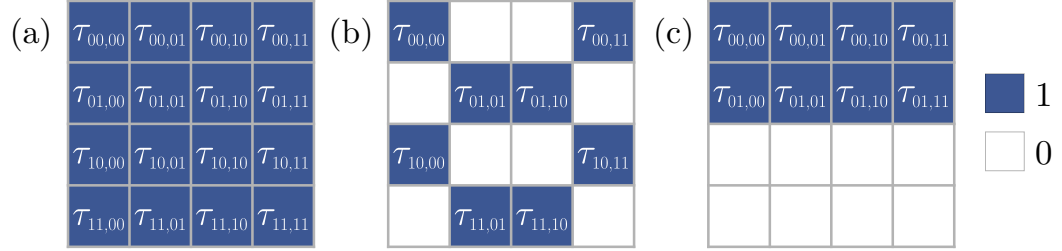
Figure 2: Three two-qubit PCE channels in the new representation.
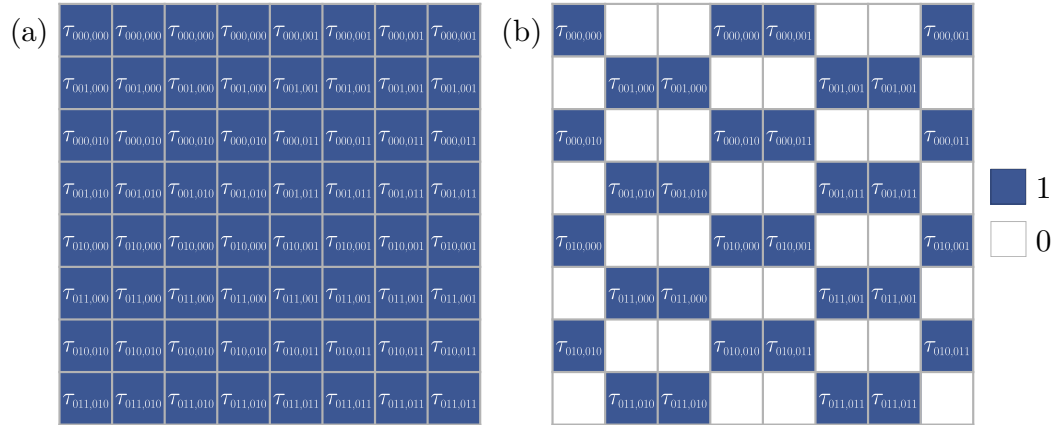
Figure 3: Two three-qubit PCE channels in the new representation.

Determining subgroups

To determine all $\tau(\vec{m}, \vec{n})$ of Weyl channels satisfying eq. (5.29) we proceed in two steps. The first step involves identifying all subgroups of $\mathcal{G}$. We begin by stating two relevant facts about finite abelian groups, and then discuss how to find the subgroups for the more general case of an abelian group $\mathcal{G}$, which encompasses the majority of our discussion in this section. After that, we describe the second step, which is how to determine all phases of $\tau_{\vec{m},\vec{n}}$ of a WCE channel by determining all homomorphisms from a subgroup to the roots of unity.

Whenever p and q are coprime, the group $\mathbb{Z}_{pq}$ is isomorphic to $\mathbb{Z}_p \oplus \mathbb{Z}_q$. Therefore, we may use the prime decomposition of d_α to separate each $\mathbb{Z}_{d_\alpha}$ as a sum of cyclic groups of prime power order. We proceed in this way for all α, and then we group the terms corresponding to different primes, so $\mathcal{G}$ can be written as

$$\mathcal{G} = \bigoplus_p \mathcal{G}_p, \tag{35}$$

with $\mathcal{G}_p = \bigoplus_i \mathbb{Z}_{p^{k_i}}$, for each prime p that appears in the decomposition of any of the d_α.

Since the direct sum of two arbitrary abelian groups of orders m and n that are coprime yield all abelian groups of order mn, we can directly construct all subgroups of $\mathcal{G}$ by finding all the subgroups of each $\mathcal{G}_p$. In other words, although $\mathcal{G}$ may have a complicated decomposition, we focus only in determining the subgroups of $\mathcal{G}_p$,

which will be convenient to write as

$$\mathcal{G}_p = \bigoplus_{\alpha=1}^{r} \mathbb{Z}_{p^{M_\alpha}} \qquad (36)$$

where M_α are in non-increasing order.

The group $\mathcal{G}_p$ is associated with the sequence $\overline{M} = M_1 \ldots M_r$, which is a *partition* of $M = \sum_\alpha M_\alpha$. Therefore, we will refer to $\mathcal{G}_p$ as a group of type $\overline{M}$. Furthermore, for any partition of M there exists an abelian group of order p^M that is unique up to an isomorphism [64]. If one has a subgroup $\mathcal{H}_p$ of $\mathcal{G}_p$, the corresponding partition, let us call it $\overline{N}$, satisfies $N_\alpha \leq M_\alpha$. On the other hand, once the choice of the non-increasing order for the partition of the group $\mathcal{G}_p$, the corresponding partitions for the subgroups $\mathcal{H}_p$ inherit a well-defined order from the group, and the corresponding partitions cannot therefore be taken in non-increasing order.

Another important fact about finite abelian groups is that they all have a basis; that is, they can be generated by the integer combinations of a set of elements. In our particular case, a simple way of choosing a basis is by picking a generating element for each cyclic group in eq. (36). We denote them $\vec{e}_\alpha$, and therefore an arbitrary $h \in \mathcal{H}$ can be *uniquely* expressed as

$$h = \sum_{\alpha=1}^{r} n_\alpha \vec{e}_\alpha, \qquad (37)$$

where $n_\alpha \in \mathbb{Z}_{p^{M_\alpha}}$, and the multiplication of a group element by an integer m is defined as the addition of the group element to itself repeated m times. The number r of elements in the basis is independent of the choice of basis and it is known as the group's rank r.

The general idea for finding all subgroups of $\mathcal{G}_p$ is to determine a subset of subgroups such that, upon applying all automorphisms $T : \mathcal{G}_p \mapsto \mathcal{G}_p$, all others are found. We will say that two subgroups of $\mathcal{G}_p$ are T-isomorphic when there is an automorphism T mapping one to the other. Then, to find the subgroups of $\mathcal{G}_p$ we first determine

any subset with the maximum number of subgroups that are not T-isomorphic. We call these "representative subgroups". By definition, applying all automorphisms T (which we describe how to find in Appendix 5.4) to the representative subgroups all other subgroups of $\mathcal{G}_p$ are found.

Note the difference between the concept of isomorphism for the subgroups, and the concept of T-isomorphism. The latter depends not only on the group structure of the subgroup $\mathcal{H}$, but also on the way in which it is embedded in the group $\mathcal{G}_p$. For instance, we can embed the group $\mathbb{Z}_2$ in the group $\mathbb{Z}_{2^2} \oplus \mathbb{Z}_2$ either as a subgroup of the first summand or as a subgroup of the second. In other words, the partition $\overline{M}$ describing the full group is $\overline{M} = 2\,1$ and the subgroup $\mathbb{Z}_2$ can be embedded with a partition $0\,1$ as well as $1\,0$. The two subgroups, being both isomorphic to $\mathbb{Z}_2$, are abstractly isomorphic, but that isomorphism cannot be extended to an isomorphism of $\mathbb{Z}_4 \oplus \mathbb{Z}_2$.

All subgroups of $\mathcal{G}_p$ are found applying all its automorphisms T to the subgroups generated by the bases

$$\mathcal{B} = \{p^{s_1}\vec{e}_1, \ldots, p^{s_r}\vec{e}_r\} \quad 0 \leq s_\alpha \leq M_\alpha. \tag{38}$$

Nevertheless, more than one different selection $\mathbb{S} = \{s_\alpha\}$ may determine two bases of subgroups T-isomorphic, in other words, that are connected by an automorphism of $\mathcal{G}_p$. For example, consider a group $\mathcal{G}_p$ of type $\overline{M} = 2\,2\,1\,1$. The partitions $\mathbb{S} = 0\,1\,0\,1$ and $\mathbb{S}' = 1\,0\,1\,1$ determine bases of T-isomorphic subgroups, because the automorphism defined as $T(\vec{e}_1) = \vec{e}_2$, $T(\vec{e}_2) = \vec{e}_1$, $T(\vec{e}_3) = \vec{e}_4$ and $T(\vec{e}_4) = \vec{e}_3$ maps one to the other. From each of these T-isomorphic sets of subgroups we can pick an arbitrary element, which will be called *the representative subgroup*.

To find the representative subgroups we need a criterion to determine when two bases $\mathcal{B}$ of the form (38) generate T-isomorphic groups. Let us denote $\tilde{M}_1, \ldots, \tilde{M}_q$ the q different values in the sequence of numbers in $\overline{M}$ (for instance, if $\overline{M} = 2211$, then $q = 2$ and $\tilde{M}_1 = 2, \tilde{M}_2 = 1$). Furthermore, we define the subset $S_j = \{s_\alpha, \forall \alpha :$

$M_\alpha = \tilde{M}_j\}$ of $\mathbb{S}$, that is, S_j is the subset of $\mathbb{S}$ formed by all the s_α whose αs correspond to the indices of the M_α that are equal to $\tilde{M}_j$. Then, the criterion is the following: two different sets $\mathbb{S}$ and $\mathbb{S}'$ determine bases of T-isomorphic subgroups whenever their corresponding subsets S_j and S_j' are the same for all j.

We are ready to describe the complete algorithm to determine all the subgroups of a given group $\mathcal{G}$. First, decompose $\mathcal{G}$ as a sum of prime power order groups $\mathcal{G}_p$. For every $\mathcal{G}_p$, find all sets $\mathbb{S} = \{s_\alpha\}$ and discriminate between them to find the only ones that determine representative subgroups. Then apply to them all automorphisms T of $\mathcal{G}_p$, so all subgroups of $\mathcal{G}_p$ will be found, albeit with repetitions. A description of the group of automorphisms of an arbitrary abelian group $\mathcal{G}$ is provided in [65], and the technique is summarized for completeness' sake in Appendix 5.4. Finally, to find the subgroups of $\mathcal{G}$ apply the direct sum between all different subgroups of each $\mathcal{G}_p$.

Furthermore, a way to count the total number of subgroups of $\mathcal{G}_p$ is already known in the literature. Since any abelian group of prime power order can only have subgroups that are also of prime power order, subgroups of order p^L, with $L < M$, can also be characterized by a partition $\overline{L}$ of L. It is shown in [64, 66] that necessary and sufficient conditions for the partition $\overline{L}$ to correspond to a possible subgroup of the group determined by the partition $\overline{M}$ of M are

$$L_\alpha = 0 \quad (\alpha > r), \tag{39a}$$

$$L_\alpha \leq M_\alpha, \tag{39b}$$

$$L_\alpha \geq L_{\alpha+1}. \tag{39c}$$

An expression for the number of different subgroups of type $\overline{L}$ is already known in the literature.

To fully determine the coefficients $\tau_{\vec{m},\vec{n}}$ with norm 1, we interpret them as a function that maps $\mathcal{H}$ to the group of roots of unity ω^j. We consider $\tau_{\vec{m},\vec{n}} = \omega^{\phi(\vec{m},\vec{n})}$, thus we are looking for all homomorphisms $\phi : \bigoplus_{M_\alpha} \mathbb{Z}_{p^{M_\alpha}} \mapsto \mathbb{Z}_{p^{M_1}}$. To determine one

of such functions uniquely, it is sufficient to specify the values of ϕ on a basis of $\mathcal{H}$, as described in Appendix 5.4.

Note that all the above remarks greatly simplify when d is a prime number. In that case the group $\mathcal{G}$ is additionally a vector space. The set of subgroups can then be described as the set of vector subspaces using the usual techniques of linear algebra. All the partitions described above then reduce to partitions of the type where M_α is either 1 or 0, and the partition is fully characterized by the number of its non-zero elements, which correspond to the subspace's *dimension*. Finally, the homomorphism τ can be described as a linear map from the vector space $\mathcal{G}$ to the field $\mathbb{Z}_d$, which is once more straightforwardly described in terms of linear algebra.

Determining homomorphisms

Here we describe the set of homomorphisms ϕ from an abelian group of the form $\mathcal{H} = \bigoplus_{\alpha=1}^{r} \mathbb{Z}_{p^{M_\alpha}}$ to the cyclic group $\mathbb{Z}_{p^{M_1}}$. As always, the numbers M_α are ordered in decreasing order.

We may as always choose a basis $\vec{e}_\alpha$ of $\mathcal{H}$, each having order p^{M_α}. The homomorphism ϕ is then uniquely determined by a set of homomorphisms ϕ_α from the cyclic groups $\mathbb{Z}_{p^{M_\alpha}}$ to $\mathbb{Z}_{p^{M_1}}$.

Whenever $M_1 = M_\alpha$, ϕ_α simply reduces to multiplication by an arbitrary r_α number modulo p^{M_1}. On the other hand, if $M_\alpha < M_1$, then ϕ_α is given by the multiplication by a number of the form $p^{M_1-M_\alpha} r_\alpha$ where r_α is an arbitrary number modulo p^{M_α}.

If we therefore define ν as the number of $M_\alpha = M_1$, so that $M_\nu \geq M_1$ but $M_{\nu+1} < M_1$, and $\nu = 0$ if $M_\alpha < M_1$ for all α, then ϕ can be expressed as follows:

$$\phi\left(\sum_\alpha c_\alpha \vec{e}_\alpha\right) \;=\; \vec{\phi} \cdot \vec{c} := \sum_\alpha \phi_\alpha c_\alpha \tag{40a}$$

$$\phi_\alpha \;=\; \begin{cases} p^{M_1-M_\alpha} s_\alpha & (\alpha \geq \nu) \\[2mm] t_\alpha & (\alpha < \nu) \end{cases} \tag{40b}$$

where s_α and t_α are numbers modulo p^{M_α} and p^{M_1} respectively.

The total number of such homomorphisms is therefore given by p^K with

$$K = \sum_{\alpha=1}^{\nu} M_\alpha + M_1(r - \nu) \tag{41}$$

Automorphisms of finite abelian groups

In the following we describe the bijective homomorphisms T of an arbitrary abelian group. Without loss of generality we limit ourselves to groups that are the direct sum of groups of the type $\mathbb{Z}_{p^M}$, specifically

$$\mathcal{G} = \bigoplus_{\alpha=1}^{r} \mathbb{Z}_{p^{M_\alpha}}. \tag{42}$$

To fix notations, we shall work with a fixed basis $\vec{e}_\alpha$, $1 \leq \alpha \leq r$, where r is the *rank* of $\mathcal{G}$. The map T is therefore uniquely determined by the values of $T\vec{e}_\alpha$. Since $\vec{e}_\alpha$ is a basis, we can write

$$T\vec{e}_\alpha = \sum_{\beta=1}^{r} t_{\alpha\beta}\vec{e}_\beta. \tag{43}$$

The $t_{\alpha\beta}$ are then uniquely determined, if we view them as homomorphisms from $\mathbb{Z}_{p^{M_\beta}}$ to $\mathbb{Z}_{p^{M_\alpha}}$. Since such homomorphisms can always be expressed through the multiplication by some appropriate number, the expression given in (43) is meaningful.

Now let us specify more precisely the range of variation of the $t_{\alpha\beta}$. We distinguish two cases

1. $M_\alpha \leq M_\beta$: in this case any number modulo p^{M_α} will do, and two different such numbers provide different homomorphisms.

2. $M_\alpha > M_\beta$: in this case, the number needs to be a multiple of $p^{M_\alpha - M_\beta}$, since otherwise it is not possible to define the map. In that case, we may describe $t_{\alpha\beta}$ as $p^{M_\alpha - M_\beta}\tau_{\alpha\beta}$, where $\tau_{\alpha\beta}$ is an arbitrary number modulo p^{M_β}

Consider the matrix T in greater detail, and just as in the main text, let us denote by $\tilde{M}_1, \cdots, \tilde{M}_q$ the *distinct* values of M_α in *strictly decreasing order*. We define ν_α to be the number of times $\tilde{M}_\alpha$ appears repeated in the original series. This defines a division of the T matrix in *blocks* of size $\nu_\alpha \times \nu_\beta$, where $1 \le \alpha, \beta \le q$.

We first take the elements $t_{\alpha\beta}$ modulo p. As a consequence of the observation (2), all blocks with $\alpha < \beta$ are filled with zeros, whereas all other blocks have arbitrary entries. It thus follows that the matrix is invertible modulo p if and only if all the diagonal blocks are invertible. The number of invertible $\nu_\alpha \times \nu_\alpha$ matrices modulo p is given by

$$I_\alpha = \prod_{\beta=1}^{\nu_\alpha} \left(p^{\nu_\alpha} - p^{\beta-1} \right). \tag{44}$$

One sees this by observing that we may first choose an arbitrary non-zero vector of length ν_α in $p^{\nu_\alpha} - 1$ different ways, then chose a second vector independent from the first, and so on.

All the other entries in the blocks below the diagonal, that is, the $t_{\alpha\beta}$ with $\alpha > \beta$, can be chosen arbitrarily. If we thus define

$$K_0 = \sum_{1 \le \beta < \alpha \le q} \nu_\alpha \nu_\beta, \tag{45}$$

then the total number of possible forms of the matrix T modulo p is

$$N(p) = p^{K_0} \prod_{\alpha=1}^{q} I_\alpha. \tag{46}$$

We now need to work out the number of ways this can be extended to the full matrix, where the entries have the full range of variation specified above. Note first that the condition of invertibility carries over automatically upon extension, as the inverse matrix of T modulo p can be extended uniquely to the inverse of the extended matrix.

To the entries on or below the diagonal, that is, with $t_{\alpha\beta}$ such that $\alpha \ge \beta$, we can add any number of the form $p\tau_{\alpha\beta}$, where $\tau_{\alpha\beta}$ is an arbitrary number taken modulo

$p^{\tilde{M}_\alpha - 1}$. So the number of possibilities of extending these blocks is given by p^{K_1}, where

$$K_1 = \sum_{1 \leq \beta \leq \alpha \leq q} (\tilde{M}_\alpha - 1)\nu_\alpha \nu_\beta. \tag{47}$$

For the blocks above the diagonal, that is, the blocks with $t_{\alpha\beta}$ such that $\alpha < \beta$, they are of the form $p^{\tilde{M}_\alpha - \tilde{M}_\beta} \tau_{\alpha\beta}$, with $\tau_{\alpha\beta}$ a number modulo $p^{\tilde{M}_\beta}$, so that the total number of ways of extending the blocks above the diagonal is p^{K_2}, with

$$K_2 = \sum_{1 \leq \alpha < \beta \leq q} \tilde{M}_\beta \nu_\alpha \nu_\beta. \tag{48}$$

The final result for the total number of automorphisms is thus given by

$$N_{tot}(M_1, \ldots, M_r) = p^{K_0 + K_1 + K_2} \prod_{\alpha=1}^{q} I_\alpha. \tag{49}$$

Pauli component erasing quantum channels

Pauli component erasing quantum channels

Jose Alfredo de Leon [1,2] Alejandro Fonseca [3,2] François Leyvraz [4] David Davalos [5] and Carlos Pineda [2,*]

[1]*Instituto de Investigación en Ciencias Físicas y Matemáticas, Universidad de San Carlos de Guatemala,*
Ciudad Universitaria, Guatemala 01012, Guatemala
[2]*Instituto de Física, Universidad Nacional Autónoma de México, Ciudad de México 01000, Mexico*
[3]*Departamento de Física, CCEN, Universidade Federal de Pernambuco, Recife 50670-901, PE, Brazil*
[4]*Instituto de Ciencias Físicas, Universidad Nacional Autónoma de México, Cuernavaca 62210, Mexico*
[5]*Institute of Physics, Slovak Academy of Sciences, Dúbravská cesta 9, Bratislava 84511, Slovakia*

Decoherence of quantum systems is described by quantum channels. However, a complete understanding of such channels, especially in the multiparticle setting, is still an ongoing difficult task. We propose the family of quantum maps that preserve or completely erase the components of a multiqubit system in the basis of Pauli strings, which we call *Pauli component erasing maps*. For the corresponding channels, it is shown that the preserved components can be interpreted as a finite vector subspace, from which we derive several properties and complete the characterization. Moreover, we show that the obtained family of channels forms a semigroup and derive its generators. We use this simple structure to determine physical implementations and connect the obtained family of channels with Markovian processes.

I. INTRODUCTION

Quantum correlations [1–3], including entanglement [4], are an important resource for a wide variety of tasks that include teleportation [5], quantum computation [6], and others [7]. However, this resource is also extremely delicate [6,8], especially for multiparticle systems [4]; that is why an important part of the efforts of the community implementing quantum technologies is devoted to tackle this issue from an experimental [9,10] and theoretical [11–13] point of view. The process by which quantum correlations are unintentionally dissipated is called *decoherence* [8,14]. One of the main tools to study the effects of decoherence are quantum channels. Quantum channels can describe quantum noise [15,16], open quantum systems dynamics [6,17], and recently even coarse graining [18,19]. One of the main difficulties in characterizing quantum channels is that, like for quantum states, the number of parameters required for their description increases quite rapidly with Hilbert-space dimension. Moreover, such parameters are constrained in a complicated way by physical conditions, such as complete positivity [20]. Describing in detail families of channels having a given property provides insight into the jungle of quantum operations. For the qubit case there are several studies concerning the unital case, for which nontrivial properties can be described using only three parameters, which in turn form the well-known tetrahedron of Pauli channels [15,16,21]. More generally, in Ref. [22] the authors study families of convex combinations of quantum-classical channels that relate to unital qubit channels with positive eigenvalues, and give a generalization of the Bloch sphere. Similarly, a generalization of Pauli channels based on mutually unbiased measurements is introduced and studied in Ref. [23]. Other studies of channels beyond the qubit can be found [24–27].

In this paper we present a generalization of idempotent Pauli channels—i.e., the qubit flip operations (bit, phase, and bit-phase when the flip probability is 1/2), total depolarizing qubit channel, and the identity channel—to the case of N qubits. The generalization is done by extending Pauli observables to *Pauli strings* (tensor products of Pauli matrices) [28,29]. The resulting maps are unital and diagonal in the Pauli strings' basis. We shall in the following refer to such maps as *Pauli component erasing* (PCE) *maps*.

The main task which we perform in this paper is the identification of the conditions which an arbitrary PCE map must satisfy in order to be completely positive. The answer turns out to involve a strikingly simple and unexpected mathematical structure that is exploited to gain deeper understanding on aforementioned channels, as we show in Sec. III B. This structure allows us, for example, to describe such channels with a much reduced set of parameters (as compared to specifying a list of all erased Pauli components) or to define an interesting semigroup structure on the set of all PCE channels. Additionally, these channels are, in a sense, the simplest possible channels, and as such can be used as building blocks of more general channels. For instance, one can combine them (through convex superposition) or compose them with unitary transformations. To summarize succinctly the final result, we show that it is possible to assign to every Pauli string a simple PCE channel, obtained by extending the system with an ancilla of a single qubit, acting on the combined system by a unitary involving the Pauli string and tracing over the ancilla.

*carlospgmat03@gmail.com

It then follows from our results that *all* PCE channels arise from such channels by composition.

The paper is organized as follows. In Sec. II we recall the properties of quantum channels needed to proceed with the definition of PCE maps. In Sec. III we diagonalize analytically the Choi matrix for arbitrary PCE maps and characterize their complete positivity by interpreting PCE quantum channels as finite vector subspaces. We study the generators of the semigroup structure associated to the set of PCE channels in Sec. IV, and we use them to derive meaningful physical interpretations of PCE channels in Sec. V, as well as Kraus operators of the generators. To finish, we conclude and discuss future perspectives and possible generalizations in Sec. VI.

II. PAULI COMPONENT ERASING MAPS

In this section we introduce the family of PCE maps. Let us start our discussion with a brief review of several basic concepts of quantum channels that will allow us to introduce some notation, and finish with the definition of PCE maps and some generalities. We further introduce a useful graphical representation for them.

A. Quantum channels

Quantum channels are the most general linear operations that a quantum system undergoes independently of its past [20,30]. The physical system under study will be associated with a Hilbert space denoted by H, and the set of linear operators over such space will be denoted by $\mathcal{B}(\mathsf{H})$. That way, a density matrix ρ of such system is an element of $\mathcal{B}(\mathsf{H})$.

The construction of quantum channels includes basically three ingredients: linearity, trace preservation, and complete positivity. Linearity is needed to map every convex combination of density matrices into a convex combination of the evolution of such density matrices. The trace preserving property is required for the process $\mathcal{E}$ to happen with probability 1, and reads $\mathrm{tr}\mathcal{E}[\rho] = \mathrm{tr}\rho = 1$. The complete positivity condition is needed to preserve positive semidefiniteness and handle the nonlocal nature of quantum theory. A linear map $\mathcal{E}$ is positive if it maps density operators to density operators, i.e., if $\mathcal{E}[\rho] \geqslant 0$ for all density matrices ρ. On the other hand, if one extends a positive map to include an ancilla, the resulting map is not always positive. If, for an ancillary system of arbitrary dimension, such extension results in a positive map, we say that the original map is completely positive [31]. Quantum channels are required to be completely positive so as to allow the proper evolution of potentially entangled states with an ancilla; to test this condition we require some additional steps.

A simple algorithm to test the complete positivity of a quantum channel was developed by Jamiokowski [32] and Choi [33]. One first exploits the isomorphism that maps a channel $\mathcal{E}$ to the state $\mathcal{D} = (\mathrm{id} \otimes \mathcal{E})[|\Omega\rangle\langle\Omega|]$, where $|\Omega\rangle = 1/\dim(\mathsf{H}) \sum_i^{\dim(\mathsf{H})} |i\rangle|i\rangle$ is a maximally entangled state between the original system and an ancilla and "id" is the identity channel. Remarkably, the map $\mathcal{E}$ is completely positive if and only if $\mathcal{D}$ (also called the Choi or dynamical matrix of $\mathcal{E}$) is positive semidefinite [32,33].
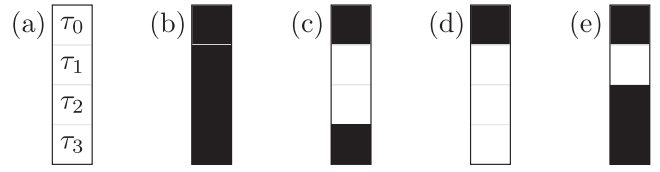
FIG. 1. In (a) we introduce the notation in the diagrams that represent the single-qubit PCE maps, so that each square corresponds to a single τ_α, $\alpha = 0, 1, 2, 3$. The diagrams in (b), (c), and (d) correspond to the identity map, completely dephasing channel, and complete depolarization, respectively, as the color of each square indicates the value attained by the corresponding τ_α, either 0 (white) or 1 (black). In (e) we show a map that only erases the component r_1, collapsing the Bloch sphere into a disk, and thus does not correspond to a quantum channel.

B. Structure of PCE maps

We have discussed the main features of quantum channels, and now we turn our attention to introduce the Pauli component erasing maps. We start by exploring the single-qubit scenario and then we treat the N-qubit case.

The most general single-qubit density matrix can be written as

$$\rho = \frac{1}{2}\sum_{\alpha=0}^{3} r_\alpha \sigma_\alpha, \tag{1}$$

with $\sigma_0 = \mathbb{1}$, and $\sigma_{1,2,3}$ the usual Pauli matrices. Normalization requires that $r_0 = 1$ and the remaining $r_{1,2,3}$ form the Bloch vector. Consider the map that projects each component in the following way:

$$r_\alpha \mapsto \tau_\alpha r_\alpha \tag{2}$$

where τ_α is either 0 or 1 (trace preserving requires that $\tau_0 = 1$). From now on we refer to any operation like that described in Eq. (2), as a single-qubit PCE map. Not every such operation is a quantum channel; for example, collapsing the entire Bloch ball to a disk on the xy plane ($\tau_1 = \tau_2 = 1$ and $\tau_3 = 0$) leads to a violation of the complete positivity conditions. Indeed, a direct evaluation of such conditions yields [15,20]

$$1 + \tau_1 + \tau_2 + \tau_3 \geqslant 0,$$
$$1 + \tau_\alpha - \tau_\beta - \tau_\gamma \geqslant 0 \ \forall \ \alpha \neq \beta \neq \gamma, \tag{3}$$

where trace preserving is already imposed, and shows that five out of the eight single-qubit PCE maps are quantum channels. These operations are the identity map, the completely depolarizing channel ($\rho \mapsto \mathbb{1}/2$), as well as the bit, phase, and bit-phase flip (with flip probability of 1/2) channels [34], and can be pictured using one column tables showing the positions of 0s and 1s (see Fig. 1).

In order to present and develop the N-qubit case, it is useful to introduce the so-called Pauli strings, defined as

$$\sigma_{\vec{\alpha}} = \sigma_{\alpha_1} \otimes \sigma_{\alpha_2} \otimes \cdots \otimes \sigma_{\alpha_N}, \tag{4}$$

where $\vec{\alpha}$ denotes a multi-index $(\alpha_1, \ldots, \alpha_N)$ and $\alpha_i = 0, 1, 2, 3$. These Hermitian operators form an orthogonal basis in the space of operators acting on N qubits. In fact, $\mathrm{tr}\sigma_{\vec{\alpha}}\sigma_{\vec{\alpha}'} = 2^N \delta_{\vec{\alpha}\vec{\alpha}'}$ and $\mathrm{tr}\sigma_{\vec{\alpha}} = 2^N \delta_{\vec{\alpha}0}$.
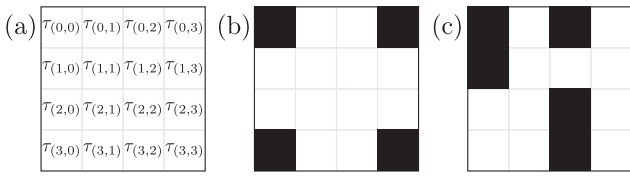
FIG. 2. In (a) we introduce the positions of two qubit diagrams. The diagram in (b) corresponds to a quantum channel that results from the tensor product of bit flip channels in each qubit [see Fig. 1(c)], and in (c) a diagram of a map that is not a quantum channel is presented.

Similarly to the single-qubit case, the density matrix ρ of a system of N qubits can be written using Pauli strings in the following way:

$$\rho = \frac{1}{2^N} \sum_{\vec{\alpha}} r_{\vec{\alpha}} \sigma_{\vec{\alpha}}, \tag{5}$$

so $r_{\vec{\alpha}} = \langle \sigma_{\vec{\alpha}} \rangle = \mathrm{tr}(\rho \sigma_{\vec{\alpha}})$ is the coefficient corresponding to the expansion of the density matrix in the normalized basis of Pauli strings. Again, normalization of the state requires that $r_{\vec{0}} = 1$. We shall refer to $r_{\vec{\alpha}}$ as the *Pauli components* of the density matrix of a system of qubits.

In general, a PCE map is a map that either preserves or completely erases the Pauli components of a density matrix. That is,

$$r_{\vec{\alpha}} \mapsto \tau_{\vec{\alpha}} r_{\vec{\alpha}}, \quad \tau_{\vec{\alpha}} = 0, 1. \tag{6}$$

In addition, for the operation to be trace preserving, it is required that $\tau_{\vec{0}} = 1$. It is worth noticing that, as for the single-qubit case, not all PCE maps are quantum operations. On the other hand, constructing and evaluating the conditions for complete positivity is nontrivial and is the main problem addressed in this paper. We shall refer to the map $r_{\vec{\alpha}} \mapsto \tau_{\vec{\alpha}} r_{\vec{\alpha}}$, with arbitrary values of $\tau_{\vec{\alpha}}$ (only restricted by complete positivity), as *Pauli diagonal maps*.

A graphical representation for PCE maps may be introduced, with the two-qubit case proving to be the most useful. Consider a N-dimensional Cartesian grid, with 4^N places. Each place has N integer coordinates, ranging from 0 to 3, so each place corresponds to a given $\vec{\alpha}$ in Eq. (5). For a given PCE, we shall fill the square if the corresponding $\tau_{\vec{\alpha}} = 1$. Otherwise, we leave it empty. Examples for $N = 1$ and 2 are provided in Figs. 1 and 2, respectively.

It is worth noticing that the set of PCE maps overlaps with the set of "Pauli diagonal channels constant on axes" defined in Ref. [22], consisting of convex combinations of *quantum-classical* channels. In particular, it can be shown that quantum-classical channels defined with the eigenbasis of some set of $2^N - 1$ commuting Pauli observables [29] yield a PCE map with exactly 2^N components equal to 1s in its diagonal. For details, we refer the reader to Appendix A.

III. MATHEMATICAL CONSIDERATIONS

This section is devoted to deriving the conditions a Pauli diagonal map needs to satisfy the complete positivity condition, i.e., that all the eigenvalues of the Choi matrix associated to the channel are non-negative. To do so, we calculate and

diagonalize the Choi matrix of a general Pauli diagonal map, first for a single qubit and then for N qubits. Finally, we restrict from Pauli diagonal maps to PCE maps, and provide a connection between a vector subspace and the set of coefficients $\{\tau_{\vec{\alpha}}\}$ in Eq. (6) of a PCE quantum channel. This allows us to derive several important properties of this particular family of channels.

A. Diagonalization of the Choi matrix

We now construct the Choi matrix of a single-qubit Pauli diagonal map $\mathcal{E}$. As described above, $\mathcal{E}$ is a linear map from $\mathcal{B}(\mathsf{H})$ to itself. We shall denote elements of $\mathcal{B}(\mathsf{H})$ by the notation $|\cdot\rangle\rangle$. Thus, for instance, $|\sigma_\alpha\rangle\rangle$ represents the Pauli matrix σ_α understood as a vector belonging to $\mathcal{B}(\mathsf{H})$, for the present case, in which $\mathsf{H} = \mathbb{C}^2$. Since the scalar product in $\mathcal{B}(\mathsf{H})$ is given by $\langle\langle A_1|A_2\rangle\rangle = \mathrm{tr}A_1^\dagger A_2$, elements of the Pauli basis satisfy the relation $\langle\langle \sigma_\alpha|\sigma_{\alpha'}\rangle\rangle = \mathrm{tr}(\sigma_\alpha^\dagger \sigma_{\alpha'}) = 2\delta_{\alpha\alpha'}$. In this language, the state of a single qubit reads $|\rho\rangle\rangle = 2^{-1} \sum_{\alpha=0}^{3} r_\alpha |\sigma_\alpha\rangle\rangle$ and the matrix form of the map $\mathcal{E}$ is

$$\hat{\mathcal{E}} = \frac{1}{2} \sum_{\alpha=0}^{3} \tau_\alpha |\sigma_\alpha\rangle\rangle\langle\langle\sigma_\alpha|. \tag{7}$$

After some steps, detailed from Eq. (B3) to Eq. (B6), it is possible to show that the Choi matrix of $\mathcal{E}$ reads

$$\mathcal{D} = \frac{1}{2} \sum_{\alpha=0}^{3} \tau_\alpha \sigma_\alpha \otimes \sigma_\alpha^*. \tag{8}$$

Notice that $|\sigma_\alpha\rangle\rangle\langle\langle\sigma_\alpha|$ and $\sigma_\alpha \otimes \sigma_\alpha^*$ are different operators. Indeed, the former acts as a linear map upon the vector space $\mathcal{B}(\mathsf{H})$, whereas the latter acts on the tensor product $\mathsf{H} \otimes \mathsf{H}$. Of course, there is a basis dependent identification between these two spaces, which is used in the construction of the Choi matrix. Surprisingly, one can in fact show that $\mathcal{D}$ is diagonal in the Pauli basis (see Appendix B for details). The eigenvalues are

$$\lambda_\alpha = \frac{1}{2} \sum_{\beta=0}^{3} a_{\alpha\beta} \tau_\beta, \tag{9}$$

where

$$a = \begin{pmatrix} 1 & 1 & 1 & 1 \\ 1 & 1 & -1 & -1 \\ 1 & -1 & 1 & -1 \\ 1 & -1 & -1 & 1 \end{pmatrix}. \tag{10}$$

We wish to add that one can replace a with $H \otimes H$, with H the Hadamard matrix, and still diagonalize the same Choi matrix $\mathcal{D}$. This is due to the fact that a corresponds to a permutation of rows of $H \otimes H$. However, we chose the aforementioned definition as some later considerations [see Eq. (32)] cannot be easily written in terms of $H \otimes H$.

The same program can be carried out for N qubits. In this case, one uses the vectorized Pauli strings:

$$|\sigma_{\vec{\alpha}}\rangle\rangle = |\sigma_{\alpha_1} \otimes \cdots \otimes \sigma_{\alpha_N}\rangle\rangle. \tag{11}$$

This vectorization must not be confused with the tensor product of all $|\sigma_{\alpha_i}\rangle\rangle$, since the tensor product and the vectorization process generally do not commute [35]. The vectors satisfy

the orthogonality relation $\langle\langle \sigma_{\vec{\alpha}} | \sigma_{\vec{\alpha}'} \rangle\rangle = 2^N \delta_{\vec{\alpha}\vec{\alpha}'}$. The matrix representation of the map corresponding to a Pauli diagonal map is

$$\hat{\mathcal{E}}_N = \frac{1}{2^N} \sum_{\vec{\alpha}} \tau_{\vec{\alpha}} |\sigma_{\vec{\alpha}}\rangle\rangle\langle\langle\sigma_{\vec{\alpha}}|. \tag{12}$$

As in the previous case, the Choi matrix $\mathcal{D}_N$ may be written in terms of tensor products of Pauli matrices:

$$\mathcal{D}_N = \frac{1}{2^N} \sum_{\vec{\alpha}} \tau_{\vec{\alpha}} \bigotimes_{j=1}^N \sigma_{\alpha_j} \otimes \sigma_{\alpha_j}^*. \tag{13}$$

This matrix is again diagonal in the (multiqubit) Pauli basis, with the eigenvalue corresponding to $|\sigma_{\vec{\alpha}}\rangle\rangle$ given by

$$\lambda_{\vec{\alpha}} = \frac{1}{2^N} \sum_{\vec{\beta}} A_{\vec{\alpha}\vec{\beta}} \tau_{\vec{\beta}}, \tag{14}$$

where

$$A = a^{\otimes N}. \tag{15}$$

Again, the proofs are provided in Appendix B. We wish to add that we could diagonalize $\mathcal{D}_N$ with $H^{\otimes 2N}$ instead of $a^{\otimes N}$, which might be more convenient for other applications.

B. PCE quantum channels as vector spaces

In this subsection we will provide a one-to-one relation between PCE quantum channels and the subspaces of a discrete vector subspace associated with the indices $\vec{\alpha}$ labeling the components of a state [see Eq. (5)]. Some established facts about vector spaces will allow us to derive the main features of PCE quantum channels.

Let us start by recalling that the problem of determining complete positivity of a PCE map can be recast as determining which coefficients $\tau_{\vec{\alpha}}$ are mapped via A to positive eigenvalues $\lambda_{\vec{\alpha}}$, as in Eq. (14). Using the fact that $a^{-1} = a/4$, and so

$$A^{-1} = \frac{1}{4^N} A, \tag{16}$$

we can directly invert Eq. (14) to obtain

$$\sum_{\vec{\beta}} A_{\vec{\alpha}\vec{\beta}} \lambda_{\vec{\beta}} = 2^N \tau_{\vec{\alpha}}, \tag{17}$$

which will serve as a starting point for our analysis. This is a remarkable equation, as it provides a method to diagonalize the Choi matrix of any Pauli diagonal map.

Two other simple but crucial observations are the following. For valid quantum channels it holds that

$$\sum_{\vec{\alpha}\in\Omega} \lambda_{\vec{\alpha}} = 0 \quad \Rightarrow \quad \lambda_{\vec{\alpha}} = 0, \forall \vec{\alpha} \in \Omega \tag{18}$$

for an arbitrary subset of multi-indices Ω, as each member of the sum is greater than or equal to zero, due to complete positivity of the underlying channel. Finally, setting $\vec{\alpha} = 0$ in Eq. (17), and taking into account the normalization condition

TABLE I. Definition of the $\oplus$ operation [see Eq. (23)]. Note that the operation is an Abelian group; in fact it corresponds to the Klein group, where the neutral element is zero. This is the reason for choosing an additive notation for the operation defined in (23).

$\oplus$	0	1	2	3
0	0	1	2	3
1	1	0	3	2
2	2	3	0	1
3	3	2	1	0

that $\tau_{\vec{0}} = 1$, we obtain

$$\sum_{\vec{\alpha}} \lambda_{\vec{\alpha}} = 2^N, \tag{19}$$

since $A_{\vec{0},\vec{\beta}} = 1$ for all $\vec{\beta}$.

Now we need a definition: to each multi-index $\vec{\alpha}$ we associate a *set* of multi-indices $\Phi(\vec{\alpha})$ as follows:

$$\Phi(\vec{\alpha}) = \{\vec{\beta} : A_{\vec{\alpha}\vec{\beta}} = 1\}. \tag{20}$$

If we now assume that $\tau_{\vec{\alpha}} = 1$, and calculate the difference between Eq. (19) and $\sum_{\vec{\beta}} A_{\vec{\alpha}\vec{\beta}} \lambda_{\vec{\beta}} = 2^N$ [which follows from Eq. (17) and $\tau_{\vec{\alpha}} = 1$], one obtains

$$\lambda_{\vec{\beta}} = 0, \quad \forall \vec{\beta} \notin \Phi(\vec{\alpha}). \tag{21}$$

Thus, if $\tau_{\vec{\alpha}} = 1$, then $\tau_{\vec{\gamma}}$ and $\tau_{\vec{\gamma}'}$ are equal if

$$A_{\vec{\beta}\vec{\gamma}} = A_{\vec{\beta}\vec{\gamma}'}, \quad \forall \vec{\beta} \in \Phi(\vec{\alpha}). \tag{22}$$

This follows from restricting the sum Eq. (17) to the indices $\vec{\beta}$ such that $\lambda_{\vec{\beta}} \neq 0$, given in Eq. (21). Condition (22) therefore connects three multi-indices, $\vec{\alpha}$, $\vec{\gamma}$, and $\vec{\gamma}'$. When such a connection exists, $\tau_{\vec{\alpha}} = 1$ implies $\tau_{\vec{\gamma}} = \tau_{\vec{\gamma}'}$.

Let us now work out the nature of the aforementioned connection. For arbitrary k we define a vector $\vec{\beta}_k$ such that $\vec{\beta}_k \in \Phi(\vec{\alpha})$ as follows: $\vec{\beta}_k$ is zero everywhere except for the kth coordinate, which takes a value β such that $a_{\alpha_k\beta} = 1$. Since $a_{\alpha 0} = 1$ for any α, this particular choice of $\vec{\beta}$ indeed belongs to $\Phi(\vec{\alpha})$, so that if Eq. (22) holds for all $\vec{\beta} \in \Phi(\vec{\alpha})$ it must hold for that particular $\vec{\beta}_k$, which leads to

$$a_{\beta\gamma_k} = a_{\beta\gamma_k'} \tag{23}$$

for all β such that $a_{\alpha_k\beta} = 1$. One can verify, by working out the different cases, that Eq. (23) is equivalently expressed as

$$\gamma_k' = \alpha_k \oplus \gamma_k \tag{24}$$

where $\oplus$ denotes the operation of the Klein group (see Table I for a detailed description).

It will be useful to think of the multi-index $\vec{\alpha}$ as an element of a vector space. To do so, we notice that any group with the property that $\alpha \oplus \alpha = 0$ is indeed a vector space under the two-element field $\{0, 1\}$. We notice that the Klein group described in Table I is actually isomorphic to the two-dimensional vector space over the field of two elements $\{0, 1\}$. Then, we build the complete vector space, with the same field, and defining $\vec{\alpha} \oplus \vec{\beta} = (\alpha_1 \oplus \beta_1, \cdots, \alpha_N \oplus \beta_N)$ [36]. We can indeed restate Eq. (24) and say that, for quantum channels, if

$\tau_{\vec{\alpha}} = 1$, then $\tau_{\vec{\gamma}} = \tau_{\vec{\alpha} \oplus \vec{\gamma}}$. For example, in Fig. 2(c) the indices that correspond to preserved components are $\vec{\alpha}^{(0)} = (0, 0)$, $\vec{\alpha}^{(1)} = (0, 2)$, $\vec{\alpha}^{(2)} = (1, 0)$, $\vec{\alpha}^{(3)} = (2, 2)$, and $\vec{\alpha}^{(4)} = (3, 2)$. However, $\vec{\alpha}^{(1)} + \vec{\alpha}^{(2)} = (1, 2)$, which is not preserved, and thus this diagram does not correspond to a quantum channel. From this view we can derive several interesting observations that will be presented in the rest of the section.

From this readily follows an amusing property: the set of all multi-indices $\vec{\gamma}$ for which $\tau_{\vec{\gamma}} = 1$ is closed under binary vector addition; in other words, it forms a vector subspace of the set of all multi-indices. A moment's consideration will further show that the above reasoning can be inverted; that is, if we set all $\tau_{\vec{\gamma}}$ equal to 1 whenever $\vec{\gamma}$ belongs to a given vector subspace of the set of all indices, then τ indeed has an image which has only positive components. In other words, there is a one-to-one correspondence between a quantum channel, and a vector subspace of the aforementioned space.

With this information, we present a procedure to generate all solutions: we start out from the solution having $\tau_{\vec{0}} = 1$, with everything else zero. We may then successively switch $\tau_{\vec{\alpha}}$'s to 1 for various values of $\vec{\alpha}$, taking care immediately to set equal to 1 the components of τ that correspond to values of $\vec{\beta}$ generated by the previously switched values of $\vec{\alpha}$ via the operation $\oplus$. Doing so, in an ordered way, allows one to generate all PCE quantum channels with a given set of preserved components, without the need of exploring the exponentially large space of all PCE maps.

We can show that all PCE quantum channels preserve 2^K components. First recall that a vector space of dimension d over a field of q elements has q^d elements [37]. Now V is a vector space on a field of two elements having dimension $2N$. We have seen earlier that

$$W = \{\vec{\alpha} : \vec{\alpha} \in V, \tau_{\vec{\alpha}} = 1\} \quad (25)$$

is a subspace of V. As such, W has a given dimension K, which means that W has 2^K elements. In other words, a set of indices $\tau_{\vec{\alpha}}$ with the property discussed above can only have 2^K elements equal to 1, for a given integer K.

It is natural to ask how many PCE quantum channels exist that preserve 2^K components. One can calculate such number, $\mathcal{S}_{N,K}$, by examining the number of different independent subsets of vectors that spawn a given vector subspace. In Appendix C we show that

$$\mathcal{S}_{N,K} = \prod_{m=0}^{K-1} \frac{2^{2N-m} - 1}{2^{K-m} - 1}. \quad (26)$$

From the above expression, it is easy to see the symmetry relation

$$\mathcal{S}_{N,K} = \mathcal{S}_{N,2N-K} \quad (27)$$

which suggests a relation between individual channels that preserve K and $2N - K$ Pauli components that for the time being has escaped our efforts to identify.

Finally, let us point out the following: if we wish to specify a PCE channel explicitly, the naive way to proceed would be simply to list all the Pauli components which are not erased. This requires in general, however, an exponential amount of information: that is, if the system has N qubits, we generally require of the order of 2^N bits to do this. If, on the other hand, we take advantage of the vector space structure of a PCE channel, we only need to specify a basis. Since a basis consists of N vectors of length N, the information required is only of N^2 bits, so that we have obtained a very substantial improvement by exploiting complete positivity. This is reminiscent of a rather similar effect in *stabilizer states* which can also be specified by N^2 bits, as opposed to an exponentially large number of basis coefficients for arbitrary states. A stabilizer state is one which is the common eigenvector to the eigenvalue 1 of a set of N commuting Pauli strings. The similarity is highly intriguing, and potentially of interest, since stabilizer states are of central importance in quantum error correction [38].

IV. GENERATORS

We now discuss the existence of a generator set for all PCE quantum channels and how to label each of them uniquely as $\mathcal{G}_{\vec{\alpha}}$ (according to its local action on every qubit in the system). Finally we will discuss a symmetry of PCE quantum channel generators and a connection between them and A [see Eq. (15)].

There exists a subset of PCE quantum channels that generates the entire set; the nature of these generators may be studied, as we shall see, with the properties of the aforementioned vector space. By standard theorems of linear algebra, any proper subspace W [see Eq. (25)] can be extended to a maximal nontrivial subspace of dimension $2N - 1$ by adjoining appropriate additional basis elements. This can be done in different ways. We therefore arrive to the set of maximal extensions of W, where every maximal subspace corresponds to a PCE quantum channel that preserves half of the Pauli components. The intersection of all the elements of this set reduces to W itself, and since intersection of subspaces translates to composition of PCE channels this implies that all PCE quantum channels can be obtained as compositions of PCE channels corresponding to maximally nontrivial subspaces, plus the identity map. In other words, the set of PCE quantum channels that preserve half of the components plus the identity map is a generator set for all PCE channels. Consider Fig. 3; Figs. 3(c)–3(e) represent nontrivial PCE generators (PCEGs) and the composition of any two of them yields the PCE channel corresponding to Fig. 3(b).

A PCEG may be characterized by its local action on every qubit in the system. This action can be encoded using a multi-index $\vec{\alpha}$, as in (4), hence each of the different 4^N multi-indices may be uniquely related to each of the PCE generators and thus denoted as $\mathcal{G}_{\vec{\alpha}}$ (see Figs. 4 and 5). The proof is simplified if one uses the Kraus representation developed in Sec. V, so we postpone the demonstration to Appendix D. For single qubits, the identity corresponds to $\mathcal{G}_0$, shown in Fig. 1(b), whereas $\mathcal{G}_3$ is shown in Fig. 1(c). The two-qubit PCE generator represented in Fig. 3(c) acts on the first qubit (first column) as a map of its Bloch sphere to the x axis, and on the second qubit (first row) as an identity, hence it is labeled $\mathcal{G}_{(1,0)}$. See Fig. 5 for the notation of all two-qubit PCE generators.

A reflection symmetry is identified for PCE generators. Consider the map $\Sigma^{(k)}$ that reflects a multi-index $\vec{\alpha}$ with respect to the kth axis. This map leaves all components of $\vec{\alpha}$ invariant, except the kth component, which is transformed
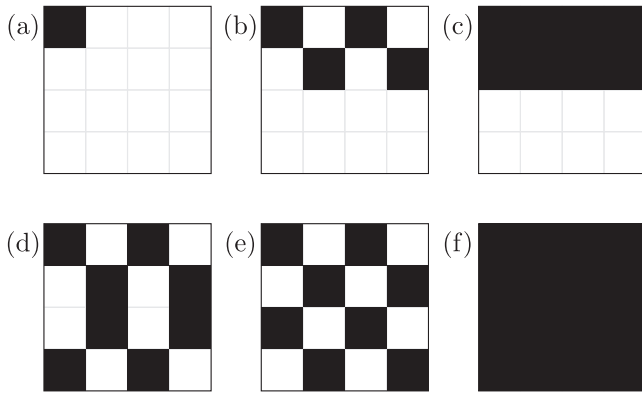
FIG. 3. Examples of diagrams for several two-qubit PCE quantum channels: (a) the totally depolarizing channel and (b) a PCE channel that preserves four components—the normalization component, one local component of qubit 2, and two correlations between the two qubits. (c), (d), and (e) show the three generators $\mathcal{G}_{(1,0)}$, $\mathcal{G}_{(3,2)}$, and $\mathcal{G}_{(2,2)}$, respectively; the combination (overlap of diagrams) of any two of them yields the channel in (b). (f) represents the identity map.

according to

$$0 \mapsto 3, \quad 3 \mapsto 0, \quad 1 \mapsto 2, \quad 2 \mapsto 1. \tag{28}$$

The maps have the following properties:

(1) $\Sigma^{(k)}(\vec{\alpha}) \oplus \Sigma^{(k)}(\vec{\beta}) = \vec{\alpha} \oplus \vec{\beta}$.

(2) $\Sigma^{(k)}(\vec{\alpha}) \neq \vec{\alpha}$.

From the first property, we now obtain

$$\vec{\alpha} = \Sigma^{(k)}(\vec{\alpha}) \oplus \Sigma^{(k)}(\vec{0}). \tag{29}$$

This implies that if $\Sigma^{(k)}(\vec{0})$ belongs to a channel then $\tau_{\vec{\alpha}} = \tau_{\Sigma^{(k)}(\vec{\alpha})}$, where we used the fact that for channels the nonzero elements are closed under $\oplus$. In other words, the components of a PCE channel are symmetric under reflection over the kth axis. Now consider the case in which $\Sigma^{(k)}(\vec{0})$ does not belong to generator. Then $\tau_{\vec{\alpha}} \neq \tau_{\Sigma^{(k)}(\vec{\alpha})}$, since the case $\tau_{\vec{\alpha}} = \tau_{\Sigma^{(k)}(\vec{\alpha})} = 1$ is forbidden due to Eq. (28) and the case $\tau_{\vec{\alpha}} = \tau_{\Sigma^{(k)}(\vec{\alpha})} = 0$ is also forbidden because for generators the codimension of the associated vector space is 1. This means that the components of a PCE channel are antisymmetric with respect to reflection over the kth axis. Indeed, the two-qubit PCE generators $\mathcal{G}_{(1,0)}$, $\mathcal{G}_{(3,2)}$, and $\mathcal{G}_{(2,2)}$ represented in Figs. 2(c), 2(d) and 2(e), respectively, are either symmetric or antisymmetric under re-
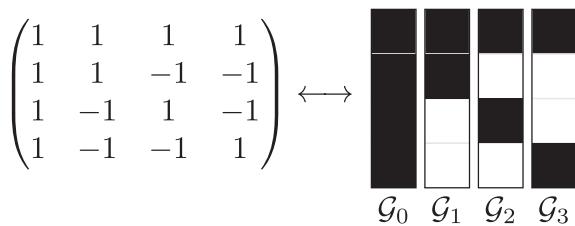
FIG. 4. The connection between rows or columns of a and single-qubit PCE generators $\mathcal{G}_\alpha$ is shown. One can identify the -1s of a with zeros in the sets $\{\tau_\alpha\}$ of preserved and erased components of each $\mathcal{G}_\alpha$. For any number of particles, such a simple relation holds see Sec. IV and Appendix D.
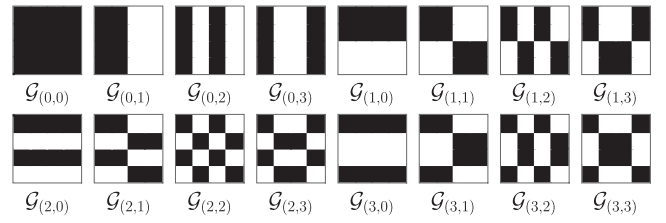
FIG. 5. PCE generators for two qubits. Notice that all generators are either symmetric or antisymmetric under horizontal and vertical reflections.

flection with respect to lines that divide the diagram in half vertically and horizontally.

Finally, it is worth pointing out that A (and thus a) [see Eq. (15)] encodes all the information of PCE generators $\mathcal{G}_{\vec{\alpha}}$ and, therefore, of all PCE quantum channels. From A, the tensor power of matrix a, one can infer the components $\{\tau_{\vec{\alpha}}\}$ of a PCE generator $\mathcal{G}_{\vec{\alpha}}$ by taking row (or column) $\vec{\alpha}$ of A and replacing -1 with 0. The proof of the connection between PCEGs and A is given in Appendix D, and in Fig. 4 we illustrate this connection for the single-qubit case.

V. PCE CHANNELS AND DECOHERENCE

Lindblad processes arise naturally in many theoretical [15,30,39–42] and experimental [43] settings and are archetypical in decoherence dynamics. Moreover, these processes lead to a monotonic (continuous) loss of information [44] and describe noninvertible channels in the asymptotic limit $t \to \infty$ [this can be seen from the monotonic (continuous) decrease of the determinant (see Ref. [30])]. It is known that not every quantum channel can be seen as a snapshot of a process arising from a traditional Lindblad equation or even a time-dependent Lindblad equation [15,30]. Therefore, an interesting question is whether PCE channels can be seen as limit points of some Markovian processes. In this section we prove that in fact they are, and give two examples of Markovian implementations. The first of them consists in identifying each PCE channel as a fixed point of some pure dissipative process, and in the second implementation we relate each PCE channel to fixed points of some memoryless collision model.

A. Kraus representation

To derive the aforementioned implementations, we exploit the existence of the PCEGs and their *Kraus representation* (or operator-sum representation) which, for an arbitrary channel $\mathcal{E}$, reads

$$\mathcal{E}[\rho] = \sum_i K_i \rho K_i^\dagger, \tag{30}$$

with $\sum_i K_i^\dagger K_i = \mathbb{1}$ (the trace-preserving condition) [45]. Inspection of the Kraus operators for two-qubit PCEGs leads to the ansatz that the Kraus operators for the generator of $\mathcal{G}_{\vec{\alpha}}$ are

$$K_0 = \frac{\mathbb{1}}{\sqrt{2}}, \quad K_1 = \frac{\sigma_{\vec{\alpha}}}{\sqrt{2}}, \tag{31}$$

since the Kraus operators corresponding to a single-qubit PCE are $\{\mathbb{1}/\sqrt{2}, \sigma_\alpha/\sqrt{2}\}$, corresponding to the operation that

leaves the component σ_α invariant [6]. Notice that according to Kraus operators the generators $\mathcal{G}_{\vec{\alpha}}$ are N-qubit flip channels with flip probability $1/2$, where the joint flip is $\rho \mapsto \sigma_{\vec{\alpha}} \rho \sigma_{\vec{\alpha}}$. In fact, tracing out all particles except the kth one gives the well-known qubit flip channels, i.e., $\mathrm{tr}_{\not k} \mathcal{G}_{\vec{\alpha}} = \mathcal{G}_{\alpha_k}$ [see Eq. (D1)]. More generally, tracing out m particles leaves a $N - m$ particles flip channel (completely dephasing).

We shall first show that the Kraus operators in Eq. (31) produce a PCE. Notice that $\sigma_\alpha \sigma_\beta \sigma_\alpha = a_{\alpha\beta} \sigma_\beta$ [see Eq. (10)], which in turn implies that

$$\sigma_{\vec{\alpha}} \sigma_{\vec{\beta}} \sigma_{\vec{\alpha}} = A_{\vec{\alpha}\vec{\beta}} \sigma_{\vec{\beta}}. \tag{32}$$

Next, consider the action of a channel with Kraus representation (31) on a N-qubit system:

$$
\begin{aligned}
\rho \mapsto & \frac{1}{2^N} \sum_{\vec{\beta}} r_{\vec{\beta}} \left(\frac{1}{2} \sigma_{\vec{\beta}} + \frac{1}{2} \sigma_{\vec{\alpha}} \sigma_{\vec{\beta}} \sigma_{\vec{\alpha}} \right) \\
= & \frac{1}{2^N} \sum_{\vec{\beta}} r_{\vec{\beta}} \frac{1 + A_{\vec{\alpha}\vec{\beta}}}{2} \sigma_{\vec{\beta}}.
\end{aligned} \tag{33}
$$

However, since $A_{\vec{\alpha}\vec{\beta}} = \pm 1$, the channel characterized by the Kraus operators in Eq. (31) is a PCE channel. Moreover, one can notice that, except for the first row, half of the matrix elements of each row are $+1$ and half are -1, which implies that the channel is a PCEG.

Observe also that a different choice of $\vec{\alpha}$ in Eq. (31) leads to different channels. This follows from the fact that if two channels were the same this would imply that the matrix representation of the corresponding superoperator of $\rho \mapsto \sigma_{\vec{\alpha}} \rho \sigma_{\vec{\alpha}}$ would have to be the same, which is clearly false. Since there are 4^n different $\vec{\alpha}$ values, this implies that all PCEGs (plus the identity map) are in one-to-one correspondence.

B. Pure dissipative implementation

In this section we show that any PCE channel can be seen as the fixed point of some decoherence process, starting with PCEGs and then extending to more general channels. Consider the following dynamical process that implements $\mathcal{G}_{\vec{\alpha}}$ when $t \to \infty$:

$$
\begin{aligned}
\mathcal{G}_{\vec{\alpha},t}[\rho] = & e^{-\gamma t} \rho + (1 - e^{-\gamma t}) \mathcal{G}_{\vec{\alpha}}[\rho] \\
= & \frac{(1 + e^{-\gamma t})}{2} \rho + \frac{(1 - e^{-\gamma t})}{2} \sigma_{\vec{\alpha}} \rho \sigma_{\vec{\alpha}},
\end{aligned} \tag{34}
$$

where $\gamma > 0$. It is easy to show that the family of channels $\mathcal{G}_{\vec{\alpha},t}$ parametrized with $t \geqslant 0$ forms a one-parametric semigroup, i.e., $\mathcal{G}_{\vec{\alpha},t_1} \mathcal{G}_{\vec{\alpha},t_2} = \mathcal{G}_{\vec{\alpha},t_1+t_2}$. Therefore $\mathcal{G}_{\vec{\alpha},t}$ describes a dissipative time-homogeneous Markovian process, which is always characterized by some Lindblad generator [39]. The Lindblad generator of $\mathcal{G}_{\vec{\alpha},t}$, denoted by $\mathcal{L}_{\vec{\alpha}}$, can be obtained using the standard procedure:

$$\mathcal{L}_{\vec{\alpha}}[\rho] = \left. \frac{d\mathcal{G}_{\vec{\alpha},t}[\rho]}{dt} \right|_{t=0} = \frac{\gamma (\sigma_{\vec{\alpha}} \rho \sigma_{\vec{\alpha}} - \rho)}{2}, \tag{35}$$

where the unique Lindblad operator associated with the relaxation ratio $\gamma/2$ is simply $\sigma_{\vec{\alpha}}$. Notice that $\sigma_{\vec{\alpha}}$ is traceless, therefore the process is purely dissipative [30].

Since PCEGs commute, we can describe easily any other PCE channel as a fixed point of a decoherence process. For

them, the Lindblad generators are the sum of the Lindbladians of the corresponding generators. As an example, consider the channel depicted in Fig. 2(b); it is equal to $\mathcal{G}_{(0,3)} \mathcal{G}_{(3,3)}$, therefore it is the fixed point of the dissipation process described with the following Lindbladian:

$$\mathcal{L}[\rho] = \frac{\gamma_{(0,3)} (\sigma_{(0,3)} \rho \sigma_{(0,3)} - \rho)}{2} + \frac{\gamma_{(3,3)} (\sigma_{(3,3)} \rho \sigma_{(3,3)} - \rho)}{2}, \tag{36}$$

where $\gamma_{(0,3)}$ and $\gamma_{(3,3)}$ are positive and correspond to the Lindblad operators $\sigma_{(0,3)}$ and $\sigma_{(3,3)}$. Notice that such election of Lindblad operators is not unique, as the PCE channel described here is also equal to $\mathcal{G}_{(0,3)} \mathcal{G}_{(3,0)}$.

C. Collision model implementation

We show now that PCE channels can also be implemented with *simple collision models* [46]. To do this, observe that employing the Stinespring dilation theorem [47] PCEGs can be implemented using a unitary over the system and an ancilla. Since PCEGs always have Kraus rank 2, one can always choose a qubit as the ancillary system. Concretely,

$$\mathcal{G}_{\vec{\alpha}}[\rho] = \mathrm{tr}_{\mathrm{qubit}}[U_{\vec{\alpha}} (\rho \otimes |0\rangle\langle 0|) U_{\vec{\alpha}}^\dagger], \tag{37}$$

where $\mathrm{tr}_{\mathrm{qubit}}$ denotes the partial trace over the ancillary qubit, with the unitary defined as follows:

$$U_{\vec{\alpha}} |\psi\rangle |0\rangle = \frac{1}{\sqrt{2}} (|\psi\rangle |0\rangle + \sigma_{\vec{\alpha}} |\psi\rangle |1\rangle), \tag{38}$$

$$U_{\vec{\alpha}} |\psi\rangle |1\rangle = \frac{1}{\sqrt{2}} (|\psi\rangle |0\rangle - \sigma_{\vec{\alpha}} |\psi\rangle |1\rangle). \tag{39}$$

Therefore, any concatenation of PCEGs can be described as a collision model with as many collisions as generators needed. In fact, generators are described with one collision. For the general case consider some PCE channel $\mathcal{E}$ generated with $\{\mathcal{G}_{\vec{\alpha}_1}, \mathcal{G}_{\vec{\alpha}_2}, \ldots, \mathcal{G}_{\vec{\alpha}_M}\}$. For this we can define an environment consisting of M qubits initially in the state $(|0\rangle\langle 0|)^{\otimes M}$, or equivalently one qubit with the additional assumption that its state is reset to $|0\rangle$ after each collision (memoryless collisions). The collision with the k-th particle is described by $U_{\vec{\alpha}_k}$, which acts solely over the system and the kth particle. Therefore $\mathcal{E}$ can be written as follows:

$$\mathcal{E}[\rho] = \mathrm{tr}_{\mathrm{E}} \left[(U_{\vec{\alpha}_1} \ldots U_{\vec{\alpha}_M}) \rho \otimes (|0\rangle\langle 0|)^{\otimes M} (U_{\vec{\alpha}_1} \ldots U_{\vec{\alpha}_M})^\dagger \right], \tag{40}$$

where tr_{E} is the partial trace over all ancillary qubits. Notice that as PCEGs commute the order of the collisions is irrelevant.

VI. CONCLUSIONS AND OUTLOOK

In this paper we introduce and characterize a set of quantum maps which either preserve or completely erase the components of a multiqubit density matrix, in the basis of Pauli strings; we call those maps *Pauli component erasing maps*. For a single qubit these include the completely depolarizing and dephasing channels. To start the characterization, we note that not all PCE maps are quantum channels, as some are not completely positive. In fact, the most laborious task of this paper was to evaluate complete positivity conditions given by the Choi-Jamiokowski isomorphism, after which we

showed that the components of PCE quantum channels form a finite vector space. This in turn allows us to unravel several properties, such as the possible number of PCE channels and the number of components preserved, while also providing advantages to study numerically this set, for example, by implying an efficient method to construct all quantum channels for a given number of qubits.

Similar to other objects in open quantum systems (for example, Lindblad processes), PCE quantum channels form a semigroup, but finite in this case. For PCE channels, the generators are generalized flip operations, i.e., channels that with probability $1/2$ apply a joint flip. This structure allows us to link this channel with multiqubit decoherence processes which can be described, say, by simple dissipative processes or memoryless collision models, which in turn may pave a way to either implement these channels or connect them with already existing decoherence families. This, together with the discovered algebraic structure that translates complete positivity into an explicit conditioned preservation of many-body correlations, encompasses an advance in the knowledge of the mathematical structures underlying general quantum channels.

In the future we might consider generalizations (such as going from qubits to qudits) as well as the geometric role of PCE channels within the set of all quantum channels to further advance the understanding of open quantum systems. We have thus described a family of quantum channels with a very special mathematical structure that allows us to widen the understanding of quantum channels in the context of many-body systems.

APPENDIX A: QUANTUM-CLASSICAL CHANNELS

A quantum-classical (QC) channel is defined by using an orthonormal basis in the Hilbert space. Let $B = \{|\psi_i\rangle\}$ be such a basis in H with $\dim(\mathsf{H}) = 2^N$; the QC channel associated to B is

$$\mathcal{E}_B^{\mathrm{QC}}[\rho] = \sum_{i=1}^{2^N} \langle\psi_i|\rho|\psi_i\rangle |\psi_i\rangle\langle\psi_i|, \qquad (\mathrm{A1})$$

that is, QC channels project density matrices onto the corresponding diagonal matrix in the basis B [22].

Consider now that the basis B is the simultaneous eigenbasis of a maximal set of commuting Pauli strings denoted by set(B); such a set contains 2^N elements (including the identity), and there are $2^N + 1$ of such sets [29]. Now we

proceed to demonstrate that the QCs defined in this way are PCE channels with 2^N 1s on their diagonal.

First we compute the components of $\mathcal{E}_B^{\mathrm{QC}}$ in the basis $2^{-N/2}\{\sigma_{\bar{\alpha}}\}$:

$$(\mathcal{E}_B^{\mathrm{QC}})_{\bar{k}\bar{l}} = \frac{1}{2^N} \sum_{i=1}^{2^N} \langle\psi_i|\sigma_{\bar{k}}|\psi_i\rangle\langle\psi_i|\sigma_{\bar{l}}|\psi_i\rangle. \qquad (\mathrm{A2})$$

To evaluate the components, observe that $\langle\psi_i|\sigma_{\bar{k}}|\psi_i\rangle^2 = 1 \;\; \forall\sigma_{\bar{k}} \in \mathrm{set}(B)$, and from the formula for the purity of $|\psi_i\rangle$,

$$1 = \frac{1}{2^N} \sum_{\bar{k}} \langle\psi_i|\sigma_{\bar{k}}|\psi_i\rangle^2, \qquad (\mathrm{A3})$$

it follows that $\langle\psi_i|\sigma_{\bar{k}'}|\psi_i\rangle = 0 \;\; \forall\sigma_{\bar{k}'} \notin \mathrm{set}(B)$ since there are only positive terms in the sum, and 2^N of them are already equal to 1. Therefore,

$$\begin{aligned}(\mathcal{E}_B^{\mathrm{QC}})_{\bar{k}\bar{k}} &= 1, \\ (\mathcal{E}_B^{\mathrm{QC}})_{\bar{k}\bar{l}'} &= (\mathcal{E}_B^{\mathrm{QC}})_{\bar{l}'\bar{l}'} = 0 \;\; \forall\sigma_{\bar{k}} \in \mathrm{set}(B) \;\; \forall\sigma_{\bar{l}'} \notin \mathrm{set}(B).\end{aligned} \qquad (\mathrm{A4})$$

To compute $(\mathcal{E}_B^{\mathrm{QC}})_{\bar{k}\bar{l}}$ for $\sigma_{\bar{k}}, \sigma_{\bar{l}} \in \mathrm{set}(B)$ with $\vec{k} \neq \vec{l}$, observe that $(\mathcal{E}_B^{\mathrm{QC}})_{\bar{k}\bar{l}} = (\mathcal{E}_B^{\mathrm{QC}})_{\bar{l}\bar{k}}$, i.e., the matrix corresponding to $\mathcal{E}^{\mathrm{QC}}$ is an orthogonal projector. Thus, considering the block,

$$\begin{bmatrix}(\mathcal{E}_B^{\mathrm{QC}})_{\bar{k}\bar{k}} & (\mathcal{E}_B^{\mathrm{QC}})_{\bar{k}\bar{l}} \\ (\mathcal{E}_B^{\mathrm{QC}})_{\bar{k}\bar{l}} & (\mathcal{E}_B^{\mathrm{QC}})_{\bar{l}\bar{l}}\end{bmatrix} = \begin{bmatrix}1 & (\mathcal{E}_B^{\mathrm{QC}})_{\bar{k}\bar{l}} \\ (\mathcal{E}_B^{\mathrm{QC}})_{\bar{k}\bar{l}} & 1\end{bmatrix}, \qquad (\mathrm{A5})$$

it is easy to check that the latter is a projector only if $(\mathcal{E}_B^{\mathrm{QC}})_{\bar{k}\bar{l}} = 0$. Since there are exactly 2^N elements of the form $(\mathcal{E}_B^{\mathrm{QC}})_{\bar{k}\bar{k}}$ with $\sigma_{\bar{k}} \in \mathrm{set}(B)$, then the channel $\mathcal{E}_B^{\mathrm{QC}}$ is PCE with 2^N 1s on its diagonal.

APPENDIX B: DIAGONALIZATION OF CHOI MATRIX $\mathcal{D}_N$

In order to simplify the derivation of the relations, let us employ pairs of binary indices instead of a single quaternary, i.e., $\alpha \to j + 2k$. For the sake of clarity, we use Latin symbols for binary indices, and reserve Greek letters for quaternary ones. We can write the elements of the Pauli basis $(\sigma_0, \sigma_1, i\sigma_2, \sigma_3)$, compactly as $\sigma_{kl} = \sum_{j=0}^{1}(-1)^{jk}|j\rangle\langle j + l(\mathrm{mod}2)|$. In vectorized form

$$|\sigma_{kl}\rangle\rangle = \sum_{j=0}^{1}(-1)^{jk}|j\rangle|j + l(\mathrm{mod}\,2)\rangle, \qquad (\mathrm{B1})$$

and its inverse relation

$$|k\rangle|k + l(\mathrm{mod}\,2)\rangle = \frac{1}{2}\sum_{j=0}^{1}(-1)^{jk}|\sigma_{jl}\rangle\rangle. \qquad (\mathrm{B2})$$

On the other hand, the matrix form of an arbitrary Pauli map $\mathcal{E}$ may be written as

$$\begin{aligned}\hat{\mathcal{E}} &= \frac{1}{2}\sum_{lm=0}^{1}\tau_{lm}|\sigma_{lm}\rangle\rangle\langle\langle\sigma_{lm}| \qquad (\mathrm{B3})\\ &= \frac{1}{2}\sum_{jklm}\tau_{lm}(-1)^{l(j+k)}\\ &\quad \times |j\rangle|j + m(\mathrm{mod}\,2)\rangle\langle k|\langle k + m(\mathrm{mod}\,2)|. \qquad (\mathrm{B4})\end{aligned}$$

After applying the reshuffling operation on $\hat{\mathcal{E}}$, we obtain the Choi matrix associated to the map. It reads

$$
\mathcal{D} = \frac{1}{2} \sum_{jklm} \tau_{lm} (-1)^{l(j+k)}
$$
$$
\times |j\rangle |k\rangle \langle j+m(\text{mod}2)|\langle k+m(\text{mod}2)|. \quad \text{(B5)}
$$

Note furthermore that the expression above may also be written as a combination of tensor products of Pauli matrices:

$$
\mathcal{D} = \frac{1}{2} \sum_{lm} \tau_{lm} \sigma_{lm} \otimes \sigma_{lm}^*. \quad \text{(B6)}
$$

Returning to Eq. (B5), let us apply the index relabeling $k \to j + k(\text{mod}2)$; then the Choi matrix reads

$$
\mathcal{D} = \frac{1}{2} \sum_{jklm} \tau_{lm} (-1)^{lk}
$$
$$
\times |j\rangle |j+k(\text{mod } 2)\rangle \langle j+m(\text{mod } 2)|\langle j+m+k(\text{mod } 2)|, \quad \text{(B7)}
$$

since $(-1)^{j+(j+k(\text{mod}2))} = (-1)^k$. To continue, we use the relation between computational and Pauli elements [Eq. (B2)], and notice that $\sum_j (-1)^{j(m\pm n)} = 2\delta_{mn}$. We arrive to the simple expression

$$
\mathcal{D} = \frac{1}{2} \sum_{jk} \left(\frac{1}{2} \sum_{lm} (-1)^{jm+kl} \tau_{lm} \right) |\sigma_{jk}\rangle\!\rangle\!\langle\!\langle\sigma_{jk}|. \quad \text{(B8)}
$$

Notice that $\mathcal{D}$ is already written in its diagonal form, and one can identify by inspection the eigenvalues. The eigenvalues read

$$
\lambda_{jk} = \frac{1}{2} \sum_{lm} (-1)^{jm+kl} \tau_{lm}, \quad \text{(B9)}
$$

or more compactly $\lambda = (1/2) H \otimes H \tau$, where H is the Hadamard matrix.

For the sake of convenience in the demonstration of several useful properties of the PCE channels, we shall reorder the eigenvalues, to write

$$
\lambda = \frac{1}{2} a \tau \quad \text{(B10)}
$$

with a the matrix shown in Eq. (10) instead of $H \otimes H$. This can be done due to the fact that both matrices (a and $H \otimes H$) are equivalent up to a permutation of rows. In other words this operation corresponds to a reordering of the eigenvalues.

N qubits

To work out the N-qubit case, we again rely on binary indices. In this case, we replace N-dimensional vector $\vec{\alpha}$ with a pair of N-dimensional vector binary indices $\vec{j}$ and $\vec{k}$ so that each entry α_i of $\vec{\alpha}$ is identified with the pair j_i and k_i as in the single-qubit case of the previous subsection. Then, all the steps leading to Eq. (B9) can be redone.

The tensor product of Pauli matrices, in vector form, will be denoted by $|\sigma_{\vec{k}\vec{l}}\rangle\!\rangle$. With this in mind, a N-qubit Pauli map can be written as

$$
\hat{\mathcal{E}}_N = \frac{1}{2^N} \sum_{\vec{l}\vec{m}} \tau_{\vec{l}\vec{m}} |\sigma_{\vec{l}\vec{m}}\rangle\!\rangle\!\langle\!\langle\sigma_{\vec{l}\vec{m}}|. \quad \text{(B11)}
$$

The generalizations of Eqs. (B1) and (B2) read

$$
|\sigma_{\vec{k}\vec{l}}\rangle\!\rangle = \sum_{\vec{j}} (-1)^{\vec{j}\cdot\vec{k}} |\vec{j}\rangle |\vec{j}+\vec{l}(\text{mod}2)\rangle, \quad \text{(B12)}
$$

$$
|\vec{l}\rangle |\vec{l}+\vec{n}(\text{mod}2)\rangle = \frac{1}{2^N} \sum_{\vec{m}} (-1)^{\vec{m}\cdot\vec{l}} |\sigma_{\vec{m}\vec{n}}\rangle\!\rangle. \quad \text{(B13)}
$$

By employing the previous relations, we can write the matrix representation of the map, $\hat{\mathcal{E}}_N$ in the N-qubit computational basis, as

$$
\hat{\mathcal{E}} = \frac{1}{2^N} \sum_{\vec{j}\vec{k}\vec{l}\vec{m}} \tau_{\vec{l}\vec{m}} (-1)^{\vec{l}(\vec{j}+\vec{k})}
$$
$$
\times |\vec{j}\rangle |\vec{j}+\vec{m}(\text{mod}2)\rangle \langle \vec{k}|\langle \vec{k}+\vec{m}(\text{mod}2)|. \quad \text{(B14)}
$$

In this way it is straightforward to apply the reshuffling operation on $\hat{\mathcal{E}}_N$ to obtain the associated Choi matrix, and then transform back to the Pauli basis and simplify to obtain

$$
\mathcal{D}_N = \frac{1}{2^N} \sum_{\vec{m}\vec{n}} \left(\frac{1}{2^N} \sum_{\vec{l}\vec{m}} \tau_{\vec{l}\vec{m}} (-1)^{\vec{l}\cdot\vec{n}+\vec{m}\cdot\vec{m}} \right) |\sigma_{\vec{m}\vec{n}}\rangle\!\rangle\!\langle\!\langle\sigma_{\vec{m}\vec{n}}|. \quad \text{(B15)}
$$

All intermediate steps, from Eq. (B3) to Eq. (B8) are similar, but with a vectorized version of the indices, and appropriate normalization constants. Again, we are left with an expression that displays explicitly the eigenvalues of the Choi matrix, so we can write

$$
\lambda_{\vec{j}\vec{k}} = \frac{1}{2^N} \sum_{\vec{l}\vec{m}} (-1)^{\vec{j}\cdot\vec{m}+\vec{k}\cdot\vec{l}} \tau_{\vec{l}\vec{m}} \quad \text{(B16)}
$$

or more compactly $\lambda = (H \otimes H/2)^{\otimes N} \tau$. Again, we prefer to reorganize the indices to be able to write

$$
\lambda = \frac{1}{2^N} A\tau, \quad \text{(B17)}
$$

where $A = a^{\otimes N}$.

APPENDIX C: NUMBER OF PCE'S FOR A FIXED NUMBER OF INVARIANT COMPONENTS

Finally, we may enumerate straightforwardly the subspaces W of dimension K. We do this in two steps: first, we evaluate $\mathcal{N}_{K,N}$, the number of all linearly independent subsets V with K elements. Each of these is the basis of one subspace of dimension K, but each subspace has a number $\mathcal{M}_K$ of different bases. The crucial point is that $\mathcal{M}_K$ is independent of the subspace under consideration: $\mathcal{M}_K$ simply describes the number of linear maps of W onto itself. The total number $\mathcal{S}_{N,K}$ of subspaces of dimension K is therefore $\mathcal{N}_{N,K}/\mathcal{M}_K$.

To evaluate $\mathcal{N}_{N,K}$ we proceed by steps: the first element of the basis can be any nonzero element, of which the number is $2^{2N} - 1$. For the basis element $m + 1$, we must choose from those which do not belong to the m-dimensional space generated by the first m basis elements, so that one chooses from $2^{2N} - 2^m$. We thus have

$$
\mathcal{N}_{N,K} = \prod_{m=0}^{K-1} (2^{2N} - 2^m). \quad \text{(C1)}
$$

On the other hand, any map of a K-dimensional vector space W onto itself is uniquely defined by a nonsingular binary $K \times K$ matrix over the field $\{0, 1\}$. To count these, we proceed as above: the first line is an arbitrary nonzero vector, of which there are $2^K - 1$. For the row $m + 1$ we must choose an arbitrary vector not belonging to those generated by the first m vectors, of which there are $2^K - 2^m$. This eventually yields

$$\mathcal{M}_K = \prod_{m=0}^{K-1} (2^K - 2^m). \tag{C2}$$

From this it follows that

$$\mathcal{S}_{N,K} = \prod_{m=0}^{K-1} \frac{2^{2N-m} - 1}{2^{K-m} - 1}. \tag{C3}$$

APPENDIX D: LOCAL ACTION AND LABELING OF PCE GENERATORS

The local action of a generator $\mathcal{G}_{\vec{\alpha}}$ on every qubit in the system depends only, as its notation suggests, on the multi-index $\vec{\alpha}$. This index has a simple meaning that can be read from the graphical representation of the channel. Recall the single-qubit PCE generators, shown in Fig. 4, denoted by $\mathcal{G}_0$ (corresponding to the identity map) and $\mathcal{G}_{1,2,3}$ (corresponding to the completely bit, phase, and bit-phase flip channels, respectively). One can easily read the diagrams in the following manner: $\alpha = 0$ corresponds to all squares black, whereas for $\alpha > 0$ we have only the zeroth and the αth squares black. Let us generalize this characterization rule for N-qubit PCE generators. Consider that the reduced density matrix of the kth qubit after generator $\mathcal{G}_{\vec{\alpha}}$ acts on the entire system

$$\text{tr}_{\not{k}} \mathcal{G}_{\vec{\alpha}}[\rho] = \frac{1}{2} \text{tr}_{\not{k}} (\rho + \sigma_{\vec{\alpha}} \rho \sigma_{\vec{\alpha}}) = \frac{\rho_k}{2} + \frac{\sigma_{\alpha_k} \rho_k \sigma_{\alpha_k}}{2}$$
$$= \mathcal{G}_{\alpha_k}[\rho_k], \tag{D1}$$

where $\not{k}$ means that all qubits except for the kth one are traced out. We can read from (D1) that α_k not only characterizes $\mathcal{G}_{\alpha_k}$ but actually tells us which single-qubit channel is acting locally on the kth qubit. The action of $\mathcal{G}_{\alpha_k}$ on the local components of the reduced density matrix ρ_k reads $r_{0,\ldots,j_k,\ldots,0} \mapsto \tau_{0,\ldots,j_k,\ldots,0} r_{0,\ldots,j_k,\ldots,0}$. The general characterization rule for all PCE generators $\mathcal{G}_{\vec{\alpha}}$ is clear now: if all $\tau_{0,\ldots,j_k,\ldots,0} = 1$, then $\alpha_k = 0$; otherwise, if $\tau_{0,\ldots,j_k,\ldots,0} = 1$ (with $j_k > 0$), then $\alpha_k = j_k$. For two-qubit PCE diagrams this means that the multi-index $\vec{\alpha}$ is encoded in the first column and row of the diagrams. For example, see $\mathcal{G}_{(0,2)}$ in Fig. 5, where all $\tau_{j_1,0} = 1$ and $\tau_{(0,2)} = 1$, and thus $\vec{\alpha} = (0, 2)$. In Fig. 5 we show all two-qubit PCE generators and their corresponding notation $\mathcal{G}_{\vec{\alpha}}$.

An interesting relation of the generators and the A matrix can be derived with the tools developed. Consider the generator $\mathcal{G}_{\vec{\alpha}}$, and its Pauli components $\tau_{\vec{\beta}}^{(\vec{\alpha})}$. We can calculate the former studying the action of the generator on the non-normalized state $\varrho = \sum_{\vec{\gamma}} \sigma_{\vec{\gamma}}$. Let us proceed with such calculation, using the Kraus decomposition Eq. (31):

$$\tau_{\vec{\beta}}^{(\vec{\alpha})} = \text{tr} \sigma_{\vec{\beta}} \mathcal{G}_{\vec{\alpha}}[\varrho] \tag{D2}$$

$$= \frac{1}{2} \sum_{\vec{\gamma}} \text{tr}[\sigma_{\vec{\beta}} \sigma_{\vec{\gamma}} + \sigma_{\vec{\beta}} \sigma_{\vec{\alpha}} \sigma_{\vec{\gamma}} \sigma_{\vec{\alpha}}] \tag{D3}$$

$$= \frac{1}{2} (1 + A_{\vec{\alpha} \vec{\beta}}) \tag{D4}$$

where we have used the orthogonality relations of Pauli matrices and Eq. (32). This means that one can read the αth generators directly from matrix A (see Fig. 4 for the $n = 1$ case). Alternatively one could construct the A matrix for $n = 2$, from Fig. 5, where the first row of this matrix is read from $\mathcal{G}_{(0,0)}$, replacing black (white) squares with 1s (-1s), the second row from $\mathcal{G}_{(0,1)}$, etc.

[1] J. S. Bell, Phys. Phys. Fiz. **1**, 195 (1964).

[2] S. Köhnke, E. Agudelo, M. Schünemann, O. Schlettwein, W. Vogel, J. Sperling, and B. Hage, Phys. Rev. Lett. **126**, 170404 (2021).

[3] H. Ollivier and W. H. Zurek, Phys. Rev. Lett. **88**, 017901 (2001).

[4] R. Horodecki, P. Horodecki, M. Horodecki, and K. Horodecki, Rev. Mod. Phys. **81**, 865 (2009).

[5] C. H. Bennett, G. Brassard, C. Crépeau, R. Jozsa, A. Peres, and W. K. Wootters, Phys. Rev. Lett. **70**, 1895 (1993).

[6] M. A. Nielsen and I. L. Chuang, *Quantum Computation and Quantum Information: 10th Anniversary Edition*, 10th ed. (Cambridge University, New York, 2011).

[7] F. Sapienza, F. Cerisola, and A. J. Roncaglia, Nat. Commun. **10**, 2492 (2019).

[8] M. Schlosshauer, Rev. Mod. Phys. **76**, 1267 (2005).

[9] G. J. Mooney, G. A. L. White, C. D. Hill, and L. C. L. Hollenberg, J. Phys. Commun. **5**, 095004 (2021).

[10] H.-J. Briegel, W. Dür, J. I. Cirac, and P. Zoller, Phys. Rev. Lett. **81**, 5932 (1998).

[11] C. H. Bennett, G. Brassard, S. Popescu, B. Schumacher, J. A. Smolin, and W. K. Wootters, Phys. Rev. Lett. **76**, 722 (1996).

[12] I. Georgescu, Nat. Rev. Phys. **2**, 519 (2020).

[13] B. M. Terhal, Rev. Mod. Phys. **87**, 307 (2015).

[14] G. Bacciagaluppi, in *The Stanford Encyclopedia of Philosophy*, edited by E. N. Zalta, Fall 2020 ed. (Metaphysics Research Lab, Stanford University, 2020).

[15] D. Davalos, M. Ziman, and C. Pineda, Quantum **3**, 144 (2019).

[16] M. B. Ruskai, S. Szarek, and E. Werner, Linear Algebra and Its Applications **347**, 159 (2002).

[17] H. Breuer and F. Petruccione, *The Theory of Open Quantum Systems* (Oxford University, New York, 2007).

[18] C. Duarte, G. D. Carvalho, N. K. Bernardes, and F. de Melo, Phys. Rev. A **96**, 032113 (2017).

[19] C. Pineda, D. Davalos, C. Viviescas, and A. Rosado, Phys. Rev. A **104**, 042218 (2021).

[20] T. Heinosaari and M. Ziman, *The Mathematical Language of Quantum Theory: From Uncertainty to Entanglement* (Cambridge University, New York, 2012).

[21] T. Rybár, S. N. Filippov, M. Ziman, and V. Bužek, J. Phys. B: At. Mol. Opt. Phys. **45**, 154006 (2012).

[22] M. Nathanson and M. B. Ruskai, J. Phys. A: Math. Theor. **40**, 8171 (2007).

[23] K. Siudzińska, Phys. Rev. A **102**, 032603 (2020).

[24] I. Sergeev, Rep. Math. Phys. **83**, 349 (2019).

[25] D. Chruściński and K. Siudzińska, Phys. Rev. A **94**, 022118 (2016).

[26] H. Ohno and D. Petz, Acta Math Hung **124**, 165 (2009).

[27] A. Fonseca, Phys. Rev. A **100**, 062311 (2019).

[28] G. Kimura, Phys. Lett. A **314**, 339 (2003).

[29] J. Lawrence, Č. Brukner, and A. Zeilinger, Phys. Rev. A **65**, 032320 (2002).

[30] M. M. Wolf and J. I. Cirac, Commun. Math. Phys. **279**, 147 (2008).

[31] I. Bengtsson and K. Zyczkowski, *Geometry of Quantum States: An Introduction to Quantum Entanglement*, 2nd ed. (Cambridge University, New York, 2017).

[32] A. Jamiołkowski, Rep. Math. Phys. **3**, 275 (1972).

[33] M.-D. Choi, Linear Algebra and Its Applications **10**, 285 (1975).

[34] M. A. Nielsen and I. L. Chuang, *Quantum Computation and Quantum Information: 10th Anniversary Edition*, 10th ed. (Cambridge University, New York, 2011).

[35] A. Gilchrist, D. R. Terno, and C. Wood, arXiv:0911.2539.

[36] We can further unravel the vector space, by identifying each index $\alpha \in \{0, 1, 2, 3\}$ with its binary notation, e.g., identify 2 with (1,0), such that to each multi-index $\bar{\alpha}$ there corresponds a binary string of length $2N$. In fact, our sum $\oplus$ would correspond to addition modulo 2 of each of the $2N$ components.

[37] S. Roman, *Advanced Linear Algebra*, 3rd ed., Graduate Texts in Mathematics Vol. 135 (Springer, New York, 2008).

[38] D. Gottesman, Stabilizer codes and quantum error correction, Ph.D. thesis, California Institute of Technology, 1997.

[39] G. Lindblad, Commun. Math. Phys. **48**, 119 (1976).

[40] A. Kossakowski, Rep. Math. Phys. **3**, 247 (1972).

[41] A. Kossakowski, Bull. Acad. Pol. Sc., Sci. Ser. Math. Astro. Phys. **20**, 1021 (1972).

[42] V. Gorini, A. Kossakowski, and E. C. G. Sudarshan, J. Math. Phys. **17**, 821 (1976).

[43] N. Boulant, T. F. Havel, M. A. Pravia, and D. G. Cory, Phys. Rev. A **67**, 042322 (2003).

[44] B. Vacchini, A. Smirne, E.-M. Laine, J. Piilo, and H.-P. Breuer, New J. Phys. **13**, 093004 (2011).

[45] K. Kraus, A. Böhm, J. D. Dollard, and W. H. Wootters, eds., States and effects, in *States, Effects, and Operations Fundamental Notions of Quantum Theory*, Lectures in Mathematical Physics at the University of Texas at Austin (Springer Berlin Heidelberg, Berlin, Heidelberg, 1983), pp. 1–12.

[46] M. Ziman and V. Bužek, in *Quantum Dynamics and Information* (World Scientific, Singapore, 2010), pp. 199–227.

[47] W. F. Stinespring, Proc. Am. Math. Soc. **6**, 211 (1955).

Weyl channels for multipartite systems

Weyl channels for multipartite systems

Tomás Basile,[1] Jose Alfredo de Leon,[2] Alejandro Fonseca,[3] François Leyvraz,[4] and Carlos Pineda[2, *]

[1]*Facultad de Ciencias, Universidad Nacional Autónoma de México, Ciudad de México 01000, Mexico*
[2]*Instituto de Física, Universidad Nacional Autónoma de México, Ciudad de México 01000, Mexico*
[3]*Departamento de Física, CCEN, Universidade Federal de Pernambuco, Recife 50670-901, PE, Brazil*
[4]*Instituto de Ciencias Físicas, Universidad Nacional Autónoma de México, Cuernavaca 62210, Mexico*

Quantum channels, a subset of quantum maps, describe the unitary and non-unitary evolution of quantum systems. We study a generalization of the concept of Pauli maps to the case of multipartite high dimensional quantum systems through the use of the Weyl operators. The condition for such maps to be valid quantum channels, i.e. complete positivity, is derived in terms of Fourier transform matrices. From these conditions, we find the extreme points of this set of channels and identify an elegant algebraic structure nested *within* them. In turn, this allows us to expand upon the concept of 'component erasing channels' introduced in earlier work by the authors. We show that these channels are completely characterized by elements drawn of finite cyclic groups. An algorithmic construction for such channels is presented and the smallest subsets of erasing channels which generate the whole set are determined.

I. INTRODUCTION

The description of open quantum systems [1, 2] serves a twofold purpose. Firstly, it lies at the core of the measurement problem [3, 4], thus bearing a fundamental interest. On the other hand, it describes quantum systems where the inevitable interaction with an environment is taken into account [5]. For most implementations of quantum devices it is crucial to understand and control such unwanted interaction. In both cases, a natural language for such a description is that of quantum channels, which have been subject of intense research [6].

The properties of a quantum channel dictate the characteristics of the associated quantum dynamics. In the realm of qubits, the set of quantum channels has been explored and thanks to a better understanding of its geometry, several physical properties of the set, such as divisibility [7–9], non-Markovianity [10, 11], channel capacity [12], among others have been unraveled. In a previous paper [13] we proposed and studied a class of channels acting on multi-qubit systems that either erased or preserved the Pauli components of the state. These are the so called Pauli component erasing (PCE) maps, which are an important subset of the Pauli maps. We found that every PCE channel corresponds uniquely to a vector subspace of a discrete vector space. Such channels can be associated with measurements and asymptotic Lindbladian evolution.

Moreover, most of the applications in the field of quantum information have been built upon qubits. Nevertheless, many real-world realizations of quantum systems have more than two levels that can be used to provide an important technical advantage. Such advantage is indeed employed to develop several important tasks like

quantum cryptography [14, 15], quantum computation [16–18], violation of Bell inequalities [19], randomness generation [20], among others. For this reason, the study of high-dimensional and multiparticle systems is of relevance.

In this article, we introduce the concept of Weyl channels for systems composed of many particles, allowing each of these to be of different dimensions. We begin defining these channels in sec. II as diagonal channels in the basis of multi-particle Weyl matrices, which are tensor products of the well-known Weyl matrices. Moving forward, we proceed to diagonalize the Choi-Jamiołkowski matrix, revealing a linear relationship between the eigenvalues and those of the channel. From this, we find two significant properties of the set of Weyl channels: (1) its extreme points in sec. III, and (2) a subgroup structure of all Weyl channels in sec. IV. Then, in sec. V we extend the notion of *component erasing* channels by introducing the Weyl erasing channels. Given its semigroup property, we describe the generator subset by means of the aforementioned algebraic structure of Weyl channels. Finally, we wrap up and conclude in sec. VI.

II. WEYL CHANNELS

A well-known generalization of the Pauli matrices to arbitrary d-dimensional Hilbert spaces was introduced by Weyl [21] and involves the following unitary matrices [22]:

$$U(m,n) = \sum_{k=0}^{d-1} \omega^{mk} |k\rangle \langle k+n|. \qquad (1)$$

Here we introduce the notation we shall use throughout: ω is the primitive d-th root of unity $\exp(2\pi i/d)$. All arithmetical operations over latin indices are taken over modulo d.

---

* carlospgmat03@gmail.com

We will further be mainly concerned with systems of N qudits, for which we introduce the following standard notations:

$$U(\vec{m}, \vec{n}) = \bigotimes_{\alpha=1}^{N} U(m_\alpha, n_\alpha) \qquad (2)$$

Greek indices will always run over a range from 1 to N, and the arithmetic operations over them will always be the usual ones. When the range is not specified, it will be from 1 to N.

We now write for example

$$U(\vec{m}, \vec{n}) = \sum_{\vec{k}} \omega^{\vec{m} \cdot \vec{k}} \left| \vec{k} \right\rangle \left\langle \vec{k} + \vec{n} \right|, \qquad (3)$$

the notational conventions being self-explanatory. Note further that all our results can routinely be extended to the more complicated case in which the different particles in the N-particle system have different dimensions, d_α. The "vectors" $\vec{m}$ are then replaced by lists of integers, with $0 \le m_\alpha \le d_\alpha - 1$. Whereas this complicates the notation considerably, no points of essential interest are thereby introduced. We thus leave it to the interested reader to develop these issues. When non-trivial points arise in this respect, we shall explicitly point this out.

These unitary matrices satisfy certain elementary properties:

$$\operatorname{tr} U(m,n)^\dagger U(m',n') = d\delta_{mm'}\delta_{nn'} \qquad (4)$$
$$U(m,n)U(m',n') = \omega^{m'n}U(m+m', n+n')$$
$$U(m,n)U(m',n') = \omega^{m'n-mn'}U(m',n')U(m,n)$$
$$U(m,n)^\dagger = \omega^{mn}U(-m,-n)$$

as well, of course, as their vectorial equivalents.

We now define Weyl maps and the corresponding channels: any density matrix on the space of N qudits, that

is, on $(\mathbb{C}^d)^{\otimes N}$, can be expressed as

$$\rho = \frac{1}{d^N} \sum_{\vec{m}, \vec{n}} \alpha(\vec{m}, \vec{n}) U(\vec{m}, \vec{n}) \qquad (5)$$

where $\alpha(\vec{m}, \vec{n})$ satisfies $\alpha(\vec{m}, \vec{n}) = \omega^{\vec{m} \cdot \vec{n}} \alpha^*(-\vec{m}, -\vec{n})$ in order for ρ to satisfy the condition of hermiticity. More intricate conditions need to be satisfied in order to yield a positive matrix, but we shall not be concerned with these.

A Weyl map is now defined as follows

$$\rho \to \rho' = \mathcal{E}[\rho] = \frac{1}{d^N} \sum_{\vec{m}, \vec{n}} \tau(\vec{m}, \vec{n}) \alpha(\vec{m}, \vec{n}) U(\vec{m}, \vec{n}). \qquad (6)$$

Here the $\tau(\vec{m}, \vec{n})$ are complex numbers, whereas ρ is the density matrix given in (5). In other words, if the $U(\vec{m}, \vec{n})$ are viewed as generators of the vector space of all Hermitian matrices, the Weyl maps act *diagonally* on this set.

We now wish to find the conditions necessary and sufficient for $\mathcal{E}$ to be a quantum channel, that is, to be trace and hermiticity preserving, as well as completely positive. For the former two conditions, we require

$$\tau(\vec{m}, \vec{n}) = \tau(-\vec{m}, -\vec{n})^*, \qquad (7\text{a})$$
$$\tau(0,0) = 1. \qquad (7\text{b})$$

To verify complete positivity, we must check the circumstances under which the Choi–Jamiołkowski matrix, given by

$$\mathcal{D} = \frac{1}{d^N} \sum_{\vec{m}, \vec{n}} \tau(\vec{m}, \vec{n}) U(\vec{m}, \vec{n}) \otimes U(\vec{m}, \vec{n})^* \qquad (8)$$

is positive semidefinite. Interestingly, eq. (8) is the corresponding Choi–Jamiołkowski matrix, even if $U(\vec{m}, \vec{n})$ are not Weyl operators, but an arbitrary basis of Hilbert-Schmidt space, as shown in Appendix A. To specify the criteria for matrix in eq. (8) to be positive semidefinite, we evaluate its eigenvalues $\lambda(\vec{m}, \vec{n})$. This is easily done after noticing that the various elements of the sum, namely the $U(\vec{m}, \vec{n}) \otimes U(\vec{m}, \vec{n})^*$ all commute for arbitrary values of $\vec{m}$ and $\vec{n}$, as readily follows from (4):

$$\left(U(m,n) \otimes U(m,n)^*\right)\left(U(m',n') \otimes U(m',n')^*\right) = \left(U(m,n)U(m',n')\right) \otimes \left(U(-m,n)U(-m',n')\right)$$
$$= \left(U(m+m', n+n')\right) \otimes \left(U(-(m+m'), n+n')\right) \qquad (9)$$

The symmetry of the final expression proves the claim, and the extension to the case of arbitrary N is straightforward.

It now remains to determine the eigenvalues of $U(\vec{m}, \vec{n})$, which given its tensor product structure [see

eq. (2)] can be reduced to the single-qudit case of $U(m, n)$. These can be calculated directly studying the recursion relation that follows from the eigenvalue equation for the Weyl operators, see Appendix B. One can then readily see that the eigenvalues $\mu(r, s)$ of $U(m, n) \otimes$

$U(m,n)^*$ take the form

$$\mu(r,s) = \omega^{mr-ns}, \qquad (10)$$

where r and s are arbitrary integers modulo d that serve as labels for the eigenvalue. The degeneracy pattern of these eigenvalues is complicated, but since our focus is on the positivity of $\mathcal{D}$, we do not need to consider these details.

The set of eigenvalues of $U(\vec{m}, \vec{n}) \otimes U(\vec{m}, \vec{n})^*$ is then given by

$$\mu(\vec{r}, \vec{s}) = \omega^{\vec{m}\cdot\vec{r}-\vec{n}\cdot\vec{s}}. \qquad (11)$$

The condition for the positive semidefiniteness of $\mathcal{D}$ is thus that, for all $\vec{r}$ and $\vec{s}$,

$$d^{-N}\sum_{\vec{m},\vec{n}} \tau(\vec{m},\vec{n})\omega^{\vec{m}\cdot\vec{r}-\vec{n}\cdot\vec{s}} = \lambda(\vec{r},\vec{s}) \geq 0. \qquad (12)$$

Note that condition (7a) on $\tau(\vec{m}, \vec{n})$ straightforwardly shows that the left-hand side of (12) is real, so that the inequality is meaningful.

The $\lambda(\vec{r}, \vec{s})$ are the eigenvalues of $\mathcal{D}$. They can also be used to characterize the Weyl channel $\mathcal{E}$. Inverting the relation (12) we get

$$\tau(\vec{m}, \vec{n}) = d^{-N} \sum_{\vec{r},\vec{s}} \lambda(\vec{r},\vec{s})\omega^{-\vec{m}\cdot\vec{r}+\vec{n}\cdot\vec{s}}, \qquad (13a)$$

$$\sum_{\vec{r},\vec{s}} \lambda(\vec{r},\vec{s}) = d^N. \qquad (13b)$$

Here (13b) follows from $\mathrm{tr}\,\mathcal{D} = d^N$, which is a consequence of (7b) and (8).

From (8) and (10) follows that the $\tau(\vec{m}, \vec{n})$ and the $\lambda(\vec{r}, \vec{s})$ are connected by the following *linear* relationship:

$$\tau(\vec{m}, \vec{n}) = \sum_{\vec{r},\vec{s}} \bigotimes_{\alpha} \left[F_\alpha \otimes F_\alpha^*\right](\vec{m}, \vec{n}; \vec{r}, \vec{s})\lambda(\vec{r}, \vec{s}), \qquad (14)$$

where F_α is the quantum Fourier transform matrix for dimension d_α in the general case, and of dimension d in the case we shall generally study (see Fig. 1).

We have therefore obtained a full characterization of Weyl channels: choosing arbitrary $\lambda(\vec{r}, \vec{s})$ that are positive and add up to d^N, the $\tau(\vec{m}, \vec{n})$ given by (13a) define a Weyl channel.

It is important to highlight that the set of channels introduced in the present work are different from other kinds of generalization of Pauli channels introduced previously [23–25]. On the other hand, similar expressions for the eigenvalues associated to random unitary channels on single d-level systems have been presented in [26, 27].

III. SET OF EXTREME POINTS

The set of Weyl channels is clearly convex, since equations (13) imply that any Weyl channel is given by a convex sum of channels of the form

$$\tau_{\vec{r}_0,\vec{s}_0}(\vec{m}, \vec{n}) = \omega^{-\vec{m}\cdot\vec{r}_0+\vec{n}\cdot\vec{s}_0}, \qquad (15)$$

where $\vec{r}_0, \vec{s}_0$ are fixed vectors whose elements are integer numbers modulo d.

Furthermore, we can see that the set of Weyl channels is in fact a $d^{2N} - 1$ dimensional simplex. Recall that all eigenvalues $\lambda(\vec{r}, \vec{s})$ of the Choi–Jamiołkowski matrix of a Weyl channel must be non-negative, and sum up to d^N [see eq. (13b)]. The set $\lambda(\vec{r}, \vec{s})$ is thus the standard $d^{2N} - 1$ dimensional simplex. Since the connection (12) between the λ's and the τ's is linear and invertible, then the set of all τ's is also a $d^{2N} - 1$ dimensional simplex. Note however that the τ's are complex, so they are actually part of a bigger $2d^{2N}$ dimensional real vector space. Nonetheless, conditions (7) (which are automatically satisfied by the formulae (12)) additionally limit the τ's so that the number of degrees of freedom is back to $d^{2N} - 1$.

Moreover, the extreme points of the simplex of Weyl channels are given by the d^{2N} channels of equation (15). This is because the extreme points of the λ's simplex are clearly

$$\lambda(\vec{r}, \vec{s}) = d^N \delta_{\vec{r},\vec{r}_0} \delta_{\vec{s},\vec{s}_0}. \qquad (16)$$

Therefore, those of the set of Weyl channels are given by applying the transformation (13a) to these extreme points, obtaining as a result the channels of equation (15). In fact, these channels are the only Weyl channels with the property that for all $\vec{m}, \vec{n}$, $|\tau(\vec{m}, \vec{n})| = 1$, as shown in the following theorem.

Theorem 1. *A Weyl channel is an extreme point of the set of Weyl channels if and only if* $|\tau(\vec{m}, \vec{n})| = 1$ *for all* $\vec{m}, \vec{n}$.

Proof. We have already proved that extreme points are of the form (15), and therefore satisfy that $|\tau(\vec{m}, \vec{n})| = 1$, so we only need to prove the converse. Equation (13a) says that

$$\tau(\vec{m}, \vec{n}) = d^{-N} \sum_{\vec{r},\vec{s}} \lambda(\vec{r}, \vec{s})\omega^{-\vec{m}\cdot\vec{r}+\vec{n}\cdot\vec{s}}. \qquad (17)$$

Recall that $d^{-N}\lambda(\vec{r}, \vec{s})$ are non-negative and add up to 1. It follows from the triangle inequality that if the sum in the right-hand side of (17) has more than one term, then $|\tau(\vec{m}, \vec{n})| < 1$. Thus, a Weyl channel with $|\tau(\vec{m}, \vec{n})| = 1$ must have all $\lambda(\vec{r}, \vec{s})$ equal to 0 except one, say $\lambda(\vec{r}_0, \vec{s}_0)$. In other words, if the Choi–Jamiołkowski matrix of a Weyl channel has only one eigenvalue $\lambda(\vec{r}_0, \vec{s}_0)$ different from zero, then that Weyl channel is an extreme point. $\square$

The simplest case that illustrates the result of this theorem are the single-qubit Weyl quantum channels. Given that the Weyl operators for $d = 2$ reduce to the Pauli operators, the extremal points for these are the vertices of the well-known tetrahedron of qubit quantum channels [28], which we illustrate in Fig. 2(a).

We can now characterize in greater detail these extreme points. For a given value of $\vec{r}_0, \vec{s}_0$, the effect of the
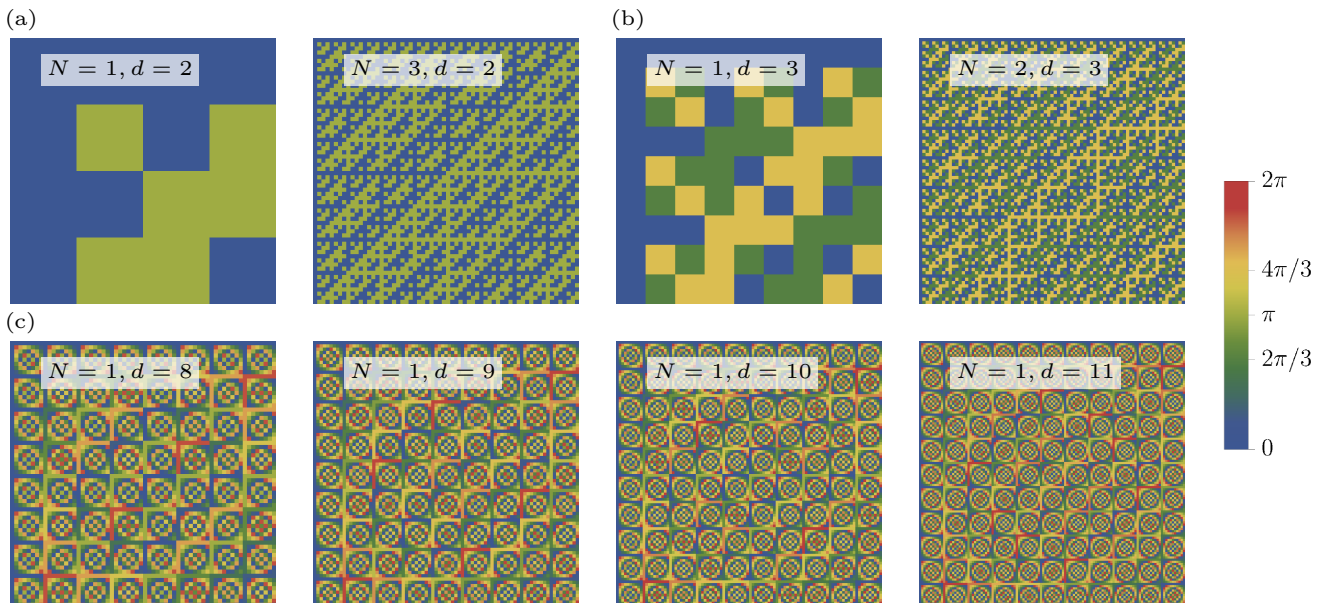
Figure 1. Visualization of the argument of the matrix elements $\bigotimes_\alpha [F_\alpha \otimes F_\alpha^*](\vec{m}, \vec{n}; \vec{r}, \vec{s})$ for different dimensions and number of particles; rows and columns are indexed by the double indices $(\vec{m}, \vec{n})$ and $(\vec{r}, \vec{s})$, respectively. This matrix map the $\tau(\vec{m}, \vec{n})$ of a Weyl map to the eigenvalues $\lambda(\vec{r}, \vec{s})$ of its Choi-Jamiołkowski matrix, see eqs (12) and (14). We show plots for systems of (a) qubits, (b) qutrits, and (c) single-qudits. Notice that not only the total dimension is relevant, but also the number of particles; for instance, compare $N = 3$, $d = 2$ with $N = 1$, $d = 8$.

channel given by (15) on a Weyl matrix $U(\vec{m}, \vec{n})$ is

$$\begin{aligned}
\mathcal{E}_{\vec{r}_0, \vec{s}_0}[U(\vec{m}, \vec{n})] &= \omega^{-\vec{r}_0 \cdot \vec{m} + \vec{s}_0 \cdot \vec{n}} U(\vec{m}, \vec{n}) \\
&= U(\vec{s}_0, \vec{r}_0) U(\vec{m}, \vec{n}) U(\vec{s}_0, \vec{r}_0)^\dagger. \quad (18)
\end{aligned}$$

We see therefore that the extreme points of the set of all Weyl channels are unitary channels. Since all Weyl channels are convex combinations of the extreme points [29], it immediately follows that all the Weyl channels are simply random unitary channels, constructed from the Weyl unitaries.

IV. A MATHEMATICAL STRUCTURE WITHIN WEYL CHANNELS

In this section, we focus on a subset of Weyl channels with physical relevance and mathematical beauty. We consider the Weyl channels, which, when iterated infinitely, converge to channels that completely erase, preserve, or introduce phases to the projections of the density matrix onto the Weyl operator basis. Our main results include the characterization of the group property of this particular subset and a method to determine these channels. Specifically, we show that the corresponding channels can be obtained by identifying all subgroups of $\mathbb{Z}_d \oplus \mathbb{Z}_d$ and their homomorphisms to $\mathbb{Z}_d$.

A. Subgroup property of Weyl channels

Theorem 2. *Let $\tau(\vec{m}, \vec{n})$ and $\tau(\vec{m}', \vec{n}')$ have both norm 1. Then so does $\tau(\vec{m} + \vec{m}', \vec{n} + \vec{n}')$ and additionally*

$$\tau(\vec{m} + \vec{m}', \vec{n} + \vec{n}') = \tau(\vec{m}, \vec{n})\tau(\vec{m}', \vec{n}') \quad (19)$$

Proof. From (13) follows that, quite generally, $\tau(\vec{m}, \vec{n})$ are convex combinations of complex numbers of the form ω^k, with k an integer. Nonetheless, the only such convex combinations having norm 1 are themselves numbers of the form ω^k, with k an integer, therefore $\tau(\vec{m}, \vec{n})$ and $\tau(\vec{m}', \vec{n}')$ are, under the hypotheses of the theorem, of the form ω^k and $\omega^{k'}$, respectively. Similarly for $\tau(\vec{m}', \vec{n}')$, which we take to be equal to $\omega^{k'}$.

Setting $\tau(\vec{m}, \vec{n}) = \omega^k$ in 13a and conveniently rewriting the equation results in

$$\omega^k = d^{-N} \sum_l \omega^l \sum_{\vec{r}, \vec{s}} \lambda(\vec{r}, \vec{s}) \delta_{-\vec{m} \cdot \vec{r} + \vec{n} \cdot \vec{s}, l} \quad (20)$$

and a similar expression for $\omega^{k'}$, replacing $\vec{m}$ and $\vec{n}$ with their primed versions. Since $\lambda(\vec{r}, \vec{s})$ are positive and sum up to d^N, it follows that the right-hand side is a convex sum of ω^l. For it to equal ω^k, an extreme point, only the term with $l = k$ can be different from zero. It follows that $\lambda(\vec{r}, \vec{s}) = 0$, whenever $-\vec{m} \cdot \vec{r} + \vec{n} \cdot \vec{s} \neq k$ or $-\vec{m}' \cdot \vec{r} + \vec{n}' \cdot \vec{s} \neq k'$. From this follows straightforwardly that again $\lambda(\vec{r}, \vec{s}) = 0$ whenever

$$-(\vec{m} + \vec{m}') \cdot \vec{r} + (\vec{n} + \vec{n}') \cdot \vec{s} \neq (k + k') \quad (21)$$

which implies

$$\tau(\vec{m} + \vec{m}', \vec{n} + \vec{n}') = \omega^{k+k'} = \tau(\vec{m}, \vec{n})\tau(\vec{m}', \vec{n}'). \quad (22)$$

$\square$

This means that the set of all $(\vec{m}, \vec{n})$, such that $\tau(\vec{m}, \vec{n})$, has norm 1 form an *additive subgroup* of the abelian group

$$\mathcal{G} = \mathbb{Z}_d^{\oplus N} \oplus \mathbb{Z}_d^{\oplus N} \quad (23)$$

with respect to vector addition modulo d. Note that this is one case where a significant difference arises when the N particles have different dimensions d_α; the vectors $(\vec{m}, \vec{n})$ would then belong to the group

$$\mathcal{G} = \left(\bigoplus_{\alpha=1}^{N} \mathbb{Z}_{d_\alpha} \right) \oplus \left(\bigoplus_{\alpha=1}^{N} \mathbb{Z}_{d_\alpha} \right). \quad (24)$$

In other words, the set $\mathcal{H} \subseteq \mathcal{G}$ on which $\tau(\vec{m}, \vec{n})$ has norm 1 forms a subgroup of $\mathcal{G}$ and τ can be seen as a homomorphism from $\mathcal{H}$ to $\mathbb{Z}_d$.

To determine all $\tau(\vec{m}, \vec{n})$ of Weyl channels satisfying eq. (19), we must proceed in 2 steps:

1. Determine all subgroups $\mathcal{H} \subseteq \mathcal{G}$.

2. Determine all homomorphisms from $\mathcal{H}$ to $\mathbb{Z}_d$.

In the following section we present an algorithm to determine all subgroups $\mathcal{H}$ of $\mathcal{G}$ and homomorphisms from $\mathcal{H}$ to $\mathbb{Z}_d$.

We wish to remark that given a quantum channel for which some of its coefficients $\tau(\vec{m}, \vec{n})$ satisfy Eq. 19, the rest of coefficients are not necessarily null. However, still these are restricted by the complete positivity condition, Eq. 12.

B. Weyl channels

To determine all $\tau(\vec{m}, \vec{n})$ of Weyl channels satisfying eq. (19) we proceed in two steps. The first step involves identifying all subgroups of $\mathcal{G}$ [cf. eq. (24)]. We begin by stating two relevant facts about finite abelian groups, and then discuss how to find the subgroups for the more general case of an abelian group $\mathcal{G}$, which encompasses the majority of our discussion in this section. After that, we describe the second step, which is how to determine all phases of $\tau(\vec{m}, \vec{n})$ of a WCE channel by determining all homomorphisms from a subgroup to the roots of unity. We refer the reader to Appendix E to illustrate with several examples the algorithm we present in this section.

Whenever p and q are coprime, the group $\mathbb{Z}_{pq}$ is isomorphic to $\mathbb{Z}_p \oplus \mathbb{Z}_q$. Therefore, we may use the prime decomposition of d_α to separate each $\mathbb{Z}_{d_\alpha}$ in eq. (24) as a sum of cyclic groups of prime power order. We proceed in this way for all α in eq. (24), and then we group

the terms corresponding to different primes, so $\mathcal{G}$ can be written as

$$\mathcal{G} = \bigoplus_p \mathcal{G}_p, \quad (25)$$

with $\mathcal{G}_p = \bigoplus_i \mathbb{Z}_{p^{k_i}}$, for each prime p that appears in the decomposition of any of the d_α.

Since the direct sum of two arbitrary abelian groups of orders m and n that are coprime yield all abelian groups of order mn, we can directly construct all subgroups of $\mathcal{G}$ by finding all the subgroups of each $\mathcal{G}_p$. In other words, although $\mathcal{G}$ in eq. (24) may have a complicated decomposition, we focus only in determining the subgroups of $\mathcal{G}_p$, which will be convenient to write as

$$\mathcal{G}_p = \bigoplus_{\alpha=1}^{r} \mathbb{Z}_{p^{M_\alpha}} \quad (26)$$

where M_α are in non-increasing order.

The group $\mathcal{G}_p$ is associated with the sequence $\overline{M} = M_1 \ldots M_r$, which is a *partition* of $M = \sum_\alpha M_\alpha$. Therefore, we will refer to $\mathcal{G}_p$ as a group of type $\overline{M}$. Furthermore, for any partition of M there exists an abelian group of order p^M that is unique up to an isomorphism [30]. If one has a subgroup $\mathcal{H}_p$ of $\mathcal{G}_p$, the corresponding partition, let us call it $\overline{N}$, satisfies $N_\alpha \leq M_\alpha$. On the other hand, once the choice of the non-increasing order for the partition of the group $\mathcal{G}_p$, the corresponding partitions for the subgroups $\mathcal{H}_p$ inherit a well-defined order from the group, and the corresponding partitions cannot therefore be taken in non-increasing order.

Another important fact about finite abelian groups is that they all have a basis; that is, they can be generated by the integer combinations of a set of elements. In our particular case, a simple way of choosing a basis is by picking a generating element for each cyclic group in eq. (26). We denote them $\vec{e}_\alpha$, and therefore an arbitrary $h \in \mathcal{H}$ can be *uniquely* expressed as

$$h = \sum_{\alpha=1}^{r} n_\alpha \vec{e}_\alpha, \quad (27)$$

where $n_\alpha \in \mathbb{Z}_{p^{M_\alpha}}$, and the multiplication of a group element by an integer m is defined as the addition of the group element to itself repeated m times. The number r of elements in the basis is independent of the choice of basis and it is known as the group's rank r.

The general idea for finding all subgroups of $\mathcal{G}_p$ is to determine a subset of subgroups such that, upon applying all automorphisms $T : \mathcal{G}_p \mapsto \mathcal{G}_p$, all others are found. We will say that two subgroups of $\mathcal{G}_p$ are T-isomorphic when there is an automorphism T mapping one to the other. Then, to find the subgroups of $\mathcal{G}_p$ we first determine any subset with the maximum number of subgroups that are not T-isomorphic. We call these "representative subgroups". By definition, applying all automorphisms T (which we describe how to find in Appendix C) to the
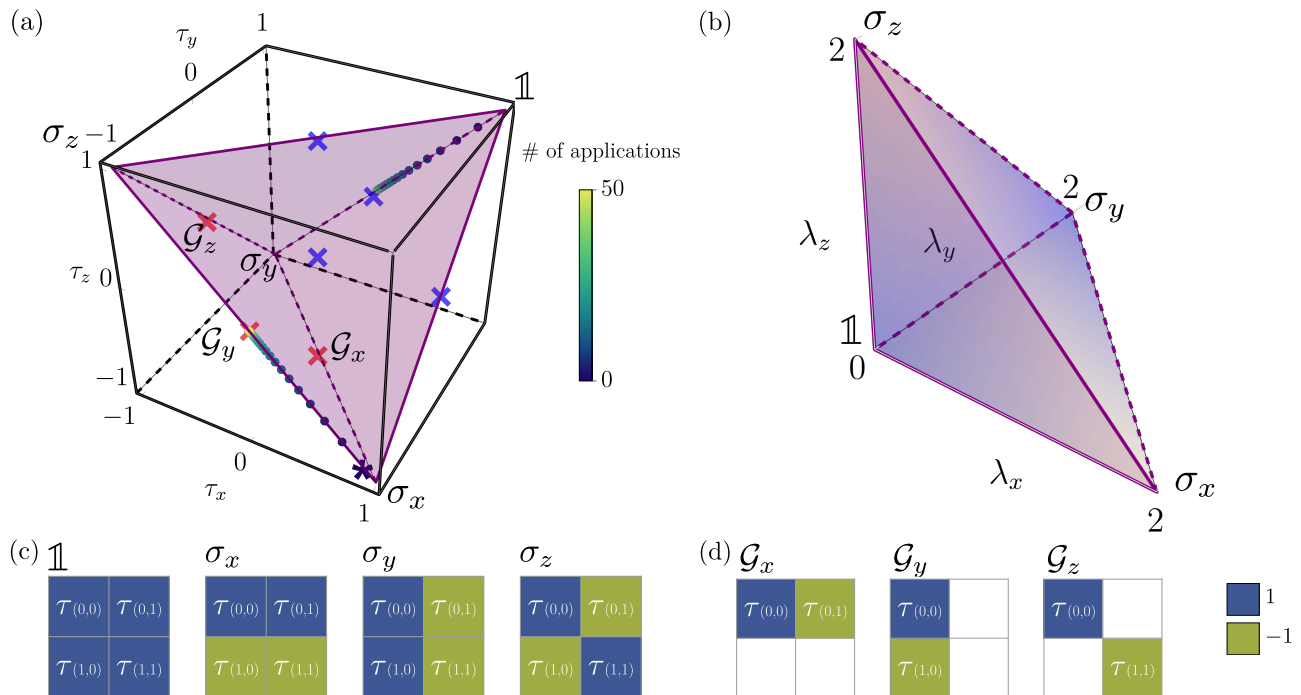
Figure 2. Simplexes of (a) the $\tau(m, n)$ of all single-qubit Weyl channels, in which we identify $\tau(0, 1) = \tau_x$, $\tau(1, 0) = \tau_y$, and $\tau(1, 1) = \tau_z$, as usual, and similarly for λs; and of (b) the eigenvalues $\lambda(m, n)$ of the corresponding Choi-Jamiołkowski matrix. Additionally, we depict in (c) and (d) the extreme points of (a) and Weyl erasing generators, respectively.

representative subgroups all other subgroups of $\mathcal{G}_p$ are found.

Note the difference between the concept of isomorphism for the subgroups, and the concept of T-isomorphism. The latter depends not only on the group structure of the subgroup $\mathcal{H}$, but also on the way in which it is embedded in the group $\mathcal{G}_p$. For instance, we can embed the group $\mathbb{Z}_2$ in the group $\mathbb{Z}_{2^2} \oplus \mathbb{Z}_2$ either as a subgroup of the first summand or as a subgroup of the second. In other words, the partition $\overline{M}$ describing the full group is $\overline{M} = 2\,1$ and the subgroup $\mathbb{Z}_2$ can be embedded with a partition $0\,1$ as well as $1\,0$. The two subgroups, being both isomorphic to $\mathbb{Z}_2$, are abstractly isomorphic, but that isomorphism cannot be extended to an isomorphism of $\mathbb{Z}_4 \oplus \mathbb{Z}_2$.

All subgroups of $\mathcal{G}_p$ are found applying all its automorphisms T to the subgroups generated by the bases

$$\mathcal{B} = \{p^{s_1}\vec{e}_1, \ldots, p^{s_r}\vec{e}_r\} \quad 0 \leq s_\alpha \leq M_\alpha. \quad (28)$$

Nevertheless, more than one different selection $\mathbb{S} = \{s_\alpha\}$ may determine two bases of subgroups T-isomorphic, in other words, that are connected by an automorphism of $\mathcal{G}_p$. For example, consider a group $\mathcal{G}_p$ of type $\overline{M} = 2\,2\,1\,1$. The partitions $\mathbb{S} = 0\,1\,0\,1$ and $\mathbb{S}' = 1\,0\,1\,1$ determine bases of T-isomorphic subgroups, because the automorphism defined as $T(\vec{e}_1) = \vec{e}_2$, $T(\vec{e}_2) = \vec{e}_1$, $T(\vec{e}_3) = \vec{e}_4$ and $T(\vec{e}_4) = \vec{e}_3$ maps one to the other. From each of these T-isomorphic sets of subgroups we can pick an arbitrary element, which will be called *the representative subgroup*.

To find the representative subgroups we need a criterion to determine when two bases $\mathcal{B}$ of the form (28) generate T-isomorphic groups. Let us denote $\tilde{M}_1, \ldots, \tilde{M}_q$ the q different values in the sequence of numbers in $\overline{M}$ (for instance, if $\overline{M} = 2211$, then $q = 2$ and $\tilde{M}_1 = 2$, $\tilde{M}_2 = 1$). Furthermore, we define the subset $S_j = \{s_\alpha, \forall \alpha : M_\alpha = \tilde{M}_j\}$ of $\mathbb{S}$, that is, S_j is the subset of $\mathbb{S}$ formed by all the s_α whose αs correspond to the indices of the M_α that are equal to $\tilde{M}_j$. Then, the criterion is the following: two different sets $\mathbb{S}$ and $\mathbb{S}'$ determine bases of T-isomorphic subgroups whenever their corresponding subsets S_j and S'_j are the same for all j.

We are ready to describe the complete algorithm to determine all the subgroups of a given group $\mathcal{G}$. First, decompose $\mathcal{G}$ as a sum of prime power order groups $\mathcal{G}_p$. For every $\mathcal{G}_p$, find all sets $\mathbb{S} = \{s_\alpha\}$ and discriminate between them to find the only ones that determine representative subgroups. Then apply to them all automorphisms T of $\mathcal{G}_p$, so all subgroups of $\mathcal{G}_p$ will be found, albeit with repetitions. A description of the group of automorphisms of an arbitrary abelian group $\mathcal{G}$ is provided in [31], and the technique is summarized for completeness' sake in Appendix C. Finally, to find the subgroups of $\mathcal{G}$ apply the direct sum between all different subgroups of each $\mathcal{G}_p$.

Furthermore, a way to count the total number of subgroups of $\mathcal{G}_p$ is already known in the literature. Since any abelian group of prime power order can only have subgroups that are also of prime power order, subgroups of order p^L, with $L < M$, can also be characterized by

a partition $\overline{L}$ of L. It is shown in [30, 32] that necessary and sufficient conditions for the partition $\overline{L}$ to correspond to a possible subgroup of the group determined by the partition $\overline{M}$ of M are

$$L_\alpha = 0 \quad (\alpha > r), \tag{29a}$$

$$L_\alpha \leq M_\alpha, \tag{29b}$$

$$L_\alpha \geq L_{\alpha+1}. \tag{29c}$$

An expression for the number of different subgroups of type $\overline{L}$ is already known in the literature. For that matter, we refer the reader to Appendix F.

To fully determine the coefficients $\tau(\vec{m}, \vec{n})$ with norm 1, we interpret them as a function that maps $\mathcal{H}$ to the group of roots of unity ω^j. We consider $\tau(\vec{m}, \vec{n}) = \omega^{\phi(\vec{m}, \vec{n})}$, thus we are looking for all homomorphisms $\phi : \bigoplus_{M_\alpha} \mathbb{Z}_{p^{M_\alpha}} \mapsto \mathbb{Z}_{p^{M_1}}$. To determine one of such functions uniquely, it is sufficient to specify the values of ϕ on a basis of $\mathcal{H}$, as described in Appendix D.

Note that all the above remarks greatly simplify when d is a prime number. In that case the group $\mathcal{G}$ is additionally a vector space. The set of subgroups can then be described as the set of vector subspaces using the usual techniques of linear algebra. All the partitions described above then reduce to partitions of the type where M_α is either 1 or 0, and the partition is fully characterized by the number of its non-zero elements, which correspond to the subspace's *dimension*. Finally, the homomorphism τ can be described as a linear map from the vector space $\mathcal{G}$ to the field $\mathbb{Z}_d$, which is once more straightforwardly described in terms of linear algebra.

V. WEYL ERASING CHANNELS

A. Generalities

In this section we focus on a particular class of Weyl channels; those for which $|\tau(\vec{m}', \vec{n}')| = 0$ or 1. In other words, we will discuss Weyl channels that completely erase, preserve or introduce specific phases to the projections of the density matrix of a system of qudits onto the Weyl matrices basis. We will refer to this subset of Weyl channels as Weyl erasing channels.

Weyl erasing channels are an interesting subset of Weyl channels, as they arise from the composition of one or more of these channels an infinite number of times. For instance, the infinite composition of any Weyl channel for which all $|\tau(\vec{m}, \vec{n})| < 1$, except $\tau(\vec{0}, \vec{0}) = 1$, results in the completely depolarizing channel. In the general case, the repeated application of a Weyl channel may not converge to a single Weyl erasing channel, however it oscillates between two or more such channels. For example, applying many times the single-qubit Weyl channel depicted with an asterisk in Fig. 2(a) asymptotically oscillates between the channel collapsing the Bloch sphere onto the y axis and other channel collapsing it onto the y axis while reflecting it across the x-z plane. This oscillation continues

indefinitely between $\vec{\tau} = (1, 0, 1, 0)$ and $\vec{\tau}' = (1, 0, -1, 0)$.

In the following, we derive a Kraus representation of Weyl erasing channels that will provide insight into the physical implementation of these channels. We then focus on deriving an expression of the eigenvalues of the Choi-Jamiołkowski matrix of Weyl erasing channels exclusively, as we already have an expression for all Weyl channels [c.f. (12)]. For this, we begin presenting an algorithm that uses the mathematical machinery developed in section IV B to find all $\tau(\vec{m}, \vec{n})$ of any Weyl erasing channel:

1. Find all sets of indices $\{(\vec{m}, \vec{n}) : |\tau(\vec{m}, \vec{n})| = 1\}$ by determining all subgroups $\mathcal{H} \subset \mathcal{G}$, with $\mathcal{G}$ that in (25).

2. Find the values of $\tau(\vec{m}, \vec{n}) = \omega^{\phi(\vec{m}, \vec{n})}$ for all $(\vec{m}, \vec{n}) \in \mathcal{H}$ by determining all homomorphisms $\phi : \mathcal{H} \mapsto \bigoplus_p \mathbb{Z}_{p^{M_1(p)}}$, with $M_1(p)$ such that $\mathbb{Z}_{p^{M_1(p)}}$ denotes the largest order cyclic group for every $\mathcal{G}_p$ in (25).

3. Assign $\tau(\vec{m}', \vec{n}') = 0$ for all $(\vec{m}', \vec{n}') \notin \mathcal{H}$.

While an exhaustive enumeration of all Weyl erasing channels for a large number N of particles is not practical, the construction provides insights into the mathematical structure of this set. In fact, we show examples of Weyl erasing channels for a single-qubit, a 4-level system and a system composed by both of them in Figs. 4-8. We remark that the algorithms to determine $\tau(\vec{m}, \vec{n})$ of Weyl and Weyl erasing channels are both the same up until determining all homomorphisms. Then, for the former one may assign any value to the $\tau(\vec{m}', \vec{n}') \notin \mathcal{H}$ as long as they keep the channel completely positive, whereas for the latter one must assign the value zero to all $\tau(\vec{m}', \vec{n}') \notin \mathcal{H}$.

Let us now evaluate the eigenvalues of the Choi matrix of a Weyl erasing channel. To be consistent with the previous section, we consider Weyl erasing channels of a system of N particles, each with dimension a power of p, so the group in question is $\mathcal{G}_p$ [see eq. (26)]. The group's rank is then $r = 2N$. Recall these channels have $\tau(\vec{m}, \vec{n}) = 0$ for all $(\vec{m}, \vec{n}) \notin \mathcal{H}$, thus, we find from (17)

$$\lambda(\vec{r}, \vec{s}) = d^{-N} \sum_{(\vec{m}, \vec{n}) \in \mathcal{H}} \tau(\vec{m}, \vec{n}) \prod_{\alpha=1}^{N} \omega_\alpha^{m_\alpha r_\alpha - n_\alpha s_\alpha} \tag{30}$$

where $\omega_\alpha = \exp\left(2\pi i / p^{M_{2\alpha}}\right)$ Since the composition of two Weyl channels is simply to multiply both sets of $\tau(\vec{m}, \vec{n})$, we can see that $\tau(\vec{m}, \vec{n})$ of Weyl erasing channels are those of an extreme Weyl channel [c.f. (15)] for all $(\vec{m}, \vec{n}) \in \mathcal{H}$, and $\tau(\vec{m}', \vec{n}') = 0$ for all $(\vec{m}', \vec{n}') \notin \mathcal{H}$. Hence, substituting $\tau(\vec{m}, \vec{n})$, and considering $\omega_{p^\alpha}^k = \omega_{p^\beta}^{p^{(\alpha-\beta)k}}$, $\alpha > \beta$, we can write

$$\lambda(\vec{r}, \vec{s}) = \sum_{(\vec{m}, \vec{n}) \in \mathcal{H}} \omega_{p^{M_1}}^{f(\vec{m}, \vec{n})}, \tag{31}$$

where $f(\vec{m}, \vec{n}) = \sum_{\alpha=1}^{N} p^{M_1 - M_{2\alpha-1}}(m_\alpha(r_\alpha - r_{0,\alpha}) - n_\alpha(s_\alpha - s_{0,\alpha}))$. To evaluate this expression we note that f is an homomorphism $f : \mathcal{G}_p \mapsto \mathbb{Z}_{p^{M_2}}$. Therefore, the sum evaluates to zero unless f maps $\mathcal{H}$ to the trivial group:

$$\lambda(\vec{r}, \vec{s}) = \begin{cases} |\mathcal{H}| & f(\vec{m}, \vec{n}) = 0 \text{ for all } (\vec{m}, \vec{n}) \in \mathcal{H} \\ 0 & \text{otherwise,} \end{cases}$$
(32)

where $|\mathcal{H}|$ is defined as the number of elements of $\mathcal{H}$. Furthermore, let us consider the group $\mathcal{H}^\perp = \{(\vec{m}, \vec{n}) : f(\vec{m}, \vec{n}) = 0\}$. The only non-zero $\lambda(\vec{r}, \vec{s})$ are those with indices $(\vec{r}, \vec{s})$ such that $(\vec{r} - \vec{r}_0, \vec{s} - \vec{s}_0) \in \mathcal{H}^\perp$.

Finally, having obtained the eigenvalues of the Choi-Jamiołkowski matrix of Weyl erasing channels we describe their canonical Kraus representation. Recall that that Weyl matrices are the Kraus operators of Weyl channels with probabilities equal to $\lambda(\vec{r}, \vec{s})$ [c.f. eq. (18)]. It then follows that Kraus operators of Weyl erasing channels are the subset of Weyl matrices $U(\vec{r}, \vec{s})$, with $(\vec{r} - \vec{r}_0, \vec{s} - \vec{s}_0) \in \mathcal{H}^\perp$, each with probability $|\mathcal{H}^\perp|/|\mathcal{G}|$.

B. Generators

In the following, we investigate the smallest subset of Weyl erasing channels which, under composition, generate the whole set. For the sake of simplicity, we start by finding the generators of Weyl channels with $\tau(\vec{m}, \vec{n}) = 0$ or 1, as these are Weyl channels characterized only by subgroups of $\mathcal{G}$. Subsequently, we move to the most general Weyl erasing channels that either preserve, erase or introduce phases to the density matrix.

We shall determine those subgroups that are Indecomposable, in the sense that they cannot be generated as the non-trivial composition of two Weyl channels. We call these the generator subgroups. We consider once again the group $\mathcal{G}$ shown in eq. (25), thus, we first discuss how to determine the generator subgroups of $\mathcal{G}_p$, and, from those, determine the generator subgroups of $\mathcal{G}$. Similarly to what we did in section IV B, the generator subgroups V_p of $\mathcal{G}_p$ can be found constructing representative generator subgroups V_p^* and applying all automorphisms of $\mathcal{G}_p$ to them.

We claim that a representative subgroup is a generator V_p of $\mathcal{G}_p$ if and only if its basis is of the form

$$\mathcal{B}_{V_p} = \{\vec{e}_1, \ldots, \vec{e}_{j-1}, p^{s_j}\vec{e}_j, \vec{e}_{j+1}, \ldots, \vec{e}_r\}, \ 1 \leq s_j \leq M_j.$$
(33)

This is verified as follows. Consider a subgroup $\mathcal{H}_p$ with basis (28) such that its set of values $\mathbb{S} = \{s_\alpha\}_\alpha$ has two (or more) values $s_\beta, s_\gamma \neq 0$. That is, $\mathcal{H}_p$ has the basis $\mathcal{B}_{\mathcal{H}_p} = \{\vec{e}_1, \ldots, \vec{e}_{\beta-1}, p^{s_\beta}\vec{e}_\beta, \ldots, \vec{e}_{\gamma-1}, p^{s_\gamma}\vec{e}_\gamma, \ldots, \vec{e}_r\}$. Then, $\mathcal{H}_p$ can be expressed as the non-trivial intersection of the group g_p' with basis $\mathcal{B}_{V_p'} = \{\vec{e}_1, \ldots, \vec{e}_{\beta-1}, p^{s_\beta}\vec{e}_\beta, \ldots, \vec{e}_r\}$ and another group V_p'' with basis $\mathcal{B}_{V_p''} = \{\vec{e}_1, \ldots, \vec{e}_{\gamma-1}, p^{s_\gamma}\vec{e}_\gamma, \ldots, \vec{e}_r\}$. Now, we check

that a group $\mathcal{H}_p$ with a basis of the form (33) cannot be expressed as an intersection of two subgroups containing $\mathcal{H}_p$ strictly. Note that groups $\mathcal{H}_p'$ satisfying $\mathcal{H}_p \subsetneq \mathcal{H}_p' \subset \mathcal{G}_p$ must have a basis of the form $\{\vec{e}_1, \cdots, p^{s_j'}\vec{e}_j, \cdots, \vec{e}_r\}$, with $s_j' < s_j$. Therefore, if we have two such groups $\mathcal{H}_p'$ and $\mathcal{H}_p''$, then the group arising from intersection $\mathcal{H}_p' \cap \mathcal{H}_p''$ has a basis $\{\vec{e}_1, \cdots, p^{\max(s_j', s_j'')}\vec{e}_j, \cdots, \vec{e}_r\}$, which doesn't generate $\mathcal{H}_p$ because the integer span of $p^{s_{j'}}\vec{e}_{j'}$ or $p^{s_{j''}}\vec{e}_{j''}$ are strictly larger than the integer span of $p^{s_j}\vec{e}_j$.

Finally, to find all generator subgroups V of $\mathcal{G} = \bigoplus_p \mathcal{G}_p$ we proceed as follows. We begin by finding the generator subgroups of $\mathcal{G}_p$. Then, the generator subgroups V are the subgroups of the form

$$V = \bigoplus_p H_p,$$
(34)

where $H_p = \mathcal{G}_p$ for all p except for one $p = p'$, for which $H_{p'} = V_{p'}$. To see this, notice that V is a generator since any other subgroup $\mathcal{H}'$ strictly containing it must also have $H_p' = \mathcal{G}_p$ for $p \neq p'$ and $H_{p'}' \subsetneq V_{p'}$. Therefore, for two such subgroups $\mathcal{H}'$ and $\mathcal{H}''$ to generate V, $H_{p'}'$ and $H_{p'}''$ should generate $V_{p'}$, which is impossible since $V_{p'}$ is a generator of $\mathcal{G}_{p'}$. On the other hand, any subgroup of $\mathcal{G}$ that is composed as the sum of groups $\mathcal{G}_p$ except for two (or more) primes p' and p'' in which the sum is of any corresponding generator subgroup, may be generated by two subgroups $\mathcal{H}$ of the form (34) with suitable generators $H_{p'} = V_{p'}$ and $H_{p''} = V_{p''}$.

To summarize up to this point: to determine the generators of Weyl erasing channels with $\tau(\vec{m}, \vec{n}) = 0, 1$ one is only required to determine the generator subgroups of the corresponding group in which the indices $(\vec{m}, \vec{n})$ of $\tau(\vec{m}, \vec{n}) = 1$ live. To determine the generators of Weyl erasing channels that also introduce phases one must still find generator subgroups, and a suitable homomorphism for each of them as well.

More specifically, a Weyl erasing generator with $|\tau(\vec{m}, \vec{n})| = 0, 1$ is completely characterized by a generator subgroup of $\mathcal{G}$ and a homomorphism $\phi : \mathcal{G} \mapsto \bigoplus \mathbb{Z}_{p^{M_2(p)}}$, with $\mathbb{Z}_{p^{M_2(p)}}$ is the largest order cyclic group for every $\mathcal{G}_p$. The composition of two channels with subgroups $\mathcal{H}_1$ and $\mathcal{H}_2$ and homomorphisms ϕ_1 and ϕ_2 yields a channel corresponding to $\mathcal{H}_1 \cup \mathcal{H}_2$ and homomorphism $\phi_1 + \phi_2$. Therefore, for every generator subgroup V, if we define a basis ϕ_V^α of the space of homomorphisms, then the set of channels corresponding to each generator subgroup V, together with any element ϕ_V^α mapping V to the whole group $\mathbb{Z}_{p^{M_2(p)}}$, form a set of generators. For instance, we show a set of Weyl erasing generators of a 4-level system in Fig. 3

To avoid misunderstandings, note that the "generators" for channels with $\tau(\vec{m}, \vec{n}) = 0, 1$, those characterized completely by a generator subgroup (and one may say that also by a homomorphism $\phi = 0$), are not generators of the whole set of Weyl erasing channels ($|\tau(\vec{m}, \vec{n})| = 0, 1$). The former channels can always be obtained through iterated composition of channels with a
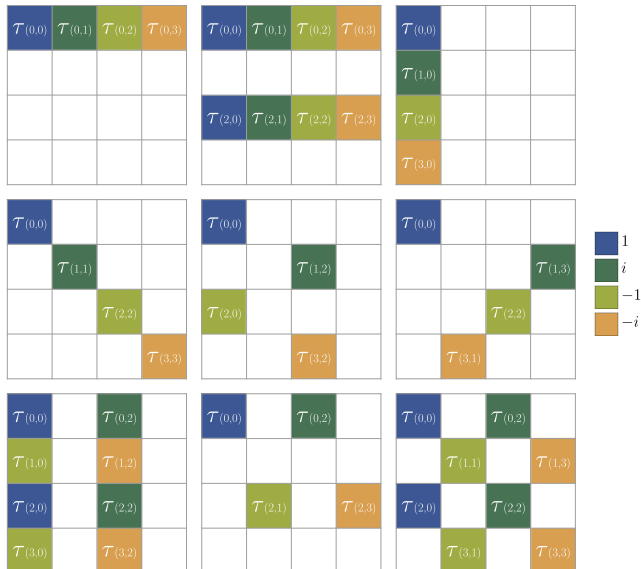
Figure 3. Weyl erasing generators for a single-particle of dimension $d = 4$. Concatenating in all possible ways the corresponding channels one obtains all the Weyl quantum channels of a 4-level system with $|\tau(m,n)| = 0, 1$.

non-zero homomorphism. For example, the single-qubit Weyl erasing channels depicted with a blue point in Fig. 2(a), except for the one located at $\vec{\tau} = (0,0,0)$, are Weyl generator channels with $\tau(m,n) = 0, 1$. However, they can be obtained from composing two times each of the three Weyl generator channels depicted with a red point. Those are the generators of all Weyl erasing channels of a single-qubit.

VI. CONCLUSIONS

In this paper, we explored a class of quantum channels of multipartite systems with different-dimensional particles. Our focus was on extending the study of Pauli and Weyl channels; the former have been studied for systems of many qubits and the latter for single d-level systems.

We begin by introducing the multi-particle Weyl operators $U(\vec{m}, \vec{n})$ to define a Weyl map as a diagonal map in this basis; its eigenvalues are denoted by $\tau(\vec{m}, \vec{n})$. We derived the constraints on $\tau(\vec{m}, \vec{n})$ for a Weyl map to preserve the trace and hermiticy of the density matrix, as well as to be completely positive. For the latter, we diagonalized its Choi-Jamiołkowski matrix and found the linear relationship between these eigenvalues and $\tau(\vec{m}, \vec{n})$.

Several features of Weyl channels emerged from our study. We identified the extreme points of the set, which correspond to Weyl operators, highlighting the random unitary nature of Weyl channels. Additionally, we established a subgroup structure within a Weyl channel, showing that the indices $(\vec{m}, \vec{n})$ of all $|\tau_{\vec{m},\vec{n}}| = 1$ is a subgroup of the direct product of groups $\mathbb{Z}_{d_\alpha} \oplus \mathbb{Z}_{d_\alpha}$, where d_α represents the dimension of the α-th particle.

Furthermore, we introduced Weyl erasing channels, which are Weyl channels that either preserve, erase, or introduce phases to the Weyl operator basis. These extend the concept of *component erasing* channels. Given that all channels of this type exhibit the subgroup structure, with the remaining $\tau_{\vec{m},\vec{n}}$ set to zero, we were able to find the smallest subset which generate, under composition, the whole set.

Our work contributes to the understanding of many-body quantum channels, and, moreover, to the dynamics of d-level systems, which have growing importance for both theoretical and practical purposes. Future research directions include investigating divisibility, non-Markovianity, channel capacity, and the subset of entanglement-breaking channels among other properties of the Weyl channel set.

Appendix A: Computation of the Choi–Jamiołkowski matrix

This appendix demonstrates that the Choi-Jamiołkowski matrix of any diagonal map $\mathcal{E}$ takes the form

$$\mathcal{D} = \frac{1}{d^N} \sum_{\vec{m}, \vec{n}} \tau(\vec{m}, \vec{n}) U(\vec{m}, \vec{n}) \otimes U(\vec{m}, \vec{n})^*, \qquad (A1)$$

whenever $U(\vec{m}, \vec{n})$ form an orthogonal basis of unitaries [23].

The Choi–Jamiołkowski matrix of a quantum map $\mathcal{E}$ is defined as follows:

$$\mathcal{D} = \frac{1}{d^N} \sum_{\vec{k}, \vec{l}} \mathcal{E}\left[\left|\vec{k}\right\rangle \left\langle \vec{l}\right|\right] \otimes \left(\left|\vec{k}\right\rangle \left\langle \vec{l}\right|\right). \qquad (A2)$$

We may now express $\left|\vec{k}\right\rangle \left\langle \vec{l}\right|$ in terms of any orthogonal basis of unitaries $U(\vec{m}, \vec{n})$

$$\left|\vec{k}\right\rangle \left\langle \vec{l}\right| = \frac{1}{d^N} \sum_{\vec{m}, \vec{n}} \text{Tr}\left(U^\dagger(\vec{m}, \vec{n}) \left|\vec{k}\right\rangle \left\langle \vec{l}\right|\right) U(\vec{m}, \vec{n}). \qquad (A3)$$

Substituting this in the expression (A2) for $\mathcal{D}$ yields.

$$\frac{1}{d^N}\sum_{\vec{k},\vec{l}}\mathcal{E}\left(\left|\vec{k}\right\rangle\!\left\langle\vec{l}\right|\right)\otimes\left|\vec{k}\right\rangle\!\left\langle\vec{l}\right| = \frac{1}{d^{2N}}\sum_{\vec{k},\vec{l},\vec{m},\vec{m}',\vec{n},\vec{n}'}\mathcal{E}\left[\mathrm{Tr}\left(U^\dagger(\vec{m},\vec{n})\left|\vec{k}\right\rangle\!\left\langle\vec{l}\right|\right)U(\vec{m},\vec{n})\right]\otimes\left[\mathrm{Tr}\left(U^\dagger(\vec{m}',\vec{n}')\left|\vec{k}\right\rangle\!\left\langle\vec{l}\right|\right)U(\vec{m}',\vec{n}')\right]$$

(A4a)

$$=\frac{1}{d^{2N}}\sum_{\vec{k},\vec{l},\vec{m},\vec{m}',\vec{n},\vec{n}'}\mathrm{Tr}\left(U^\dagger(\vec{m},\vec{n})\left|\vec{k}\right\rangle\!\left\langle\vec{l}\right|\right)\mathrm{Tr}\left(U(\vec{m}',\vec{n}')\left|\vec{l}\right\rangle\!\left\langle\vec{k}\right|\right)\tau(\vec{m},\vec{n})U(\vec{m},\vec{n})\otimes U(\vec{m}',\vec{n}')^*,$$

(A4b)

where we have used the complex conjugate of (A3). Then, using the definition of trace it follows

$$=\frac{1}{d^{2N}}\sum_{\vec{k},\vec{l},\vec{m},\vec{m}',\vec{n},\vec{n}'}\langle l|U^\dagger(\vec{m},\vec{n})|k\rangle\,\langle k|U(\vec{m}',\vec{n}')|l\rangle\,\tau(\vec{m},\vec{n})U(\vec{m},\vec{n})\otimes U(\vec{m}',\vec{n}')^* \qquad (A4c)$$

$$=\frac{1}{d^N}\sum_{\vec{m},\vec{n}}\tau(\vec{m},\vec{n})U(\vec{m},\vec{n})\otimes U(\vec{m},\vec{n})^*. \qquad (A4d)$$

This expression can also be obtained also using a recently result of Siewert, in which he derives an expression for the maximally entangled state in terms of an arbitrary orthogonal basis [33].

Appendix B: Eigenvalues of $U(m,n)$ and of $U(m,n)\otimes U(m,n)^*$

We will find the eigenvalues of $U(m,n)$. Since it is unitary, we will express the eigenvalues as ω^c, with $c\in\mathbb{R}$. Let us consider an eigenvector $|\phi\rangle = \sum_r \phi(r)|r\rangle$ with eigenvalue $\xi = \omega^c$. The eigenvalue equation for $U(m,n)$ leads to the following relation:

$$\phi(r+n) = \omega^{-mr}\omega^c\phi(r). \qquad (B1)$$

Starting with an arbitrary index r and applying this recursion equation $l-1$ times, we obtain

$$\phi(r+nl) = \omega^{-lmr-\frac{1}{2}l(l-1)mn+cl}\phi(r). \qquad (B2)$$

In the particular case in which $l = l' := \dfrac{d}{\gcd(d,n)}$ we may use that $l'n$ is a multiple of d, so:

$$\phi(r) = \omega^{-l'mr-\frac{1}{2}l'(l'-1)mn+cl'}\phi(r), \qquad (B3)$$

which implies that (for values of r such that $\phi(r)\neq 0$):

$$-l'mr - \frac{1}{2}l'(l'-1)mn + cl' = sd \qquad (B4)$$

for some integer s. Therefore:

$$c = \frac{sd}{l'} + \frac{1}{2}(l'-1)mn + mr = \gcd(d,n)s + mr + \frac{1}{2}(l'-1)mn. \qquad (B5)$$

So we conclude that all eigenvalues of $U(m,n)$ necessarily have the form

$$\omega^{\gcd(d,n)s+mr+\frac{1}{2}(l'-1)mn} \qquad (B6)$$

for s and r integers.

Furthermore, taken modulo d, the set $\{\gcd(d,n)s + mr \mid s,r\in\mathbb{Z}_d\}$ is equivalent to $\{ns + mr \mid s,r\in\mathbb{Z}_d\}$ which is also equivalent to $\{\gcd(m,n)k \mid k\in\mathbb{Z}_d\}$. Therefore, the d eigenvalues of $U(m,n)$ have are

$$\xi = \omega^{\gcd(m,n)k+\frac{1}{2}(l'-1)mn}. \qquad (B7)$$

From this, it is straightforward that the eigenvalues of $U(m,n)\otimes U(m,n)^*$ are

$$\mu(r,s) = \omega^{\gcd(m,n)k-\gcd(m,n)h}. \qquad (B8)$$

This set is equivalent to

$$\mu(r,s) = \omega^{mr-ns} \qquad (B9)$$

where r,s are integers modulo d.

Appendix C: Automorphisms of finite abelian groups

In the following we describe the bijective homomorphisms T of an arbitrary abelian group. Without loss of generality we limit ourselves to groups that are the direct sum of groups of the type $\mathbb{Z}_{p^M}$, specifically

$$\mathcal{G} = \bigoplus_{\alpha=1}^r \mathbb{Z}_{p^{M_\alpha}}. \qquad (C1)$$

To fix notations, we shall work with a fixed basis $\vec{e}_\alpha$, $1\le\alpha\le r$, where r is the *rank* of $\mathcal{G}$. The map T is therefore uniquely determined by the values of $T\vec{e}_\alpha$. Since $\vec{e}_\alpha$ is a basis, we can write

$$T\vec{e}_\alpha = \sum_{\beta=1}^r t_{\alpha\beta}\vec{e}_\beta. \qquad (C2)$$

The $t_{\alpha\beta}$ are then uniquely determined, if we view them as homomorphisms from $\mathbb{Z}_{p^{M_\beta}}$ to $\mathbb{Z}_{p^{M_\alpha}}$. Since such homomorphisms can always be expressed through the multiplication by some appropriate number, the expression given in (C2) is meaningful.

Now let us specify more precisely the range of variation of the $t_{\alpha\beta}$. We distinguish two cases

1. $M_\alpha \leq M_\beta$: in this case any number modulo p^{M_α} will do, and two different such numbers provide different homomorphisms.

2. $M_\alpha > M_\beta$: in this case, the number needs to be a multiple of $p^{M_\alpha - M_\beta}$, since otherwise it is not possible to define the map. In that case, we may describe $t_{\alpha\beta}$ as $p^{M_\alpha - M_\beta} \tau_{\alpha\beta}$, where $\tau_{\alpha\beta}$ is an arbitrary number modulo p^{M_β}

Consider the matrix T in greater detail, and just as in the main text, let us denote by $\tilde{M}_1, \cdots, \tilde{M}_q$ the *distinct* values of M_α in *strictly decreasing order*. We define ν_α to be the number of times $\tilde{M}_\alpha$ appears repeated in the original series. This defines a division of the T matrix in *blocks* of size $\nu_\alpha \times \nu_\beta$, where $1 \leq \alpha, \beta \leq q$.

We first take the elements $t_{\alpha\beta}$ modulo p. As a consequence of the observation (2), all blocks with $\alpha < \beta$ are filled with zeros, whereas all other blocks have arbitrary entries. It thus follows that the matrix is invertible modulo p if and only if all the diagonal blocks are invertible. The number of invertible $\nu_\alpha \times \nu_\alpha$ matrices modulo p is given by

$$I_\alpha = \prod_{\beta=1}^{\nu_\alpha} \left(p^{\nu_\alpha} - p^{\beta-1} \right). \qquad (C3)$$

One sees this by observing that we may first choose an arbitrary non-zero vector of length ν_α in $p^{\nu_\alpha} - 1$ different ways, then chose a second vector independent from the first, and so on.

All the other entries in the blocks below the diagonal, that is, the $t_{\alpha\beta}$ with $\alpha > \beta$, can be chosen arbitrarily. If we thus define

$$K_0 = \sum_{1 \leq \beta < \alpha \leq q} \nu_\alpha \nu_\beta, \qquad (C4)$$

then the total number of possible forms of the matrix T modulo p is

$$N(p) = p^{K_0} \prod_{\alpha=1}^{q} I_\alpha. \qquad (C5)$$

We now need to work out the number of ways this can be extended to the full matrix, where the entries have the full range of variation specified above. Note first that the condition of invertibility carries over automatically upon extension, as the inverse matrix of T modulo p can be extended uniquely to the inverse of the extended matrix.

To the entries on or below the diagonal, that is, with $t_{\alpha\beta}$ such that $\alpha \geq \beta$, we can add any number of the form

$p \tau_{\alpha\beta}$, where $\tau_{\alpha\beta}$ is an arbitrary number taken modulo $p^{\tilde{M}_\alpha - 1}$. So the number of possibilities of extending these blocks is given by p^{K_1}, where

$$K_1 = \sum_{1 \leq \beta \leq \alpha \leq q} (\tilde{M}_\alpha - 1)\nu_\alpha \nu_\beta. \qquad (C6)$$

For the blocks above the diagonal, that is, the blocks with $t_{\alpha\beta}$ such that $\alpha < \beta$, they are of the form $p^{\tilde{M}_\alpha - \tilde{M}_\beta} \tau_{\alpha\beta}$, with $\tau_{\alpha\beta}$ a number modulo $p^{\tilde{M}_\beta}$, so that the total number of ways of extending the blocks above the diagonal is p^{K_2}, with

$$K_2 = \sum_{1 \leq \alpha < \beta \leq q} \tilde{M}_\beta \nu_\alpha \nu_\beta. \qquad (C7)$$

The final result for the total number of automorphisms is thus given by

$$N_{tot}(M_1, \ldots, M_r) = p^{K_0 + K_1 + K_2} \prod_{\alpha=1}^{q} I_\alpha. \qquad (C8)$$

Appendix D: Homomorphisms from $\mathcal{H}$ to the cyclic group $\mathbb{Z}_d$

Here we describe the set of homomorphisms ϕ from an abelian group of the form $\mathcal{H} = \bigoplus_{\alpha=1}^{r} \mathbb{Z}_{p^{M_\alpha}}$ to the cyclic group $\mathbb{Z}_{p^{M_1}}$. As always, the numbers M_α are ordered in decreasing order.

We may as always choose a basis $\vec{e}_\alpha$ of $\mathcal{H}$, each having order p^{M_α}. The homomorphism ϕ is then uniquely determined by a set of homomorphisms ϕ_α from the cyclic groups $\mathbb{Z}_{p^{M_\alpha}}$ to $\mathbb{Z}_{p^{M_1}}$.

Whenever $M_1 = M_\alpha$, ϕ_α simply reduces to multiplication by an arbitrary r_α number modulo p^{M_1}. On the other hand, if $M_\alpha < M_1$, then ϕ_α is given by the multiplication by a number of the form $p^{\tilde{M}_1 - M_\alpha} r_\alpha$ where r_α is an arbitrary number modulo p^{M_α}.

If we therefore define ν as the number of $M_\alpha = M_1$, so that $M_\nu \geq M_1$ but $M_{\nu+1} < M_1$, and $\nu = 0$ if $M_\alpha < M_1$ for all α, then ϕ can be expressed as follows:

$$\phi \left(\sum_\alpha c_\alpha \vec{e}_\alpha \right) = \vec{\phi} \cdot \vec{c} := \sum_\alpha \phi_\alpha c_\alpha \qquad (D1a)$$

$$\phi_\alpha = \begin{cases} p^{M_1 - M_\alpha} s_\alpha & (\alpha \geq \nu) \\ t_\alpha & (\alpha < \nu) \end{cases} \qquad (D1b)$$

where s_α and t_α are numbers modulo p^{M_α} and p^{M_1} respectively.

The total number of such homomorphisms is therefore given by p^K with

$$K = \sum_{\alpha=1}^{\nu} M_\alpha + M_1(r - \nu) \qquad (D2)$$

Appendix E: Examples

To illustrate the application of the mathematical tools presented in the main text, we will provide detailed examples of how to identify the Weyl channels as is described in section IV. Remember that said channels are characterized by a subgroup $\mathcal{H}$ of the group of indices $\mathcal{G}$ (which corresponds to the indices whose τ's have norm 1) and an homomorphism (which gives the phases to each τ). The examples will be arranged in increasing generality, starting with a system of one qudit with prime dimension and ending with the most general case of many qudits of arbitrary dimensions.

1. Single particle with prime dimension

Here we show how to follow the algorithm described in section IV for the case of one qudit with prime dimension $d = p$. In this case, the group of indices for the τ's is simply $\mathbb{Z}_p \oplus \mathbb{Z}_p$ and we search for all its subgroups

and then all homomorphisms to $\mathbb{Z}_p$. While we do this in general, we simultaneously show the specific case for $p = 2$ (a single qubit).

We start determining the types of subgroups of $\mathbb{Z}_p \oplus \mathbb{Z}_p$ and a representative subgroup of each type. For that, we take the following steps:

- We select a basis for $\mathbb{Z}_p \oplus \mathbb{Z}_p$, the simplest would be $\{\vec{e}_1, \vec{e}_2\} := \{(1,0), (0,1)\}$.

- Define M_α as the number such that p^{M_α} is the order of $\vec{e}_\alpha$. In this case, $M_1 = M_2 = 1$ and therefore the partition for the group is $\bar{M} = M_1 M_2 = 11$.

- Find all the sets $\mathbb{S} = \{s_\alpha\}$ with $0 \leq s_\alpha \leq M_\alpha$. In this case, there are four said sets: $\{0,0\}, \{0,1\}, \{1,0\}, \{1,1\}$

- For each set, we define the basis $\mathcal{B} = \{p^{s_1}\vec{e}_1, p^{s_2}\vec{e}_2\}$, and therefore get the following bases:

$$\mathbb{S} = \{0,0\} \rightarrow \mathcal{B} = \{p^0\vec{e}_1, p^0\vec{e}_2\} = \{\vec{e}_1, \vec{e}_2\} \, , \, \mathbb{S} = \{0,1\} \rightarrow \mathcal{B} = \{p^0\vec{e}_1, p^1\vec{e}_2\} = \{\vec{e}_1\}, \tag{E1}$$

$$\mathbb{S} = \{1,0\} \rightarrow \mathcal{B} = \{p^1\vec{e}_1, p^0\vec{e}_2\} = \{\vec{e}_2\} \, , \, \mathbb{S} = \{0,0\} \rightarrow \mathcal{B} = \{p^0\vec{e}_1, p^0\vec{e}_2\} = \{\}. \tag{E2}$$

Notice that $p\vec{e}_\alpha = (0,0)$, which doesn't contribute to the basis.

- Now we only keep bases that are not T-isomorphic, so as to avoid unnecessary redundancies when applying automorphisms in the next step.

  As mentioned in the main text, we do so by first defining the sequence of numbers $\tilde{M}_1, \cdots, \tilde{M}_q$ given by the q different values in the sequence of numbers in $\bar{M}$. In this case, as $\bar{M} = 11$, there is only one number in said sequence, being $\tilde{M}_1 = 1$. Then, we define the subsets $S_j = \{s_\alpha, \forall \alpha : M_\alpha = \tilde{M}_j\}$. In this case, we only have one such subset, which happens to be the whole set, $S_1 = \{s_1, s_2\}$. As described in the main text, two different bases of the ones described in the previous step are T-isomorphic if all their sets S_j are the same. In this case, this means that the bases constructed from $\mathbb{S} = \{1,0\}$ and $\mathbb{S} = \{0,1\}$ are T-isomorphic. Therefore, we may only keep one of those bases, let's say we keep $\{0,1\}$ and discard the other one, so that the representative bases are:

$$\{\vec{e}_1, \vec{e}_2\}, \{\vec{e}_1\}, \{\}. \tag{E3}$$

The subgroups generated by these bases are the "representative subgroups". Then, to find all possible

subgroups, we need to find all automorphisms of $\mathbb{Z}_p \oplus \mathbb{Z}_p$ and apply them to these representative groups, so that we can obtain all subgroups of each type starting from the representatives.

As shown in eq.(C2), automorphisms of $\mathbb{Z}_p \oplus \mathbb{Z}_p$ are determined by a matrix $t_{\alpha\beta}$ with dimensions $r \times r$, where r is the number of elements in the basis of the group. Therefore, in this case the automorphisms are characterized by 2×2 matrices, where each entry $t_{\alpha\beta}$ can be a number modulo p.

Furthermore, these entries are constrained by the conditions given in Appendix C, and since in this case $M_1 = M_2$, all $t_{\alpha\beta}$ fall into case 1 of the aforementioned conditions. This implies that all $t_{\alpha\beta}$ are numbers modulo $p^{M_\alpha} = p$. This gives a total of p^4 possible matrices, but we need to only keep those that are invertible. For example, for the especial case of one qubit, we construct all 2×2 matrices such that all entries $t_{\alpha\beta}$ are numbers modulo 2, and out of these 16 matrices, only 6 of them are invertible:

$$T_1 = \begin{pmatrix} 0 & 1 \\ 1 & 1 \end{pmatrix}, \quad T_2 = \begin{pmatrix} 1 & 0 \\ 1 & 1 \end{pmatrix}, \quad T_3 = \begin{pmatrix} 1 & 1 \\ 0 & 1 \end{pmatrix}, \quad \text{(E4)}$$

$$T_4 = \begin{pmatrix} 1 & 1 \\ 1 & 0 \end{pmatrix}, \quad T_5 = \begin{pmatrix} 0 & 1 \\ 1 & 0 \end{pmatrix}, \quad T_6 = \begin{pmatrix} 1 & 0 \\ 0 & 1 \end{pmatrix}. \quad \text{(E5)}$$

Therefore, these matrices represent the 6 possible

automorphisms of $\mathbb{Z}_2 \oplus \mathbb{Z}_2$.

To find all the subgroups, we simply apply all automorphisms on each representative subgroup found in eq.(E3). For the case of one qubit, the result would be as follows:

- $\{\vec{e}_1, \vec{e}_2\}$: The group generated by this basis is the whole gruop, and when we apply any automorphism, we always get back the whole group because automorphisms are invertible. Therefore, the only group here is the whole group $\mathbb{Z}_p \oplus \mathbb{Z}_p$.

- $\{\vec{e}_1\}$: For this basis, the representative subgroup it generates is $\{(0,0), (1,0)\}$. As before, we apply all the automorphisms to this subgroup. We can see an example for the case of one qubit, when applying T_1 to the element$(1,0)$, we get as a result $(0,1)$, so applying T_1 to the subgroup gives as a result $\{(0,0), (0,1)\}$. Similarly, when using the other automorphisms in the case of one qubit, we get the following subgroups (excluding repetitions):

$$\{(0,0), (1,0)\}, \quad \{(0,0), (0,1)\}, \quad \{(0,0), (1,1)\}. \quad \text{(E6)}$$

- $\{\}$: In this case, the representative subgroup is the trivial $\{(0,0)\}$ and applying any automorphism leaves this subgroup intact.

Therefore, we have found all subgroups of $\mathbb{Z}_p \oplus \mathbb{Z}_p$. For the case of $p = 2$, they are: the complete group, the subgroups obtained in eq. (E6) and the trivial subgroup $\{(0,0)\}$, see Fig 4. That is, up until this point we have found the sets of indices $\{m, n\}$ for which $\tau(m, n)$ can have norm 1 in a Weyl channel.
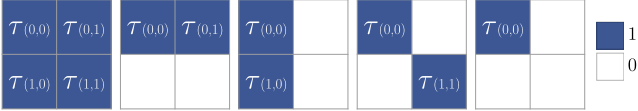

Figure 4. Single-qubit Weyl erasing channels with $\tau(m, n) = 0, 1$. These are completely characterized by the sets $\{(m,n) : \tau(m, n) = 1\}$, which are the subgroups of $\mathbb{Z}_2 \oplus \mathbb{Z}_2$.

Now we find all homomorphisms $\phi : \mathbb{Z}_p \oplus \mathbb{Z}_p \to \mathbb{Z}_p$. A homomorphism is characterized by its value in each element in the basis, $\phi_\alpha := \phi(\vec{e}_\alpha)$. To know the possible values of ϕ_α, we first define ν like in Appendix D, as the number such that $M_\nu \geq n$ but $M_{\nu+1} < n$ (where n is the exponent of the co-domain of ϕ, in this case the co-domain is $\mathbb{Z}_p$, so that $n = 1$ and we can see that $\nu = 2$). The possible values of ϕ_α are given by the cases in eq. (D1b):

- ϕ_1: Since $\alpha = 1 < \nu = 2$, we have the second case and therefore ϕ_1 is a number modulo $p^n = p$.

- ϕ_2: Since $\alpha = 2 \geq \nu = 2$, we have the first case, so that $\phi_2 = p^{n-M_2} s_s = s_2$ with s_2 a number modulo $p^{M_2} = p$. Therefore, ϕ_2 is also a number modulo p.

To find all possible homomorphisms, we determine all possible pairs ϕ_1, ϕ_2. Since ϕ_1, ϕ_2 can be any number modulo p, we have a total of p^2 homomorphisms. In the special case of one qubit, they are: $\phi_1 = \phi_2 = 0$; $\phi_1 = 0, \phi_2 = 1$; $\phi_1 = 1, \phi_2 = 0$; and $\phi_1 = \phi_2 = 1$. We show in Fig. 5 all Weyl erasing channels of a single qubit.
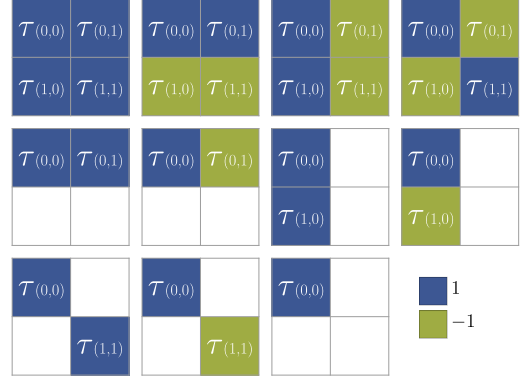

Figure 5. Single-qubit Weyl erasing channels with $|\tau(m, n)| = 0, 1$. These are completely characterized by two elements: (i) the sets $\{(m, n) : |\tau(m, n)| = 1\}$, which are the subgroups of $\mathbb{Z}_2 \oplus \mathbb{Z}_2$, and (ii) all homomorphisms $\phi : \mathbb{Z}_2 \oplus \mathbb{Z}_2 \mapsto \mathbb{Z}_2$.

2. Single particle with $d = p^n$

Now we generalize to the case of a single particle with $d = p^n$. To have a concrete example to show, we consider a particle with $d = 2^2 = 4$.

- We select a basis of $\mathbb{Z}_{p^n} \oplus Z_{p^n}$, for example, $\{\vec{e}_1, \vec{e}_2\} = \{(1, 0), (0, 1)\}$.

- Define M_α as the number such that p^{M_α} is the order of $\vec{e}_\alpha$. In this case, $M_1 = M_2 = n$, so the partition of the group is $\bar{M} = M_1 M_2 = nn$. For the special case of a 4-level system, the partition is $\bar{M} = 22$.

- Find all the sets $\mathbb{S} = \{s_\alpha\}$ with $0 \leq s_\alpha \leq M_\alpha$. For the case of a 4-level system, there are nine said sets: $\{0, 0\}, \{0, 1\}, \cdots, \{2, 1\}, \{2, 2\}$.

- For each set, we define a basis $\mathcal{B} = \{p^{s_1} \vec{e}_1, p^{s_2} \vec{e}_2\}$. For example, for a 4-level system, the bases are:

$$\mathbb{S} = \{0,0\} \to \mathcal{B} = \{\vec{e}_1, \vec{e}_2\}, \ \mathbb{S} = \{0,1\} \to \mathcal{B} = \{\vec{e}_1, 2\vec{e}_2\}, \ \mathbb{S} = \{0,2\} \to \mathcal{B} = \{\vec{e}_1\}, \tag{E7}$$

$$\mathbb{S} = \{1,0\} \to \mathcal{B} = \{2\vec{e}_1, \vec{e}_2\}, \ \mathbb{S} = \{1,1\} \to \mathcal{B} = \{2\vec{e}_1, 2\vec{e}_2\}, \ \mathbb{S} = \{1,2\} \to \mathcal{B} = \{2\vec{e}_1\}, \tag{E8}$$

$$\mathbb{S} = \{2,0\} \to \mathcal{B} = \{\vec{e}_2\}, \ \mathbb{S} = \{2,1\} \to \mathcal{B} = \{2\vec{e}_2\}, \ \mathbb{S} = \{2,2\} \to \mathcal{B} = \{\}. \tag{E9}$$
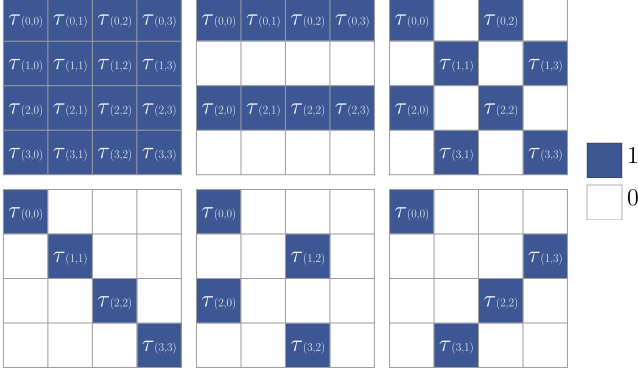

Figure 6. Some 4-level system Weyl erasing channels with $\tau(m,n) = 0,1$. Each of those is completely characterized by a set $\{(m,n) : \tau(m,n) = 1\}$, which is a subgroup of $\mathbb{Z}_4 \oplus \mathbb{Z}_4$.

Figure 7. Some Weyl erasing channels, with $d = 4$, $N = 1$, and $|\tau(m,n)| = 0,1$. Each of those is completely characterized by (1) a set $\{(m,n) : |\tau(m,n)| = 1\}$, which is a subgroup of $\mathbb{Z}_4 \oplus \mathbb{Z}_4$, and (2) an homomorphism $\phi : \mathbb{Z}_4 \oplus \mathbb{Z}_4 \mapsto \mathbb{Z}_4$.

- We define the sequence of numbers $\tilde{M}_1, \cdots, \tilde{M}_q$ given by the q different values in the sequence $\bar{M}$. In this case, we only have $\tilde{M}_1 = n$. Then, we define the subsets $S_j = \{s_\alpha, \forall \alpha : M_\alpha = \tilde{M}_j\}$; in this case we only have $S_1 = \{s_1, s_2\}$. As said before, different bases are T-isomorphic if all sets S_j are the same, and we only need to keep one of them. Therefore, for the case of one 4-level system, we only have to keep the following bases, which generate the representative subgroups:

$$\{\vec{e}_1, \vec{e}_2\}, \ \{\vec{e}_1, 2\vec{e}_2\}, \ \{\vec{e}_1\}, \ \{2\vec{e}_1, 2\vec{e}_2\}, \ \{2\vec{e}_1\}, \ \{\}.$$

Once again, automorphisms are characterized by 2×2 matrices $t_{\alpha\beta}$. Since $M_1 = M_2 = n$, all $t_{\alpha\beta}$ fall into the first case of Appendix C, which implies that all $t_{\alpha\beta}$ are numbers modulo $p^{M_\alpha} = p^n$. This gives a total of p^{4n} possible matrices, of which we only keep those that are invertible (have non-zero determinant modulo p). For example, in the case of a 4-level system, there are 96 such matrices.

Find all subgroups: As before, to find all subgroups of $\mathbb{Z}_d \oplus \mathbb{Z}_d$, we apply all automorphisms to each of the representative subgroups found in the first step and omit duplicates. As always, these subgroups describe the indexes $\tau(m,n)$ which can have norm 1. We show in Fig. 6 some Weyl erasing channels of a 4-level system that are completely characterized by subgroups of $\mathbb{Z}_4 \oplus \mathbb{Z}_4$.

We find all homomorphisms $\phi : \mathbb{Z}_{p^n} \oplus \mathbb{Z}_{p^n} \to \mathbb{Z}_{p^n}$. As for the last case, the homomorphism is characterized by two values $\phi_1 = \phi(\vec{e}_1), \phi_2 = \phi(\vec{e}_2)$. Using Appendix D, we find that ϕ_1 and ϕ_2 are both numbers modulo p^n.

To find all possible homomorphisms, we determine all possible pairs of ϕ_1, ϕ_2 which gives a total total of p^{2n} homomorphisms. For the case of a 4-level system, the 16 homomorphisms are given by all pairs of numbers ϕ_1, ϕ_2 modulo 4. We show in Fig. 7 some Weyl erasing channels for a 4-level system.

3. Single particle with arbitrary dimension

Now we consider a single particle with arbitrary dimension d, which can be written with its prime factorization as $d = \prod_{i=1}^{K} p_i^{n_i}$. In this case, what we have done in the last examples does not apply, since it only applies for groups of the form $\mathbb{Z}_{p^{M_1}} \oplus \mathbb{Z}_{p^{M_2}} \oplus \cdots \oplus \mathbb{Z}_{p^{M_K}}$ (notice that all the groups in the sum are powers of the same prime).

However, we can still find the subgroups of $\mathbb{Z}_d \oplus \mathbb{Z}_d$. To do it, we use the fact that $\mathbb{Z}_{pq} \simeq \mathbb{Z}_p \oplus \mathbb{Z}_q$ whenever p and q are coprime. Therefore, $\mathbb{Z}_d \simeq \mathbb{Z}_{p_1^{n_1}} \oplus \cdots \oplus \mathbb{Z}_{p_K^{n_K}}$, and after reordering we have that:

$$\mathbb{Z}_d \oplus \mathbb{Z}_d \simeq \bigoplus_{i=1}^{K} \mathbb{Z}_{p_i^{n_i}} \oplus \mathbb{Z}_{p_i^{n_i}}. \tag{E10}$$

Furthermore, it is a well known fact that subgroups of $F_1 \oplus F_2$ with F_1 and F_2 groups of coprime orders, are obtained as cartesian products of subgroups of F_1 with subgroups of F_2. Therefore, because of the decomposition of eq.(E10), we can find the subgroups of $\mathbb{Z}_d \oplus \mathbb{Z}_d$ by obtaining all the subgroups of each $\mathbb{Z}_{p_i^{n_i}} \oplus \mathbb{Z}_{p_i^{n_i}}$ (which can be done as in the last example) and then taking all their possible cartesian products.

To find the homomorphisms $\phi : \mathbb{Z}_d \oplus \mathbb{Z}_d \rightarrow \mathbb{Z}_d$, we picture the ϕ as going from $\bigoplus_{i=1}^{K} \mathbb{Z}_{p_i^{n_i}} \oplus \mathbb{Z}_{p_i^{n_i}}$ to $\bigoplus_{i=1}^{K} \mathbb{Z}_{p_i^{n_i}}$. Any such homomorphism can be written as the direct sums of homomorphisms $\phi_i : \mathbb{Z}_{p_i^{n_i}} \oplus \mathbb{Z}_{p_i^{n_i}} \rightarrow \mathbb{Z}_{p_i^{n_i}}$, which we obtained in the last example. Therefore, by constructing all such direct sums, we obtain all the homomorphisms we were looking for.

For example, if $d = 12$ all we need to do is find all the subgroups and homomorphisms of $\mathbb{Z}_4 \oplus \mathbb{Z}_4$ and of $\mathbb{Z}_3 \oplus \mathbb{Z}_3$ and then take cartesian products of these subgroups and the direct sum of the homomorphisms.

4. N particles of dimension of prime power dimension

Now we consider a system consisting of N particles, each with dimension p^{n_i} for $i = 1, \cdots, N$, ordered such that $n_1 \geq n_2 \geq \cdots \geq n_N$ (notice that the prime p is the same for all particles). In this case, the problem is to find all the subgroups of $\mathcal{G} = \mathbb{Z}_{p^{n_1}} \oplus \mathbb{Z}_{p^{n_1}} \oplus \cdots \mathbb{Z}_{p^{n_N}} \oplus \mathbb{Z}_{p^{n_N}}$ and homomorphisms from $\mathcal{G}$ to $\mathbb{Z}_{p^{n_1}}$. As an example, we will develop a system of one qubit and one 4-level system.

Similarly to the other examples, to find the representative subgroups we take the following steps:

- Select a basis of $\mathcal{G}$. For example, in the case of a qubit and a 4-level system, the group is $\mathcal{G} = \mathbb{Z}_4 \oplus \mathbb{Z}_4 \oplus \mathbb{Z}_2 \oplus \mathbb{Z}_2$, and we can choose a basis $\{\vec{e}_1, \vec{e}_2, \vec{e}_3, \vec{e}_4\}$, with $\vec{e}_1 = (1, 0, 0, 0)$ $\vec{e}_2 = (0, 1, 0, 0)$ $\vec{e}_3 = (0, 0, 1, 0)$ $\vec{e}_4 = (0, 0, 0, 1)$, where the first two entries add mod 4 and the last two add mod 2.

- Next, we find the partition of $\mathcal{G}$. For the qubit and 4-level system, the orders of $\vec{e}_1$ and $\vec{e}_2$ are 4 and the orders of $\vec{e}_3, \vec{e}_4$ are 2, so that the partition of the group is $\bar{M} = M_1 M_2 M_3 M_4 = 2211$.

- We find all the sets $\mathbb{S} = \{s_\alpha\}$ with $0 \leq s_\alpha \leq M_\alpha$, in this case there are 36 said sets.

- For each set $\mathbb{S}$, we define the basis $\mathbb{B} = \{p^{s_1}\vec{e}_1, p^{s_2}\vec{e}_2, p^{s_3}\vec{e}_3, p^{s_4}\vec{e}_4\}$.

- As before, some of the bases created this way are redundant, since they are T-isomorphic. To eliminate this redundancy, we first define $\tilde{M}_1, \cdots, \tilde{M}_q$ given by the q different values of numbers in $\bar{M}$. In the example of a 4-level system and a qubit, we have that $\tilde{M}_1 = 2, \tilde{M}_2 = 1$. Then, we define the sets $S_j = \{s_\alpha, \forall \alpha : M_\alpha = \tilde{M}_j\}$, which in this case are $S_1 = \{s_1, s_2\}$ and $S_2 = \{s_3, s_4\}$. Finally, bases are $T-$isomorphic if their corresponding sets S_j are equal. For example, the bases that come from the sets $\mathbb{S} = \{2, 1, 1, 0\}$ and $\mathbb{S}' = \{1, 2, 0, 1\}$ are $T-$isomorphic, since $S_1 = S_1' = \{2, 1\}$ and $S_2 = S_2' = \{1, 0\}$. Therefore, after eliminating redundant bases and keeping only one of each batch, we get the following 18 bases:

$$\mathbb{S} = \{0, 0, 0, 0\} \rightarrow \mathcal{B} = \{\vec{e}_1, \vec{e}_2, \vec{e}_3, \vec{e}_4\}, \quad \mathbb{S} = \{0, 0, 0, 1\} \rightarrow \mathcal{B} = \{\vec{e}_1, \vec{e}_2, \vec{e}_3\}, \quad \mathbb{S} = \{0, 0, 1, 1\} \rightarrow \mathcal{B} = \{\vec{e}_1, \vec{e}_2\},$$
$$\mathbb{S} = \{0, 1, 0, 0\} \rightarrow \mathcal{B} = \{\vec{e}_1, 2\vec{e}_2, \vec{e}_3, \vec{e}_4\}, \quad \mathbb{S} = \{0, 1, 0, 1\} \rightarrow \mathcal{B} = \{\vec{e}_1, 2\vec{e}_2, \vec{e}_3\}, \quad \mathbb{S} = \{0, 1, 1, 1\} \rightarrow \mathcal{B} = \{\vec{e}_1, 2\vec{e}_2\},$$
$$\mathbb{S} = \{0, 2, 0, 0\} \rightarrow \mathcal{B} = \{\vec{e}_1, \vec{e}_3, \vec{e}_4\}, \quad \mathbb{S} = \{0, 2, 0, 1\} \rightarrow \mathcal{B} = \{\vec{e}_1, \vec{e}_4\}, \quad \mathbb{S} = \{0, 2, 1, 1\} \rightarrow \mathcal{B} = \{\vec{e}_1\},$$
$$\mathbb{S} = \{1, 1, 0, 0\} \rightarrow \mathcal{B} = \{2\vec{e}_1, 2\vec{e}_2, \vec{e}_3, \vec{e}_4\}, \quad \mathbb{S} = \{1, 1, 0, 1\} \rightarrow \mathcal{B} = \{2\vec{e}_1, 2\vec{e}_2, \vec{e}_3\}, \quad \mathbb{S} = \{1, 1, 1, 1\} \rightarrow \mathcal{B} = \{2\vec{e}_1, 2\vec{e}_2\},$$
$$\mathbb{S} = \{2, 1, 0, 0\} \rightarrow \mathcal{B} = \{2\vec{e}_2, \vec{e}_3, \vec{e}_4\}, \quad \mathbb{S} = \{2, 1, 0, 1\} \rightarrow \mathcal{B} = \{2\vec{e}_2, \vec{e}_3\}, \quad \mathbb{S} = \{2, 1, 1, 1\} : \{2\vec{e}_2\},$$
$$\mathbb{S} = \{2, 2, 0, 0\} \rightarrow \mathcal{B} = \{\vec{e}_3, \vec{e}_4\}, \quad \mathbb{S} = \{2, 2, 0, 1\} \rightarrow \mathcal{B} = \{\vec{e}_3\}, \quad \mathbb{S} = \{2, 2, 0, 0\} \rightarrow \mathcal{B} = \{\}$$

As in the other cases, these bases form the representative subgroups of the group.

As before, the automorphisms are described by matrices $t_{\alpha\beta}$. For the special case of a qubit and 4-level system, the matrices are of dimensions 4×4 (because there are 4 elements in the basis) and the conditions on the entries $t_{\alpha\beta}$ can be found using the cases described in Appendix C, which lead to:

- t_{11}: $M_1 = M_1$ so that t_{11} is a number modulo $p^{M_1} = 2^2 = 4$.

- t_{12}: $M_1 = M_2$ so that t_{12} is a number modulo $p^{M_1} = 2^2 = 4$.

- t_{13}: $M_1 > M_3$ so that $t_{13} = p^{M_1 - M_3}\tau_{13} = 2\tau_{13}$ with τ_{13} a number modulo $p^{M_3} = 2$. Therefore, the possible values are 0 and 2.

- The same can be done for the rest of the values, and we find that $t_{11}, t_{12}, t_{21}, t_{22} \in \{0, 1, 2, 3\}$; $t_{13}, t_{14}, t_{23}, t_{24} \in \{0, 2\}$ and $t_{31}, t_{32}, t_{33}, t_{34}, t_{41}, t_{42}, t_{43}, t_{44} \in \{0, 1\}$.

Then, running through all possible matrices with these entries and keeping only the invertible ones, we find 147456 matrices.

As before, to find all subgroups, we apply these automorphisms to every representative subgroup and discard
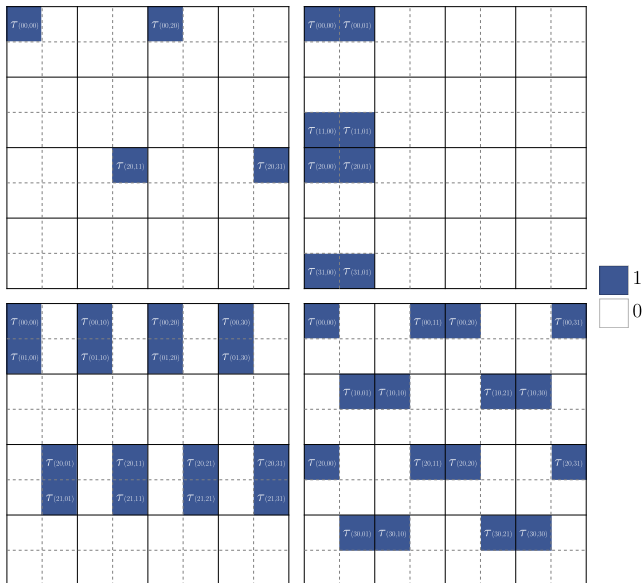
Figure 8. Some Weyl erasing channels of a system with a 4-level particle and a qubit, with $\tau(\vec{m}, \vec{n}) = 0, 1$. Recall that (m_α, n_α) corresponds to α-th particle.

repetitions. This procedure gives us the 249 subgroups of $\mathbb{Z}_4 \oplus \mathbb{Z}_4 \oplus \mathbb{Z}_2 \oplus \mathbb{Z}_2$, some of which are shown in fig. (8).

Finally, we find the homomorphisms $\phi : \mathcal{G} \to \mathbb{Z}_{p^{n_1}}$. For the case of a qubit and a 4-level system, we need the homomorphisms $\phi : \mathbb{Z}_4 \oplus \mathbb{Z}_4 \oplus \mathbb{Z}_2 \oplus \mathbb{Z}_2 \to \mathbb{Z}_4$. As before, we need to follow the procedure mentioned in Appendix D. In this case, $n = 2$ and therefore $\nu = 2$. The homomorphisms ϕ are characterized by the values in the basis $\phi_\alpha = \phi(\vec{e}_\alpha)$ which have to follow the conditions of eq.(D1b), that lead to:

- ϕ_1: Since $\alpha = 1 < 2 = \nu$, we are in the second case of eq.(D1b), thus ϕ_1 is a number modulo $p^n = 4$.

- ϕ_2: Since $\alpha = 2 = 2 = \nu$, we are in the first case of eq. (D1b), thus $\phi_2 = p^{n-M_2} s_2 = s_2$ with s_2 a number modulo $p^{M_2} = 4$.

- ϕ_3 : Since $\alpha = 3 > 2$, $\phi_3 = p^{n-M_3} s_3 = 2s_3$ with s_3 a number modulo $p^{M_3} = 2$, so that $\phi_3 = 0, 2$.

- ϕ_4 : Equivalently to ϕ_3 we find that $\phi_4 = 0, 2$.

Therefore, the homomorphisms for a qubit and a 4-level system are given by the 4 numbers $\phi_1, \phi_2, \phi_3, \phi_4$ with

$\phi_1, \phi_2 \in \{0, 1, 2, 3\}$ and $\phi_3, \phi_4 \in \{0, 2\}$ for a total of 64 possibilities.

5. Most General Case

In the most general case we have N particles, each with arbitrary dimension d_i and so the group under consideration is $\mathcal{G} = \bigoplus_{i=1}^N \mathbb{Z}_{d_i} \oplus \mathbb{Z}_{d_i}$.

Then, in this direct sum, we can first separate each $\mathbb{Z}_{d_i}$ as a sum of cyclic groups of prime power orders, such as it was done in section E 3 of this appendix. Then, having written $\mathcal{G}$ as a direct sum of cyclic groups with prime power order, we collect together the cyclic groups of order that is a power of 2, then cyclic groups of order power of 3, 5, 7, and so on for each prime.

After this, we can find the subgroups and homomorphisms of each of these collections as it was done in section E 4. Finally, the subgroups of $\mathcal{G}$ can be found as cartesian products of subgroups of different collections.

Appendix F: Number of subgroups per type $\overline{L}$

An expression for the number of different subgroups of type $\overline{L}$ is already known in the literature. To introduce this expression we first need to consider the Ferrers graph of $\overline{L}$, that is, L squares of which the first L_1 are in the first row, the next L_2 in the second, and so on. Then, the conjugate partition $\overline{L}'$ is defined as the Ferrers graph of $\overline{L}$ obtained by inverting rows and columns. Similarly, the partition $\overline{M}'$ is defined as the conjugate partition of $\overline{L}$. The number of subgroups $\mathcal{H}$ of type $\overline{L}$ of $\mathcal{G}_p$ is given by

$$\prod_{\alpha \geq 1} p^{M'_{\alpha+1}(L'_\alpha - M'_\alpha)} \begin{bmatrix} L'_\alpha - M'_{\alpha+1} \\ M'_\alpha - M'_{\alpha+1} \end{bmatrix}_p, \qquad \text{(F1)}$$

where the symbol

$$\begin{bmatrix} n \\ m \end{bmatrix}_p = \prod_{s=1}^m \frac{p^{n-s+1} - 1}{p^{m-s+1} - 1} \qquad \text{(F2)}$$

denotes the number of vector subspaces of dimension m in a vector space of dimension n over the field $\mathbb{Z}_p$. The proof is rather intricate, and we refer the reader to the relevant literature, such as [32, 34]. However, the key fact is that the number of subgroups obtained by our algorithm can be compared with (F1) to check that all subgroups of a given partition $\overline{L}$ have been found.

[1] H.-P. Breuer and F. Petruccione, *The Theory of Open Quantum Systems* (Oxford University Press, 2007).
[2] A. Rivas and S. F. Huelga, *Open quantum systems*, Vol. 10 (Springer, 2012).
[3] M. Schlosshauer, Decoherence, the measurement problem, and interpretations of quantum mechanics (2004), arXiv:0312059 [quant-ph].
[4] W. H. Zurek, Rev. Mod. Phys. **75**, 715 (2003).

[5] M. A. Nielsen and I. L. Chuang, *Quantum Computation and Quantum Information: 10th Anniversary Edition* (Cambridge University Press, 2010).

[6] M. M. Wilde, *Quantum Information Theory*, 2nd ed. (Cambridge University Press, 2017).

[7] M. M. Wolf, J. Eisert, T. S. Cubitt, and J. I. Cirac, Phys. Rev. Lett. **101**, 150402 (2008).

[8] D. Davalos, M. Ziman, and C. Pineda, Quantum **3**, 144 (2019).

[9] T. Heinosaari and M. Ziman, *The mathematical language of quantum theory: from uncertainty to entanglement* (Cambridge University Press, 2011).

[10] Á. Rivas, S. F. Huelga, and M. B. Plenio, Reports on Progress in Physics **77**, 094001 (2014).

[11] H. P. Breuer, E. M. Laine, J. Piilo, and B. Vacchini, Reviews of Modern Physics **88**, 021002 (2016).

[12] L. Gyongyosi, S. Imre, and H. V. Nguyen, IEEE Communications Surveys & Tutorials **20**, 1149 (2018).

[13] J. A. de Leon, A. Fonseca, F. Leyvraz, D. Davalos, and C. Pineda, Physical Review A **106**, 42604 (2022), arXiv:2205.05808.

[14] D. Bruß and C. Macchiavello, Physical Review Letters **88**, 127901 (2002).

[15] N. J. Cerf, M. Bourennane, A. Karlsson, and N. Gisin, Physical Review Letters **88**, 127902 (2002).

[16] T. C. Ralph, K. J. Resch, and A. Gilchrist, Physical Review A - Atomic, Molecular, and Optical Physics **75**, 022313 (2007), arXiv:0806.0654.

[17] E. T. Campbell, Physical Review Letters **113**, 230501 (2014).

[18] Y. Wang, Z. Hu, B. C. Sanders, and S. Kais, Frontiers in Physics **8**, 1 (2020), arXiv:2008.00959.

[19] T. Vértesi, S. Pironio, and N. Brunner, Physical Review Letters **104**, 060401 (2010), arXiv:0909.3171.

[20] P. Skrzypczyk and D. Cavalcanti, Physical Review Letters **120**, 260401 (2018), arXiv:1803.05199.

[21] H. Weyl, Zeitschrift für Physik **46**, 1 (1927).

[22] R. A. Bertlmann and P. Krammer, Journal of Physics A: Mathematical and Theoretical **41**, 235303 (2008), arXiv:0806.1174.

[23] M. Nathanson and M. B. Ruskai, Journal of Physics A: Mathematical and Theoretical **40**, 8171 (2007).

[24] H. Ohno and D. Petz, Acta Mathematica Hungarica **124**, 165 (2009).

[25] D. Chruściński and K. Siudzińska, Physical Review A **94**, 022118 (2016), arXiv:1606.02616.

[26] D. Chruściński and F. A. Wudarski, Physics Letters, Section A: General, Atomic and Solid State Physics **377**, 1425 (2013), arXiv:1212.2029.

[27] D. Chruściński and F. A. Wudarski, Physical Review A - Atomic, Molecular, and Optical Physics **91**, 012104 (2015), arXiv:1408.1792.

[28] I. Bengtsson and K. Życzkowski, *Geometry of Quantum States* (Cambridge University Press, 2017).

[29] G. Dahl, An introduction to convexity (2010).

[30] W. Burnside, *Theory of groups of finite order* (The University Press, 1911).

[31] C. Hillar and D. Rhea, The American Mathematical Monthly **114**, 917 (2007).

[32] G. Birkhoff, Proceedings of the London Mathematical Society **2**, 385 (1935).

[33] J. Siewert, Journal of Physics Communications **6**, 055014 (2022).

[34] L. Butler, Proceedings of the American Mathematical Society **101**, 771 (1987).

Bibliographic references

[1] Z. Hu, R. Xia, and S. Kais, "A quantum algorithm for evolving open quantum dynamics on quantum computing devices", Scientific reports **10**, 3301 (2020), arXiv:1904.00910 [quant-ph].

[2] F. Caruso, V. Giovannetti, C. Lupo, and S. Mancini, "Quantum channels and memory effects", Rev. Mod. Phys. **86**, 1203–1259 (2014).

[3] M. A. Nielsen and I. L. Chuang, *Quantum computation and quantum information: 10th anniversary edition*, 10th (Cambridge University Press, USA, 2011).

[4] I. Bengtsson and K. Życzkowski, *Geometry of quantum states: an introduction to quantum entanglement*, 2nd. (Cambridge University Press, 2017).

[5] Y. Mafi, P. Kazemikhah, A. Ahmadkhaniha, H. Aghababa, and M. Kolahdouz, "Bidirectional quantum teleportation of an arbitrary number of qubits over a noisy quantum system using 2 n bell states as quantum channel", Optical and Quantum Electronics **54**, 568 (2022).

[6] L. Gyongyosi and S. Imre, "Advances in the quantum internet", Communications of the ACM **65**, 52–63 (2022).

[7] D.-G. Im et al., "Optimal teleportation via noisy quantum channels without additional qubit resources", npj Quantum Information **7**, 86 (2021).

[8] A. Gilyén, S. Lloyd, I. Marvian, Y. Quek, and M. M. Wilde, "Quantum algorithm for petz recovery channels and pretty good measurements", Physical Review Letters **128**, 220502 (2022).

[9] E. Fontana, N. Fitzpatrick, D. M. n. Ramo, R. Duncan, and I. Rungger, "Evaluating the noise resilience of variational quantum algorithms", Phys. Rev. A **104**, 022403 (2021).

[10] S. Choi, Y. Bao, X.-L. Qi, and E. Altman, "Quantum error correction in scrambling dynamics and measurement-induced phase transition", Physical Review Letters **125**, 030505 (2020).

[11] V. Sivak et al., "Real-time quantum error correction beyond break-even", Nature **616**, 50–55 (2023).

[12] S. J. Beale, J. J. Wallman, M. Gutiérrez, K. R. Brown, and R. Laflamme, "Quantum error correction decoheres noise", Physical review letters **121**, 190501 (2018).

[13] A. A. Abbott, J. Wechs, D. Horsman, M. Mhalla, and C. Branciard, "Communication through coherent control of quantum channels", Quantum **4**, 333 (2020).

[14] S. Pirandola, "End-to-end capacities of a quantum communication network", Communications Physics **2**, 51 (2019).

[15] H.-Y. Ku et al., "Quantifying quantumness of channels without entanglement", PRX Quantum **3**, 020338 (2022).

[16] J. Cotler et al., "Entanglement wedge reconstruction via universal recovery channels", Physical Review X **9**, 031011 (2019).

[17] S. Harraz, S. Cong, and J. J. Nieto, "Enhancing quantum teleportation fidelity under decoherence via weak measurement with flips", EPJ Quantum Technology **9**, 1–12 (2022).

[18] N Abouelkhir, H. E. Hadfi, A Slaoui, and R. A. Laamara, "A simple analytical expression of quantum fisher and skew information and their dynamics under decoherence channels", Physica A: Statistical Mechanics and its Applications **612**, 128479 (2023).

[19] W.-C. Li et al., "Dynamics of multipartite quantum steering for different types of decoherence channels", Scientific Reports **13**, 3798 (2023).

[20] E. Chitambar and G. Gour, "Quantum resource theories", Reviews of Modern physics **91**, 025001 (2019).

[21] M. Schlosshauer, "Decoherence, the measurement problem, and interpretations of quantum mechanics", Rev. Mod. Phys. **76**, 1267–1305 (2005).

[22] T. Heinosaari and M. Ziman, *The mathematical language of quantum theory: from uncertainty to entanglement* (Cambridge University Press, 2011).

[23] D. Davalos, M. Ziman, and C. Pineda, "Divisibility of qubit channels and dynamical maps", Quantum **3**, 144 (2019), arXiv:`1812.11437`.

[24] M. Beth Ruskai, S. Szarek, and E. Werner, "An analysis of completely-positive trace-preserving maps on M_2", Linear Algebra and its Applications **347**, 159–187 (2002), arXiv:`quant-ph/0101003`.

[25] D. Bruß and C. Macchiavello, "Optimal Eavesdropping in Cryptography with Three-Dimensional Quantum States", Phys. Rev. Lett. **88**, 127901 (2002).

[26] N. J. Cerf, M. Bourennane, A. Karlsson, and N. Gisin, "Security of Quantum Key Distribution Using d-Level Systems", Phys. Rev. Lett. **88**, 127902 (2002).

[27] T. C. Ralph, K. J. Resch, and A. Gilchrist, "Efficient Toffoli gates using qudits", Phys. Rev. A **75**, 022313 (2007), arXiv:`0806.0654`.

[28] E. T. Campbell, "Enhanced Fault-Tolerant Quantum Computing in d -Level Systems", Phys. Rev. Lett. **113**, 230501 (2014).

[29] Y. Wang, Z. Hu, B. C. Sanders, and S. Kais, "Qudits and High-Dimensional Quantum Computing", Front. Phys. **8**, 1–24 (2020), arXiv:`2008.00959`.

[30] T. Vértesi, S. Pironio, and N. Brunner, "Closing the detection loophole in Bell experiments using qudits", Phys. Rev. Lett. **104**, 060401 (2010), arXiv:0909. 3171.

[31] P. Skrzypczyk and D. Cavalcanti, "Maximal Randomness Generation from Steering Inequality Violations Using Qudits", Phys. Rev. Lett. **120**, 260401 (2018), arXiv:1803.05199.

[32] M. Nathanson and M. B. Ruskai, "Pauli diagonal channels constant on axes", Journal of Physics A: Mathematical and Theoretical **40**, 8171 (2007).

[33] K. Siudzińska, "Geometry of pauli maps and pauli channels", Phys. Rev. A **100**, 062331 (2019), arXiv:1909.07722 [quant-ph].

[34] Chruściński, Dariusz and Siudzińska, Katarzyna, "Generalized pauli channels and a class of non-markovian quantum evolution", Phys. Rev. A **94**, 022118 (2016).

[35] I. Sergeev, "Generalizations of 2-dimensional diagonal quantum channels with constant frobenius norm", Reports on Mathematical Physics **83**, 349–372 (2019).

[36] A. Fonseca, "High-dimensional quantum teleportation under noisy environments", Phys. Rev. A **100**, 062311 (2019).

[37] H. Ohno and D. Petz, "Generalizations of pauli channels", Acta Mathematica Hungarica **124**, 165–177 (2009).

[38] J. Sakurai and J. Napolitano, *Modern Quantum Mechanics* (Cambridge University Press, 2017).

[39] H.-P. Breuer and F. Petruccione, *The theory of open quantum systems* (Oxford University Press, USA, 2002).

[40] C. Gerry and P. L. Knight, *Introductory quantum optics* (Cambridge university press, 2005).

[41] B. C. Hall, "Systems and subsystems, multiple particles", in *Quantum theory for mathematicians* (Springer, 2013), pp. 419–440.

[42] F. Nathan and M. S. Rudner, "Universal lindblad equation for open quantum systems", Physical Review B **102**, 115109 (2020).

[43] V. Y. Shishkov, E. S. Andrianov, A. A. Pukhov, A. P. Vinogradov, and A. A. Lisyansky, "Relaxation of interacting open quantum systems", Physics-Uspekhi **62**, 510 (2019).

[44] M.-D. Choi, "Completely positive linear maps on complex matrices", Linear Algebra and its Applications **10**, 285–290 (1975).

[45] A. Jamiołkowski, "Linear transformations which preserve trace and positive semidefiniteness of operators", Reports on Mathematical Physics **3**, 275–278 (1972).

[46] M. Jiang, S. Luo, and S. Fu, "Channel-state duality", Phys. Rev. A **87**, 022310 (2013).

[47] K. Kraus, "General state changes in quantum theory", Annals of Physics **64**, 311–335 (1971).

[48] E. Sudarshan, P. Mathews, and J. Rau, "Stochastic dynamics of quantum-mechanical systems", Physical Review **121**, 920 (1961).

[49] W. F. Stinespring, "Positive functions on C^*-algebras", Proceedings of the American Mathematical Society **6**, 211–216 (1955).

[50] M. Beth Ruskai, S. Szarek, and E. Werner, "An analysis of completely-positive trace-preserving maps on m2", Linear Algebra and its Applications **347**, 159–187 (2002).

[51] C. King and M. Ruskai, "Minimal entropy of states emerging from noisy quantum channels", IEEE Transactions on Information Theory **47**, 192–209 (2001), arXiv:quant-ph/9911079.

[52] A. Fujiwara and P. Algoet, "One-to-one parametrization of quantum channels", Phys. Rev. A **59**, 3290–3294 (1999).

[53] A Fujiwara and P Algoet, "Affine parameterization of quantum channels", in Proceedings. 1998 ieee international symposium on information theory (cat. no. 98ch36252) (IEEE, 1998), p. 87.

[54] X. Mi et al., "Information scrambling in quantum circuits", Science **374**, 1479–1483 (2021), arXiv:2101.08870 [quant-ph].

[55] S. T. Flammia and J. J. Wallman, "Efficient estimation of pauli channels", ACM Transactions on Quantum Computing **1**, 1–32 (2020).

[56] J. A. de Leon, A. Fonseca, F. Leyvraz, D. Davalos, and C. Pineda, "Pauli component erasing quantum channels", Phys. Rev. A **106**, 042604 (2022), arXiv:2205.05808v2 [quant-ph].

[57] Y. J. Ionin and M. S. Shrikhande, *Combinatorics of symmetric designs*, New Mathematical Monographs (Cambridge University Press, 2006).

[58] M. M. Wolf and J. I. Cirac, "Dividing quantum channels", Communications in Mathematical Physics **279**, 147–168 (2008).

[59] F. Ciccarello, S. Lorenzo, V. Giovannetti, and G. M. Palma, "Quantum collision models: open system dynamics from repeated interactions", Physics Reports **954**, 1–70 (2022).

[60] H. Weyl, "Quantenmechanik und gruppentheorie", Zeitschrift für Physik **46**, 1–46 (1927).

[61] R. A. Bertlmann and P. Krammer, "Bloch vectors for qudits", Journal of Physics A: Mathematical and Theoretical **41**, 235303 (2008), arXiv:0806.1174 [quant-ph].

[62] T. Basile, J. A. de Leon, A. Fonseca, F. Leyvraz, and C. Pineda, *Weyl channels for multipartite systems*, 2023, arXiv:2310.10947 [quant-ph].

[63] K. M. R. Audenaert and S. Scheel, "On random unitary channels", New Journal of Physics **10**, 023011 (2008).

[64] W. Burnside, *Theory of groups of finite order* (The University Press, 1911).

[65] C. Hillar and D. Rhea, "Automorphisms of finite abelian groups", Am. Math. Mon. **114**, 917–923 (2007).

[66] G. Birkhoff, "Subgroups of abelian groups", Proc. London Math. Soc. **2**, 385–401 (1935).

Colophon

This thesis is based on a template developed by Matthew Townson and Andrew Reeves. It was typeset with $\LaTeX\,2_\varepsilon$. It was created using the *memoir* package, maintained by Lars Madsen, with the *madsen* chapter style. The font used is Latin Modern, derived from fonts designed by Donald E. Kunith.